Nairn, Neil J (2011) *A Pilot Study for the digital replacement of a distorted dentition acquired by Cone Beam Computed Tomography (CBCT).* MSc(R) thesis.

http://theses.gla.ac.uk/3019/

A Pilot Study for the digital replacement of a distorted dentition acquired by Cone Beam Computed Tomography (CBCT).

Neil James Nairn

This thesis was submitted in fulfilment of the requirements for the Degree of MSc by research, College of Medicine, Veterinary & Life Sciences University of Glasgow.

October 2011

Dedication

This thesis is dedicated in loving memory of my uncle, Jack Elder. He was my childhood hero who inspired and influenced me throughout his life. Sadly missed but never forgotten.

This thesis is also dedicated to my parents Alex and Helen and my brother Alex, who have been a guiding light throughout my life and for all their support, love and encouragement in recent times.

And to my wonderful son, Lewis Alexander Nairn, who was born on the 23rd of October 2007 - he shows me what is important in life.

Acknowledgements

I wish to express my sincere thanks to my supervising committee Professor Ashraf Ayoub, Professor Khursheed Moos, Professor Joseph Barbenel and in particular my immediate supervisor Dr Balvinder Khambay. Their expert advice, guidance and unfailing patience has been overwhelming throughout this thesis. I would also like to thank them, on behalf of my family for their faith, belief and pastoral support through some challenging circumstances in which it was written.

I would also like to thank Laetitia Brocklebank, Liz Weldon and Angela Holmes and all the staff in the radiology department in the Glasgow Dental Hospital & School for all their and time support, often out of hours.

Special thanks to Carol McIvor for all her encouragement and assistance with patient recruitment and of course the cups of tea when it was needed most.

I'd like to thank Dr John Whitters who was my advisor of studies, and introduced me to the staff at Strathclyde University, who very kindly allowed me the use of their facilities.

Extended thanks go to my colleagues and friends, in particular David and Jacqueline Kilpatrick for their tolerance and encouragement throughout the writing of this thesis.

Abstract

Introduction: Cone beam CT (CBCT) is becoming a routine imaging modality designed for the maxillofacial region. Imaging patients with intra-oral metallic objects cause streak artefacts. Artefacts impair any virtual model by obliterating the teeth. This is a major obstacle for occlusal registration and the fabrication of orthognathic wafers to guide the surgical correction of dentofacial deformities.

Aims and Objectives: To develop a method of replacing the inaccurate CBCT images of the dentition with an accurate representation and test the feasibility of the technique in the clinical environment.

Materials and Method: Impressions of the teeth are acquired and acrylic baseplates constructed on dental casts incorporating radiopaque registration markers. The appliances are fitted and a preoperative CBCT is performed. Impressions are taken of the dentition with the devices in situ and subsequent dental models produced. The models are scanned to produce a virtual model. Both images of the patient and the model are imported into a virtual reality software program and aligned on the virtual markers. This allows the alignment of the dentition without relying on the teeth for superimposition. The occlusal surfaces of the dentition can be replaced with the occlusal image of the model.

Results: The absolute mean distance of the mesh between the markers in the skulls was in the region of 0.09mm ± 0.03mm; the replacement dentition had an absolute mean distance of about 0.24mm ± 0.09mm. In patients the absolute mean distance between markers increased to 0.14mm ± 0.03mm. It was not possible to establish the discrepancies in the patient's dentition, since the original image of the dentition is inherently inaccurate.

Conclusion: It is possible to replace the CBCT virtual dentition of cadaveric skulls with an accurate representation to create a composite skull. The feasibility study was successful in the clinical arena. This could be a significant advancement in the accuracy of surgical prediction planning, with the ultimate goal of fabrication of a physical orthognathic wafer using reverse engineering.

Table of Contents

List of Tables

List of Figures

Chapter 4 Results

Chapter 5   Discussion

Declaration

I declare that this thesis is the result of my own work and has not been submitted for any other degree at the University of Glasgow or any other institution.

Chapter One

Introduction and Literature Review

Introduction and Literature Review

1.1   Orthognathic surgery

The correction of dentofacial deformities by orthodontic and surgical intervention involves repositioning teeth and bone in three dimensions within the constraints of aesthetics, stability and function (Hajeer *et al.,* 2002).

Precise diagnosis and treatment planning for orthognathic surgery are essential for improving aesthetic and functional problems in severe dentofacial deformities (Proffit and White, Jr., 1990; Uechi *et al., 2006;* Chapuis *et al., 2007)*. Current methods of planning surgery in the maxillofacial region are based on two dimensional (2D) techniques, panoramic x-rays, facial and intraoral photographs and lateral cephalometric tracings (Harrell, Jr. *et al., 2002;* Xia *et al.,* 2001). These 2D images only represent the vertical and horizontal axis (x and y) and not the anteroposterior depth axis (z) (Hajeer *et al.,* 2004a). Two dimensional views are limited and rotational and head positioning errors will alter the normal anatomy which is not accurately represented, some elements can be obscured and calibration of the views is difficult. Patients are often unable to relate to the post-surgical profile prediction plan. A patient's main concern is their frontal facial view as this is experienced every day by looking in a mirror. Lateral photographs and 2D radiographs are unable to provide sufficient information to identify realistically and accurately the 3D configuration of the face and skull (Ayoub *et al.,* 2007; Harrell, Jr. *et al.,* 2002; Olszewski and Reychler, 2004).

The diagnostic information currently gained from the 2D techniques has been used in conjunction with study cast prediction in order to formulate a treatment plan (Bamber *et al.,* 2001; Uechi *et al.,* 2006). Once that treatment plan was established intermediate and final occlusal wafers were fabricated for the mid and post-operative model relationships for model surgery.

1.2 Orthognathic model surgery

Orthognathic model surgery has been a classical technique used to simulate orthognathic surgical cases on dental casts (Bamber *et al., 2001*). The model surgery has been used to simulate the final correction of facial deformity and malocclusion. The outcome of this model surgery allows the three-dimensional movements to be transferred and applied to the surgical correction of complex dentofacial deformities (Sharifi *et al.*, 2008). In order to achieve accurate model surgery the dental occlusion is recorded in the retruded contact position and the face bow recordings must accurately reflect the maxillary position relative to the skull.

1.2.1 Face bow and articulator systems

The face-bow is a device used for recording the relationship of the maxilla to the hinge axis in three planes of space, and the articulator is a device which mimics the position of the maxillary and mandibular teeth in contact in the centric position. Semi and fully adjustable articulators are able to simulate additional movements of the temporomandibular joints or mandible (O'Malley and Milosevic, 2000).

When the face bow position has been recorded, the recording is then transferred to a semiadjustable articulator and used to mount the upper dental cast on an articulator. A wax wafer is commonly used to record the retruded contact point position and this is then attached to the upper dental cast and the lower model is positioned in the correct intercuspal position and mounted on the lower section of the articulator prior to any model surgery. The articulated upper model is then optimally repositioned for surgery in the three planes of space and by the prescribed measurements and an intermediate and final wafer is fabricated to guide the surgeon perioperatively for the repositioning of the jaws (Bamber and Vachiramon, 2005; Barbenel *et al.,* 2010). This technique is still widely used, but it has been well documented that each stage has inherent errors (Bowley *et al.,* 1992; Nattestad and Vedtofte, 1994; Renzi *et al.,* 2002).

There are currently available a large number of differing face bows and articulators, varying from simple hinge articulators to semiadjustable systems that have been designed for prosthodontic purposes but not specifically for orthognathic surgical planning (Walker *et al.,* 2008a; Walker *et al.,* 2008b). Orthognathic predictive planning cannot be achieved precisely in many cases with current model surgery and face bow transfer systems (Renzi *et al.,* 2002). It is now well recognised that the current systems used are inaccurate for planning the correction of dentofacial deformities where the skeletal base may be abnormal (O'Neil *et al.,* 2010).

It is claimed that most face bows and their articulators are designed with the Frankfort horizontal plane and the upper cross member of the articulator as being parallel and horizontal (Gateno *et al.,* 2001; Walker *et al.,* 2008b). However it has been repeatedly shown that the orientation of dental models mounted on articulators using conventional facebows was inaccurate when replicating the orientation of a patient's jaws and teeth and this has introduced a systematic error (Ellis III, 1990; Gateno *et al.,* 2001; Gold and Setchell, 1983; O'Malley and Milosevic, 2000).

In a further study to establish an orthognathic surgery planning protocol, the validation of two orthognathic model surgery techniques was conducted. The Lockwood keyspacer and the Eastman anatomical-orientated systems were compared. The results obtained indicated that neither of the techniques provided a treatment plan with an acceptable degree of accuracy; however the Eastman technique was shown to be more accurate and this could have been clinically more helpful (Bamber *et al.,* 2001).

1.2.2 The outcome of orthognathic surgery

In a study to determine the accuracy of model surgery prediction and identify possible errors associated with the process (Sharifi *et al.,* 2008). It was found that the maxilla was more under-advanced and over-impacted anteriorly than had been predicted and the mandibular setback was more than had been predicted. This may be a result of inaccuracies with the face bow recording, the intermediate wafer, and the auto-rotation of the mandible in the supine or

anaesthetised patient. Barbenel *et al*. (2010) found that simulated model surgery on an articulator resulted in the planned vertical surgical movement not being fully achieved, the degree of maxillary impaction and downgraft was less than had been predicted. It was also found that planning for a 10mm maxillary forward movement without vertical change resulted in less advancement and a simultaneous downward movement of 3.3mm. Maxillary forward and upward prediction planning produced a greater advancement and 50% of the maxillary impaction in relation to the horizontal and vertical reference planes.

Walker *et al*. (2008) designed a new face bow and orthognathic articulator system incorporating a spirit level designed to overcome the problems associated with conventional facebows and articulators. These new systems allowed the mounting of study casts for asymmetric faces, accurately reproducing their clinical anatomy. These were evaluated by comparing measurements of anatomical features from the cephalometric radiographs against the corresponding features on the casts mounted on the orthognathic articulator. It was shown that although the measurements suffered from inter-subject variability the angulations of the occlusal cant, horizontal and maxillary occlusal plane and intercondylar widths did not significantly differ. It was concluded that the ability to mount casts accurately that simulated the clinical condition of patients would be more accurate in orthognathic predictive model surgery.

1.2.2.1   Summary

The literature clearly illustrated that the actual result of orthognathic surgery may differ significantly from the planned results from model surgery; this was recognised and it was recommended that precision and accuracy in orthognathic surgery could be improved with the application of current and future computer graphic systems for the prediction of surgical techniques (Nattestad and Vedtofte, 1994). Even though published literature highlighted the shortcomings of manual techniques the methods of preoperatively performing the planned osteotomy on dental casts is still regarded as the gold standard for planning the postoperative dental occlusion (Plooij *et al.*, 2011).

1.3 Current methods and techniques of capturing three dimensional (3D) data

Maxillofacial surgery requires precise 3D measurements of the human face and skull. The introduction of the digital era has revolutionised the techniques and procedures that can be used for prediction in craniofacial surgery.

There are a variety of techniques available to capture 3D data, each of which has potential advantages and disadvantages. Broadly speaking the methods available can be divided into two categories:

- **Surface data:** These scanners acquire surface three dimensional data of an object. This can be achieved by scanning an object by physical touch with the use of a stylus, emitting some form of light or by photographic capture.

- **Volumetric data:** These scanners are capable of acquiring and reconstructing 3D data of internal structures of an object with the use of x-ray, ultrasound or magnetic impulse.

1.4 Surface data imaging

The Principle methods are:
- Coordinate measuring machine
- 3D Facial Morphometry
- 3D Cephalometry
- Holography
- Laser
- Morphoanalysis
- Stereophotogrammetry
- Reflex Metrograph

1.4.1 Coordinate measuring machine (CMM)

The CMM was first introduced in the 1950's by the Ferranti company (Scotland) and was predominantly developed for use within the mechanical engineering, oil and gas, automotive and aerospace industries (Veselko *et al.,* 1998). It consisted of a stylus which needed to physically touch the object. The stylus was capable of moving within the three axes of motion (x, y & z); and a computer processed the information with the appropriate software.

The use of CMM measuring machines has been described previously in the dental literature. Ayoub *et al.* (2003) described a technique where a CMM was used to measure five landmarks on 21 stone models of infants with cleft palates. CMM became established as the gold standard for obtaining the x, y and z co-ordinates of an object. Khambay *et al.* (2008) used a CMM scanner for validating stereophotogrammetry.

Spencer *et al.* (1996) described a technique for constructing a 3D image of the mandible using a Ferranti co-ordinate measuring machine with the use of a specialised surface modelling software programme for image regeneration. They concluded that the major advantage of using CMM was its accuracy of representation and with the development of software would provide a more detailed representation of deformities in 3D.

Although this method of scanning was precise and capable of measuring to an accuracy of 0.001mm (Veselko *et al.,* 1998), it was not possible to apply this to a live patient as the CMM could only scan the surfaces of an object. In addition to this the scanning procedure was slow and relied on physical contact, this had the potential to distort or damage the surface being scanned i.e. the soft tissues.

CMM was both tedious and time consuming and if it were to be more widely used within the maxillofacial field there was a need to develop faster data capturing, even if this resulted in a small loss of accuracy (Spencer *et al.,* 1996).

1.4.2 3D facial morphometry

The technique of 3D facial morphology comprised of a system with two infrared charge coupled device cameras (CCD) that acquired images of the subject in real time. Hemispheric reflective markers were carefully positioned on a patients face to clearly identify landmarks and specialised software was used to reconstruct the x, y and z coordinates in relation to a referencing system (Ferrario *et al.*, 1996).

Three dimensional facial morphology had the advantages that it was non-invasive and did not subject the patients to harmful radiation; it appeared to be better at evaluating the relationships between the craniofacial structures and it was used as a research tool. It was subsequently adapted to the clinical situation as an addition to cephalometric analysis, predominantly for younger patients, so that any potential growth imbalance might be identified (Ferrario *et al.*, 1995).

There were significant disadvantages associated with 3D facial morphology. The placement of landmarks on patients was very time consuming and they were not readily reproduced. Patients were likely to change their facial expression between captures which increased the errors, life-like models showing natural soft tissues could not be produced, and therefore this technique could not be used as a communication medium for orthognathic or orthodontic patients, nor could it be used as a 3D treatment prediction tool (Hajeer *et al.*, 2002; Hajeer *et al.*, 2004a).

1.4.3 3D cephalometry

Early 20th century techniques of measuring dental and facial irregularities were predominantly undertaken by orthodontists who studied the inter-relationships of the teeth and jaws both before and after treatment. This often involved invasive techniques of obtaining landmarks of the skull by entering through the skin and soft tissues (Broadbent, 1931).

Broadbent (1931) developed a new form of cephalometric analysis by developing the Broadbent-Bolton Roentgenographic Cephalometer (BBRC) (Dean *et al.,* 2000). The BBRC held the head in a static and standard position. Two x-ray sources captured a biorthogonal frontal (posteroanterior) and lateral views, as opposed to the more common and less accurate method of turning the patient through 90 degrees in front of a single x-ray source (Savara, 1965). This simultaneous x-ray method had the advantage of increasing the landmark identification accuracy.

Manual 3D cephalometry had the advantage of not requiring any specialised equipment other than a standard x-ray machine, this meant that it was inexpensive and exposed patients to a relatively low dosage of radiation (Mori *et al.,* 2001).

The disadvantages of manual 3D cephalometry included difficulties associated with accurately locating the same two landmarks on different x-ray views, the length of time associated with undertaking this procedure, the absence of substantial soft tissue outlines, the overlapping of images creating poor visualisation of individual structures, errors associated with the projection procedure and the inability to identify true skeletal asymmetries when they were present (Hajeer *et al.,* 2002; Valiathan *et al.,* 2007). Mori *et al.* (2001) developed a 3D cephalometric system that not only corrected the magnification associated with Cephalometry, but also addressed cephalic malpositioning, the accuracy of which was evaluated by the use of measurements for dry skulls.

A more recent study (Popat and Richmond, 2009), described a new commercially available software programme specifically designed for 3D orthognathic surgery which integrated 2D Cephalograms images with 3D cone beam computed tomograms.

1.4.4 Holography

Holography is a technique that enables a user to record the light that is scattered from the surface of an object and then later reconstructed within the virtual environment in the form of a hologram (Young and Altshuler, 1977a).

The image appeared as if it was still present and in exactly the same position and orientation on the x, y & z axis. Holography was first demonstrated in 1947 by Dennis Gabor (Gabor, 1948), but it was not until 1963 that Yuri Denisyuk was able to record a 3D object (Denisyuk, 1962) and then Leith and Upatnieks investigated the practical applications of holography (Leith and Upatnieks, 1962).

The physical principles behind holography differed from photography; however the process had similarities in that both required a camera, a developing system and a visualisation system (Romeo *et al.*, 1995).

A hologram could be viewed by using a low-powered laser beam as the light source. A single laser beam is directed on to a hologram plate, this divides the beam back into its original object and reference beams. The object is then reconstructed and displayed, composed of light reconstructed in the monochromatic colour of the laser light, but having no mass and appearing at the identical distance from the hologram plate as the original object (Young and Altschuler, 1977b).

Martensson and Ryden, (1992) detailed a new holographic technique called the holodent system. This system was designed to produce holograms and would facilitate three-dimensional measuring. They discovered that metal and plaster had good light reflection, making the contours of the individual holographic image sharp and distinct and that a unique advantage of this system was its ability to allow the user to observe two dentitions at the same time. They also noted that when attempting to superimpose two holographic images or a hologram on a corresponding image this caused a blurring and the upper holographic image obscured details of the hologram in the lower position. Precision in the z axis was consistently lower than the positions in the x and y positions, which might have been due to a parallax error. Patients who had measurements recorded on reference points within the dental arch were not reliable, in these cases the rugae of the palate were used as the reference.

A unique advantage of this holographic technique of observing dental models was the ability to study two dentitions simultaneously and changes in tooth

positioning could be measured and visualised with the two dental arches superimposed on each other.

A method was developed for study models to be scanned as holographic films to record three dimensional, measurable images that would provide a substitute for gypsum study casts that were time consuming to construct, expensive to store and susceptible to breakage or abrasion (Keating *et al.,* 1984). Models should be retained for eleven years or until the patient is 26 years old (Bell *et al.,* 2003). Holographic images of dental casts were proven to provide a sufficiently accurate representation of orthodontic study models 0.05mm – 0.2mm (Romeo *et al.,* 1995). Holograms might be able to assist in solving the problems associated with gypsum study casts (Rossouw *et al.,* 1991).

A study substituting holograms for study casts on 56 patients over a 6 month period found that three clinicians believed holograms to be equally or more convenient and informative than conventional study casts, but one clinician found holograms to be inferior to study casts in both respects. It was concluded that currently available holograms merited further investigations and should be refined to further improve their convenience, informativeness and economic benefits so that holographic images could be stored indefinitely (Harradine *et al.,* 1990).

Holograms would be expensive and difficult to produce, and although the image captured by holography was 3D, it was stored in a static form and could not be manipulated in the same manner as gypsum study casts. The advantage of holography was that films could be stored with patient's medical records and this was a step forward for archiving dental study casts virtually, however as yet it could not totally replace original models and the information they provided might be limited (Bell *et al.,* 2003).

1.4.5 Laser

A laser is a device that generates and amplifies coherent electromagnetic energy at optical frequencies; it produces a coherent, extremely bright light of a single

colour (Young and Altshuler, 1977b). The name laser is an acronym for "light amplification by stimulated emission of radiation".

Albert Einstein in his 1917 paper *Zur Quantēntheorie der Strahlung* laid the foundation for the development of the laser and its predecessor the maser. Maser is the acronym for "microwave amplification by stimulated emission of radiation" (Young and Altshuler, 1977b).

A 3D scanner is a non-invasive means of rapidly collecting three dimensional surface data of an object. Laser scanners generally emit a laser beam that sweeps over the surface of an object and a detector gathers millions of measurements. The data is collected and grouped into compressed point cloud data bases that can be manipulated with the use of a computer. The resulting data can be viewed, navigated and analysed.

Lasers can be categorised as either non-contact active, where some form of radiation or light is emitted and the reflection is detected to produce a recording of an object. Non-contact passive scanners detect reflected ambient radiation and do not emit any kind of radiation (El-Hakim *et al.*, 1995).

1.4.5.1   Time of flight

A time of flight laser scanner emits a pulse of light at an object and the time it takes to be reflected and detected is timed. The accuracy of this type of scanner is dependent on how precisely the time can be recorded. A time of flight scanner can only detect the distance of a single point in its direction of view. Developments of these types of scanners have incorporated mirrors that are able to rotate at high speed allowing a greater number of points to be recorded, approximately 10,000-100,000 points per second.

1.4.5.2   Triangulation

A triangulation scanner emits a laser beam on to a subject and uses a camera to identify the position of the laser dot. Depending on the distance the laser comes into contact with a surface this will determine where the dot will appear in the camera's field of view. The technique is referred to as triangulation since

the dot, the camera and the source emitting the laser form a triangle (Mayer, 1999). Triangulation scanners project a laser stripe to speed up the acquisition process.

1.4.5.3   Structured light

Structured light scanners project a sweeping pattern of laser light on to an object and a camera is offset from the light source and analyses the deformation of the pattern on the object. A major advantage of structured light 3D scanners is speed. They are able to scan multiple points or an entire field of view (F.O.V.) at once, significantly reducing the distortion created by a moving object (Rocchini *et al.,* 2001).

1.4.5.4   Phase-based / modulated light

In phase-based or modulated based scanners a light source is modulated with a sine wave, this causes the amount of light that the laser emits to vary. In a similar way to the time of flight method a laser is emitted and reflected from an object. The speed of measurement in a phase-based/modulated laser scanner can be up to 100 times faster than that of a time of flight scanner.

Zhang and Yau, (2006) described a high-resolution, 3D absolute coordinate measurement system based on the phase-shifting method which was able to acquire a 3D shape at 30 frames per second and containing 266,000 points per frame. They applied the technique to human hands and faces. They concluded that such a system could have applications in manufacturing, inspection, entertainment, security and medical imaging.

1.4.5.5   Facial surface laser scanning

Laser scanning provides a non-intrusive and safe method of capturing the face for planning or evaluating the outcome of orthodontic or maxillofacial surgical treatment (Hajeer *et al.,* 2004a).

A system has been developed with a high spatial resolution for longitudinal studies of post surgery soft tissue changes in growing individuals. The system

was repeatable, safe and involved no direct contact with a patient's face (Moss *et al.,* 1987). The patients head was immobilized with a cephalostat, and a laser scan of the whole head and neck was performed with eyes closed (Papadopoulos *et al.,* 2002). The system consisted of two vertically fanned out low power helium-neon laser beams which were projected onto the face and viewed from an oblique angle using a television camera, following a similar method that had been previously developed (Arridge *et al.,* 1985).

In a study by McCance, 16 skeletal class III adult patients were laser scanned prior to surgery, 3 months post surgery and 1 year post retention and were compared with a control group of the same population to establish 3D soft tissue changes (McCance *et al.,* 1992). It was found that laser scanning was a simple non-invasive method of auditing surgical outcomes and measuring surgical relapse and that the results were independent of the spatial orientation of the profile and free from subjective judgement. However several questions remained unresolved (McCance *et al.,* 1997):

1. No clear statistical method had been established for comparing shape.
2. What would be the criteria by which any change would be judged, at least two criteria were necessary, the first being a numerical comparison between the before and after surgery, and the second a measure of the consequent change which the error had on a facial appearance.

3D laser scanning systems have increased in usage for assessing facial shape and contour analysis (Kau *et al.,* 2004; Kau *et al., 2005)*. McCance *et al.* (1997) applied it to adult cleft palate patients, Da Silveira *et al.* (2003) applied laser scanning to cleft palate infant patients. Soncul and Bamber, (2004) used a laser scanner to evaluate the soft changes following correction of class III dentoskeletal deformity cases. Further developments led to a colour millimetric scale being used in conjunction with laser scanned data. This proved to be a very useful tool for analysing surgical outcome and for illustrating it in a clear and easily understood way (McCance *et al.,* 1997).

Cephalographs and laser scanned images were compared by measuring the lip-incisor relationship, the naso-labial angle, nasal tip projection, the naso-facial

angle, the naso-mental angle and the labio-mental angle in pre and post operative orthognathic patients. The results indicated that the two methods were comparable, but the laser scan would be superior in pre and post operative assessment of soft tissue changes as a result of surgery due to its clarity and potential three dimensional application (Soncul and Bamber, 1999).

The accuracy and reproducibility of generating 3D object reconstructions using a laser scanner were assessed by testing them on a geometrical calibrated cylinder, a dental study cast and a plaster facial model (Kusnoto and Evans 2002). The tests were conducted at varying distances and found that the scanner was accurate to 0.5mm (± 0.1mm) in the vertical dimension and 0.3mm (± 0.3mm) in the horizontal dimension when applied to the cylinder. The study cast scan was accurate in measuring molar width to 0.2mm (± 0.1mm) and 0.7mm in the palatal vault and a facial model could be scanned to an accuracy of 1.9mm (± 0.8mm), which was regarded as not acceptable for orthognathic surgery. The authors concluded that laser scanning had a great research potential for growth, surgical simulations, treatment changes and it had a variety of orthodontic applications which could be used three dimensionally.

When capturing the head and neck region with a laser scanner the patients head should be immobilised using a cephalostat so that the laser scan can cover the whole head and neck (Papadopoulos *et al.,* 2002). This provides the clinician with data that enables more a precise treatment outcome to be predicted, as well as the prognosis, treatment planning and an evaluation of the results of treatment (O'Grady and Antonyshyn, 1999).

1.4.5.6   Intra-oral laser scanning

The first hand held intra-oral scanner that was developed in America was based on the structured light technique. A video camera recorded the light distortions on the clinical crowns as the light passed over them, which took approximately one minute. A computer then merged all the scans captured to create a complete dental arch (Hajeer *et al., 2004b*).

A further development of the intra oral scanning system was based on the principles of laser triangulation. The initial size of the systems restricted its

15

application to plaster casts. A new system was developed which would be compared to that of the currently available commercial intra-oral system with a coordinate measuring table used as the gold standard. The measurement distances were shown to have a maximum deviation of 0.2mm. However further developments are required in order to reduce the size of the equipment with the use of more precise device components (Commer *et al.*, 2000).

1.4.5.7   Laser scanning models

Dental study models are regarded as an integral part of dental practice and research and they are routinely used in the physical recording of orthodontic treatment (Bell *et al.,* 2003., Papadopoulos *et al.,* 2002). Dental study models are also routinely used in research, audit and teaching (Asquith *et al.,* 2007). Dental study models have several disadvantages (Papadopoulos *et al.,* 2002):

- Storage/Cost
- Archiving
- Weight
- Susceptibility to fracture
- Surface abrasion
- The methodology for the recording of measurements

An efficient and reproducible method of capturing a 3D virtual study model using a laser scanner was developed by Keating *et al.* (1984).   Thirty randomly selected intact white study models were selected. These were measured in the three planes using a digital calliper (accurate to 0.01mm). The same models were captured using a laser scanner and then compared. The results indicated that there was no statistically significant difference in the measurements taken on the original plaster model compared to those obtained using the laser scanner; therefore laser scanning would help with a number of the problems associated with study models, producing durable images without any fear of loss or damage to the original casts (Hajeer *et al.,* 2004b).

It has been shown statistically that almost 50% of the study casts handled by non-specialised personnel reach the clinical environment fractured (Harradine *et*

al., 1990). There have been a number of studies carried out that utilise laser scanners as a means of capturing and storing dental casts with the ultimate goal of reducing the problems associated with the dental cast (Hirogaki *et al.,* 2001; Lu *et al.,* 2000; Motohashi and Kuroda, 1999).

The repeatability and accuracy with the use of a laser scanner and a touch probe scanner has been evaluated in an attempt to produce an accurate representation of a tooth or teeth that could be used to serve as input data in a manufacturing system suitable for fixed dental prostheses. Ten dies were prepared for complete crowns and the surfaces were digitized 3 times each with the laser optical scanner and with the touch probe scanner. The repeatability and accuracy of the laser scanner was comparable with the touch probe surface digitisation device (Persson *et al.,* 2006).

Several studies have been carried out to assess the accuracy, reproducibility and reliability of laser scanned digital models. Santoro *et al.* (2003) evaluated the reliability of the OrthoCAD (Cadent, Fairview, NJ) system. Two independent examiners measured tooth size, overbite and overjet on both digital and plaster models. The results showed a statistically significant difference between the 2 groups for tooth size and overbite. However the magnitude of these differences ranged from 0.16mm to 0.49mm and was considered clinically insignificant for orthodontic and maxillofacial cases.

Asquith *et al.* (2007) examined the accuracy and reproducibility of measurements made on digital models by sampling 10 sets of orthodontic study casts, marking specific points and scanning them using the Arius3D laser scanner (Inition, London, UK). Two examiners measured study casts and the 3D models independently. They determined that systematic errors of measurement were detected, but were clinically insignificant.

In a study evaluating the systematic errors associated with producing plaster or computer-based models experiments which were conducted on a standardised plastic model which was regarded as the gold standard, accuracy, reproducibility, efficacy and effectiveness were tested by comparing the measurements of the 3D models with plaster models. Measurements made from

the 3D models appeared to be as accurate and reliable as measurements from the plaster models (Quimby *et al.,* 2004). Therefore 3D models would be a clinically acceptable alternative to conventional plaster models (Kusnoto and Evan, 2002).

1.4.5.8   Disadvantages of laser scanning

- Laser scanning may prove difficult to apply to a live patient due to the possibility of movement during the scan, in addition to possible safety issues related to the scanner (Hajeer *et al.,* 2004b).

- 3D scanning of dental casts by laser scanning can be time consuming (Papadopoulos *et al.,* 2002).

- Difficulty in measuring beneath overhangs, such as the anterior oral vestibule in the dental model with severe labio-lingual tipping of anterior teeth (Hajeer *et al.,* 2004b; Motohashi and Kuroda, 1999).

- The inability to capture soft tissue texture. This results in difficulties in identification of land marks that are dependent on surface colour (Hajeer *et al.,* 2002).

- Visualisation of the true size, location, or relationship of the roots of the teeth and other anatomy (Harrell *et al.,* 2002).

1.4.6 Morphanalysis

Clinical morphanalysis began at the Mount Vernon Centre for plastic and maxillofacial surgery, Northwood in 1963. The centre for morphanalysis was established in 1966 to provide a service to conduct clinical research, it then moved to the department of human Morphology at Southampton University where the technique was further developed (Rabey, 1977).

Morphanalysis is a technique of acquiring 3D records using photographs, radiographs and study casts of a patient Hajeer *et al.* (2002). Rabey (1971) claimed that the major advantages of morphanalysis in orthognathic surgery

were analytic validity, statistical validity, accuracy and superior communications.

1.4.6.1 Disadvantages of morphanalysis

- The equipment used in morphanalysis is expensive, highly elaborate, complicated and time consuming and would not be practical to apply to everyday use (Hajeer *et al.,* 2002; Khambay *et al.,* 2002).

1.4.7 Stereophotogrammetry

Photogrammetry can be defined as the science or art of obtaining reliable measurements by means of photography (Hajeer *et al.,* 2002). This eliminates the need to acquire facial dimensional data by the use of direct contact with a patient's face (Burke and Beard, 1967). Stereophotogrammetry refers to a case where two cameras are configured to work in unison to record the same object at different angles and record 3D distances of features by means of triangulation. The 3D image can be rotated, translated and dilated on a computer screen (Hajeer *et al.,* 2004a; Von and Rivett, 1982).

Stereophotogrammetry can provide an accurate evaluation of the face; multiple stereo-pair views can be incorporated to increase the amount of 3D data that can be obtained to generate a 3D model. Inaccuracies created by movement are eliminated since all the captured photographs are taken simultaneously (Hajeer *et al.,* 2002). Due to the fast capture speed and relative ease of use, 3D digital stereophotogrammetry is rapidly becoming the preferred facial surface imaging modality serving as an objective digital archive of patient's faces without the exposure of radiation (Heike *et al.,* 2010).

1.4.7.1 Stereophotogrammetry in the clinical environment

A new concept was demonstrated of quantifying facial morphology and detecting changes in facial morphology during growth and development using stereophotogrammetry (Ras *et al.,* 1996). Burke *et al.* (1983) described how stereophotography was used to measure soft tissue changes on a patient who was about to undergo surgery to their mandible.

A non-invasive and cost effective vision based three dimensional facial data capture system was introduced and developed for the planning of maxillofacial orthognathic operations. Facial images were captured using two sets of stereo-paired cameras and a scale-space-based stereo matching system was used to recover correspondences between the stereo-pairs with a spatial accuracy of 0.5mm (Ayoub e*t al.,* 1998). This system was further developed by the introduction of a process which allowed the 3D geometry of soft tissue captured by stereophotogrammetry to be registered with a 3D image of the underlying skeletal hard tissue to an accuracy of between 1.25mm and 1.5mm (Khambay *et al.,* 2002).

In order to acquire consistent high quality 3D facial captures the following protocol needed to be applied to optimise image quality (Heike *et al.,* 2010):

- A space should be dedicated with ample room and sufficient ambient lighting.
- Appropriate seating should be available to facilitate rapid positioning, especially when working with children.
- Scalp hair should be appropriately positioned so that all relevant surfaces of anatomy are not obscured, and any reflective objects would be required to be removed.
- Ensure that the subject achieves a neutral facial expression in a resting position that can be repeated if post-operative images are required.
- The patient's head should be positioned so that areas of interest are visible to the system's cameras to maximise facial surface coverage.
- Batch processing should be undertaken if multiple images are to be acquired in a limited amount of time.

1.4.7.2 Stereophotogrammetry applied to study casts

A biostereometric technique for digitally recording and storing dental casts was introduced by Ayoub *et al.* (1997). In a study to assess the accuracy it was concluded that the technique was an accurate and reproducible method for recording and storing study models. The digitised models could be viewed from

a variety of angles and positions with measurements being made to a precision of 0.27mm (Bell *et al.,* 2003).

1.4.7.3   Disadvantages of stereophotogrammetry

- Stereophotogrammetry requires specially trained staff to operate the system.
- Only the surface of an object is captured and it is not capable of capturing or displaying the underlying hard tissue (McCance *et al.,* 1992).
- Stereophotogrammetry relies on the texture of the image for pinpointing landmarks; monochrome study casts are not ideally suited for this type of image capture.
- Severe areas of undercut may not be visible in the cameras line of sight, therefore study models would be reconstructed with areas which are incomplete.

1.4.8 Reflex metrograph

The reflex Metrograph is an optical plotter that is connected directly to a microcomputer. It is able to capture directly 3D landmarks of irregular shaped objects up to 300mm without physically contacting the object (Speculand *et al.,* 1988a; Speculand *et al.,* 1988b).

The reflex Metrograph consists of a corrected semi-reflecting mirror, a mirror mount, an object table and an orthogonally movable measuring mark (a 0.3mm diameter pinpoint light spot) (Takada *et al.,* 1983).

The light spot is positioned on an adjustable three-dimensional slide system which can be manipulated in the three planes of x, y, and z. Rack driven encoders supply the co-ordinate data which is analysed by the computer. When in use the light spot moves so that it appears to lie superimposed upon a chosen point or landmark when viewed through the mirror.

If the operator moves their head they can use the parallax effect to optimise the location of the light spot/landmark. When the light spot is in the correct

position the operator can transmit the co-ordinates to a PC (Speculand *et al.*, 1988a).

Several dental and maxillofacial studies have used reflex metrography to record anatomical points. Matteson *et al.* (1989) undertook a study to investigate the value of three-dimensional images compared with cephalometric techniques in assessing craniofacial deformity. Takada *et al.* (1983) used the reflex metrograph to measure points on a dental cast and found that operators with no previous experience were able to determine points to an accuracy of ± 0.1mm. Bishara *et al.* (1994) used a reflex metrograph to digitize points on dental casts and combined it with measurements taken from cephalograms to study the dentofacial changes occurring between 25 and 46 years of age in an untreated normal sample.

1.4.8.1 Disadvantages of reflex metrograph

- An object being scanned must be inanimate as any movement would render the system useless and therefore this could not be applied to live subjects.
- The reflex metrograph only measures specific points or landmarks and would not be able to reproduce a realistic image of an object.

1.5 Volumetric data imaging

- Computed Tomography (CT).
- Spiral Computed Tomography.
- Cone Beam Computed Tomography (CBCT).
- Magnetic Resonance Imaging (MRI).
- Ultrasonography.

1.5.1 Computed tomography (CT)

Conventional radiographic images capture all the structures within a field of view with very similar fidelity. This can be a significant disadvantage where the

structures imaged are superimposed on each other, and this can result in the structure or area of interest being obscured or completely masked.

Tomography provides a method for the selection of an anatomical image that requires to be focused in the area of interest and it enhances the radiographic contrast and tends to blur the information on either side of that area.

Computed tomography (CT), is a highly specialized method of tomography made possible through the development of modern computer technology, which in 2D provided anatomical image slices through the body. This was developed in 1972 by Sir Godfrey Hounsfield and Allan McLeod Cormack and initially manufactured by EMI (Kalender, 2006).

Conventional x-ray images are produced when radiation passes through the body and the structures of differing densities create shadows. CT also utilises these images, but in a different way. Conventional tomography was also referred to as axial tomography since the plane in which the patient was scanned was parallel to the long axis of the body, resulting in coronal and sagittal images. CT differs in that transaxial or transverse images are produced and are at right angles to the long axis of the body.

In conventional CT there is no standard image receptor, like an x-ray film or an image intensifier tube. Instead the scanner consisting of a rotating gantry with an x-ray source transmits multiple small collimated x-ray beams which traverse specific areas of the body in an axial plane of the patient. The subsequent attenuated image is captured by a radiation detector and forwarded to a computer. The strength of these x-ray beams are recorded and measured by complex multi detectors that are rotating on the opposing side of the beam source. The information is then analysed; and the initial image is produced.

Once CT was accepted as a diagnostic modality, several manufacturing companies in addition to EMI began to develop and produce CT scanners. Although these differed in design they all followed the same original basic principles.

Over an initial period four generations of CT scanner were developed, which were characterised by the nature of the x-ray source and the detector movement.

1.5.1.1 First-generation imaging scanners

The original scanners designed by EMI worked on a principle known as translation/rotation. The x-ray source tube produced a finely collimated pencil beam and two detectors were located on the opposing sides of the tube to detect the radiation produced, so that two adjacent slices could be imaged during each procedure. Following each linear tube movement (translation) the assembly was rotated by one degree and the translation repeated 180 times. The fundamental drawback of this procedure was time. It would take up to 5 minutes per scan, which would require the patient to lie perfectly still for relatively long periods of time; as a result of this, early CT was almost exclusively used for neurological examinations.

1.5.1.2 Second-generation imaging scanners

First generation scanners were regarded as almost a demonstration project in that they demonstrated that it was feasible to have the x-ray source and detector working together in unison to produce an image.

Second-generation scanners still incorporated translation and rotation technology; however the x-ray source then produced a fan-shaped beam instead of a pencil beam and units were fitted with a multi-detector assembly unit of approximately 30 detectors tightly fitted together. The assembly still rotated, but now it was in increments of 10 degrees, which meant that only 18 translations would be required. The introduction of these changes meant that a scan time could be reduced to about 20 seconds, but the time required completing a CT examination was still regarded as too long and the introduction of a fan beam created problems:

- There was a significant increase in scatter radiation that had a detrimental effect on the final image.

- There was an increase of intensity of the beam towards the edges due to the shape of the beam; this was compensated for by using a special filter.

1.5.1.3   Third-generation imaging scanners

Third-generation scanners consisted of a much larger configuration of detectors (up to 750) and a fan beam of 30-60 degrees. A rotational movement was introduced; this meant that both the x-ray source and detectors rotated concurrently around the patient ensuring a constant x-ray source to detector distance, this in turn increased the quality of image reconstruction by ensuring improved x-ray beam collimation and reduced the effects of potential scatter radiation.

CT examination time was reduced to 1-10 seconds, making it less likely that a patient would move, eliminating the likelihood of motion artefacts. Continuing advancements in computer technology increased the speed in which the images could be reconstructed, therefore reducing overall examination time.

A disadvantage of third-generation scanners was the appearance of ring artefacts, which occurred when any of the detectors failed. The signal that had not been detected created interferences producing a ring on the reconstructed image.

1.5.1.4   Fourth-generation imaging scanners

Fourth-generation scanners introduced a rotational-static movement. The x-ray source rotated around the patient with multiple detectors (approximately 4000) arranged throughout the circumference of a circular gantry. The x-ray source produced a fan shaped beam, although this meant that there was no longer a constant x-ray source to detector distance this did not create a problem since each detector was able to be calibrated during image acquisition. This eliminated the problem of ring artefacts that were associated with third-generation scanners. Fourth-generation scanners were capable of achieving image acquisition in under a second and compensated for variations in slice thickness with automatic pre-patient collimation.

Disadvantages of fourth-generation scanners were their increased cost due to the number of detectors installed. More importantly the dosage of radiation a patient was subjected to was significantly increased.

1.5.1.5   Digital image matrix

In order to create a digital image from a CT scan an image matrix is created. This matrix is a complex arrangement of numbers that are arranged in a sequence of columns and rows, each square of the matrix is referred to as a picture element and when arranged in the matrix these elements are known as pixels. The thickness of the slices creates an additional volume element or voxel, the combination of the voxels and pixels create a cube of information each containing a CT number or Hounsfield unit (HU).

1.5.1.6   Hounsfield units (HU)

A HU is the number that is assigned to each individual pixel within the matrix and is displayed on a monitor as a level of brightness or on a photograph as a level of optical density. The CT number assigned is dependent on the relative comparison of an x-ray attenuation coefficient of the tissue that is present within the voxel compared to an equal volume of water. Water is used as the reference material as it has a uniform density and is abundant within the human body; therefore it is assigned a HU value of zero. Molecular structures that are denser than water are assigned with a positive HU value and structures that have less density are assigned with a negative HU value. The range of values varies from -1000 for air to +4000 for metals, Figure 1.1.

Substance	HU value
Air	-1000
Lungs	-250 ranging to -850
Fat	-100
Water	0
Blood	+20 ranging to +75
Bone	+150 ranging to +1000
Metal	+2000 ranging to +4000

Figure 1.1   Hounsfield units (HU).

In order to view an image each pixel is displayed as a shade of grey. The level of grey present corresponds to the CT number that has been assigned to that pixel.

As CT imaging continues to develop, further advances in image resolution and reduction in patient dosage are being introduced; these include differing motions of the x-ray source and the detector configuration. As yet no design has been acclaimed as the fifth-generation, but Spiral CT is leading the field.

1.5.2 Spiral/helical computed tomography

Spiral CT can also be referred to as Helical CT and was first introduced in 1989. It differs from previous described CT scanners in that during spiral CT the gantry is continually rotating and emitting a narrow fan shaped x-ray beam. The table that the patient is positioned on simultaneously passes through the aperture of the gantry. The combination of the movements from the table and the gantry creates the spiral effect scanning a volume of tissue as opposed to a group of individual slices.

This technique was possible with the development of slip-ring technology. Slip rings are electromechanical devices that conduct electrical signals through an array of rings and brushes from a rotating surface onto a fixed surface. This meant that there was no cable between the gantry and generator so there was no interference and the gantry was able to continually rotate.

1.5.2.1　Multi-slice spiral/helical CT

In the early 1990's a company developed an improvement to spiral CT by introducing multiple rows of elements along the z axis. This meant that the scanning time was significantly reduced. These new types of scanners are referred to as Volume CT (VCT) systems as entire sections of body could be scanned in a single breath.

Multi-slice systems allow viewing in all orientations (isotropic), faster scanning times, increased spatial resolution due to an increase in voxel size and greater anatomical coverage.

Computed tomography has been used for several years within the field of dentistry for providing cross-sectional implant imaging (Yajima *et al.*, 2006), for evaluating a variety of infections, cysts, tumours and trauma within the maxillofacial region (White and Pharoah, 2008a). CT also provides essential 3D information on dental and craniofacial anatomy for the diagnosis and treatment planning of clinical procedures such as craniofacial reconstruction (Mah *et al.*, 2003a).

It is now widely acknowledged that CT has introduced a new epoch in dentistry and is now widely used in the area of oral and maxillofacial predictive surgery planning (Nandini *et al.*, 2008; Park *et al.*, 2007). CT allows the user to access the internal morphology and skeletal structures of bone and teeth in a virtual environment. When displayed in a 3D format it can provide valuable information as the images provide clear information about the patient in a variety of directions as well as cross-sections (Gateno *et al.*, 2003; Nkenke *et al.*, 2004a; Sohmura *et al.*, 2005).

CT usage has significantly increased over the past thirty years with approximately 5 million images captured in the United States in 1983. This figure sharply increased with a rise to 20 million images in 1995 (Mah *et al.*, 2003b).

For orthognathic treatment planning these images can be used in addition to conventional radiographs, cephalometric analysis, photographic imaging and study casts (Nkenke *et al.*, 2004a; Troulis *et al.*, 2002). CT is now widely recognised as the gold standard for capturing hard tissue and it has applications for a range of situations:

- Assisting patients to visualise their appearance following surgery
- Operative procedures can be simulated and used for teaching purposes
- Soft tissue changes following osteotomy surgery can be simulated and agreed upon
- Assist in Quality assurance

In comparison to conventional cephalograms, CT does not have errors due to the superimposition of anatomic structures and differential enlargement in different areas. More accurate measurements have been reported on planar two dimensional (2D) CT images (Kragskov *et al.*, 1997; Vannier *et al.*, 1997).

Chapuis *et al.* (2007) developed a technique which incorporated 3D digital technology from a CT image with existing conventional techniques for computer-aided preoperative surgical planning and navigation during surgery. The system was applied to one patient who was receiving a bi-maxillary osteotomy. The authors reported an improved assessment of pathology and increased precision; however the technique is extremely complicated, time consuming and would be compromised by the presence of metallic objects creating artefacts.

1.5.2.2 Resolution and accuracy problems associated with CT

- CT devices expose patients to an increased amount of radiation in comparison to conventional two dimensional x-ray images and CBCT. It has been suggested the use of 3D CT images should limited to morphological analysis of malocclusion and follow-up of treatment in clinical orthodontics (Hajeer *et al.*, 2004a; White and Pharoah, 2008a).
- CT scanning is likely to have increased waiting times and be relatively expensive in comparison to conventional radiography which limits its usefulness in daily clinical practice (Hajeer *et al.*, 2004b).
- Patients who currently have metallic restorations, implants or stainless steel orthodontic brackets can create distortions in the CT image referred to as artefacts. These significantly impair the information on the dentition, occlusion and maxillomandibular relationships (Nkenke *et al.*, 2004a; Park *et al.*, 2007; Sohmura *et al.*, 2005).
- Conventional CT images, when viewed in 2D depict the craniofacial region as a number of image slices instead of one image, making it difficult to evaluate different points on multiple images (Kragskov *et al.*, 1997).
- The image quality that is obtained from CT has not sufficient detail on the occlusal surfaces and of intercuspal relationships, this create significant difficulties in predicting the position of the mandible after surgery (Gateno *et al.*, 2003; Uechi *et al.*, 2006).

- A dedicated work station with a high image processing capacity and highly specialised operators are required to operate the system (Okumura *et al.,* 1999). Conventional CT machines are large in size and this creates problems in areas where space is paramount if a dedicated machine is required; however in most instances this is a shared facility (Arai *et al.,* 1999).

- Although CT exposes patients to a higher dosage of radiation, there may be instances when superior quality images are required, especially when obtaining information on the surrounding soft tissues (White and Pharoah, 2008a).

1.5.3 Cone beam computed tomography (CBCT)

Cone beam computed tomography (CBCT) is a relatively recent innovation and has very similar characteristics to that of conventional CT. CBCT was developed over the last 20 years and has gained broad acceptance in dentistry in the last 5 years (White and Pharoah, 2008a). CBCT was specifically designed for use in the maxillofacial region for the visualisation of hard tissue (Yajima *et al.,* 2006), Figure 1.2.

CBCT has been regarded as one of the more exciting and revolutionary forms of imaging in dentistry (Mah and Hatcher, 2004), CBCT can also be referred to as cone-beam volumetric tomography (CBVT). CBCT differs from conventional CT in a number of ways:

1. The x-ray source in CT is from a high output rotating anode generator; CBCT can use a low energy fixed anode tube similar to dental panoramic machines.

2. CT scanners image patients in a series of axial plane slices that can be either stacked or form a continuous spiral motion over an axial plane; CBCT captures the image in one 360° rotation similar to a panoramic dental radiograph machine. Image data can be collected for the whole maxillofacial region or can be specified to capture a limited regional area of interest.
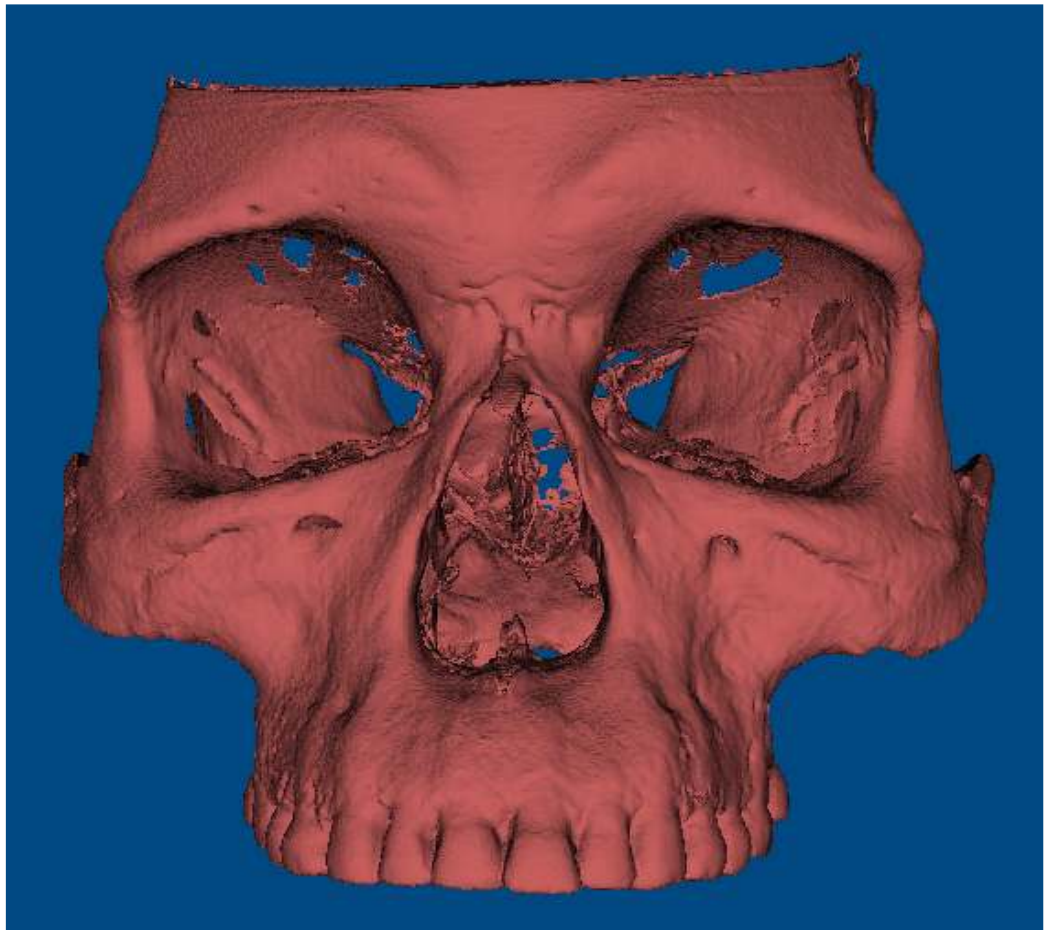
Figure 1.2   Image of a maxilla created using CBCT.

The CBCT machine includes a rotating gantry to which an x-ray source or projector and detector are attached. The x-ray source projects a cone-shaped beam of ionising radiation through the centre of the area of interest and is captured by a 2D flat panel detector on the opposing side. The gantry rotates once around the region of interest projecting and capturing between 150 to potentially more than 600 sequential planar projection images in the field of view and this action is normally completed within 10-30 seconds (Scarfe and Farman, 2008).

As in spiral/helical CT scanners CBCT information is digital, therefore advanced computer programmes construct a three dimensional volume from the 2D images captured. The term voxel is used in CBCT terminology as opposed to pixel. The voxel as previously mentioned is a unit of volume and not a 2 dimensional area. The image files created are in a DICOM system (Digital Imaging and Communications in Medicine); this is the universal format for 3D images in the medical field.

CBCT differs from that of conventional CT in a number of ways, some of which are regarded as advantageous and others as disadvantageous.

1.5.3.1   Advantages of CBCT over CT

- CBCT significantly reduces the dosage of harmful radiation to which a patient would be exposed. This is approximately 20% of a conventional CT device and which can equate to a full mouth periapical series (Mah e*t al.,* 2003b). However this depends on the setting selected and the particular model of CBCT device that is being used, but this can range from 29 μSv to 477 μSv compared with the conventional CT output of 2000 μSv (Scarfe and Farman, 2008).

- CBCT devices are significantly smaller and less expensive than conventional CT (Palomo *et al.,* 2006), this being approximately one quarter to one fifth of the cost (Scarfe and Farman, 2008).

- The projection images are captured in one single rotation of the device; therefore artefacts created by patient movement are significantly reduced (Scarfe and Farman, 2008).

- Depending on the type of CBCT device being used, the x-ray beam can be limited to the area of interest creating an optimum field of view (Scarfe and Farman, 2008).

- Images from the CBCT are created with a submillimeter isotropic resolution ranging from 0.076mm – 0.4mm. The images produced achieve a level of spatial resolution accurate enough to be measured for maxillofacial applications where a high level of accuracy in the three planes of x, y and z is paramount (Scarfe and Farman, 2008).

- CBCT imaging quality is comparable or in some cases even superior to conventional CT depending on the situation it is being used for, with CBCT having a higher spatial resolution (Al-Rawi *et al.,* 2010). Variability still exists between the different types of CBCT machines being used especially in depicting delicate structures within the maxillofacial region (Liang *et al.,* 2009).

1.5.3.2 Disadvantages of CBCT over CT

- CBCT images will produce more interference, creating a grainy effect. This is because CT has superior collimation of the exit beam; however this results in patients receiving a much greater dosage of radiation (White and Pharaoh, 2008a).

- CBCT does not provide an extensive range of contrast resolution compared to CT. Therefore CT imaging should be considered in situations where soft tissue detail is required e.g. for maxillofacial surgery (White and Pharaoh, 2008a).

- As with CT, CBCT suffers from some of the same problems in that it is not possible to reproduce an accurate representation of the occlusal surfaces of the teeth. When imaging patients using CBCT, any intra-oral metallic objects (e.g. restorations, jewellery, implants and orthodontic appliances) create streak artefacts (Nkenke *et al.,* 2004b; Sohmura *et al.,* 2005; Swennen *et al.,* 2009b). These artefacts can obliterate the occlusal surfaces of the images of the teeth, rendering the virtual model useless in predicting intercuspal relationship and orthognathic wafer construction (Uechi *et al.,* 2006).

- CBCT imaging with a flat panel detector (FPD) provides excellent spatial resolution; however the contrast resolution is compromised due to increased x-ray scatter.

- Compared with cone beam computed tomography (CBCT), CT images contain much less interference; there is also a substantially larger range of contrast resolution, which can display soft tissue information which is not available on CBCT (White and Pharoah, 2008a).

1.5.4 Magnetic resonance imaging (MRI)

Magnetic resonance imaging (MRI) was developed in July 1977 (Lewis *et al.,* 2008). MRI has similarities to CT in that it is a computer based cross- sectional imaging modality. However the principles of MRI differ from CT and conventional radiography as no harmful x-rays are emitted to generate the MRI image and the image can be obtained in any plane (Bearcroft, 2007; Strauss and Burgoyne, 2008).

MRI uses electromagnetic energy produced by a powerful magnet, radiowaves and computer analysis to produce images of soft tissues. A powerful magnetic field is generated which aligns the hydrogen atoms within the body. Radio waves are transmitted to alter this alignment causing the hydrogen to emit a weak radio signal that is amplified by the scanner (Tasaki and Westesson, 1993). MRI has equal resolution but much greater soft tissue contrast than CT scanning which allows a more detailed visualisation of the soft tissues (Strauss and Burgoyne, 2008). MRI can be extremely useful in dentistry for the evaluation of soft tissue abnormalities of the temporomandibular joint and for evaluating soft tissue disease (White and Pharoah, 2008). Therefore MRI is currently regarded as the gold standard for the imaging of soft tissue (Lewis *et al.,* 2008), but currently MRI is of limited value for the imaging of hard tissues.

1.5.4.1   Disadvantages of MRI

- MRI machines are large, expensive and noisy. To obtain an image normally takes several minutes (Strauss and Burgoyne, 2008).

- Patients often feel claustrophobic while in the gantry tube (Strauss and Burgoyne, 2008).

- MRI is contraindicated in pregnant women and in patients who have implanted metallic devices; however titanium implants are not a contraindication (Lewis *et al.,* 2008).

- MRI does not provide the natural photographic appearance of the texture of the facial surface (Ayoub *et al.,* 1998).

- MRI can produce distorted facial reconstruction due to artefacts created by metallic objects e.g. fillings, restorations and orthodontic brackets present within the oral environment (Ayoub *et al.,* 1998; Eggers *et al.,* 2005).

1.5.5 Ultrasonography

Ultrasonography is a technique that delivers a reflection picture by transmitting pulses of sound from a probe connected to a patient's skin through a gel. When the sound wave reaches a substance with a differentiation in density part of the wave is reflected back, it is detected as an echo by the probe (Hell, 1995). The duration of time for the echo to be detected is measured and the depth of tissue calculated. Three dimensional images are created by acquiring multiple cross sectional 2D images.

3D Ultrasonography is regarded as a relatively new imaging technique and has the advantages that it is relatively inexpensive, there is no patient radiation exposure, the patient is comfortable and the procedure is repeatable. Ultrasonography was mainly developed for foetal visualisation and diagnosis in obstetrics (Papadopoulos *et al.,* 2002), it has applications in maxillofacial surgery for diagnostic treatment planning as well as investigating temporomandibular disorders (Akizuki *et al.,* 1990; McCann *et al.,* 2000). The use of ultrasonography as an imaging technique for maxillofacial surgery planning is still at an experimental stage, and there are major problems associated with data acquisition, reduction and storage (Khambay *et al.,* 2002).

1.5.5.1   Disadvantages of ultrasonography

- Ultrasonography is able to provide the 3D coordinates of specific landmarks, but will not produce a 3D image (Hajeer *et al.*, 2002).
- Ultrasound images can present with artefacts and can be distorted. This can produce multiple and misleading false information.   The most common errors are the false-positive and false-negative images produced that can be so intense that they mislead the clinician in making a diagnosis (Papadopoulos *et al.*, 2002).
- The procedure is time consuming and requires a compliant patient as well as a highly skilled operator (Hajeer *et al.*, 2002).
- Ultrasonography is not able to visualise bone abnormalities (Bearcroft, 2007).
- Any head motion during data acquisition will introduce errors, and probe touching and depression of the patients skin may cause distortions of their spatial positions (Hajeer *et al.*, 2002).

1.5.5.2   Summary

Cone beam CT is widely regarded as the gold standard for acquiring hard tissue and is rapidly becoming a routine imaging modality specifically designed for the maxillofacial region.   CBCT scan technology has played a major role in the evolution of diagnostic imaging for dental and surgical applications.   The ability to visualise a patient's anatomy with an interactive 3D assessment eradicates any guesswork and allows clinicians to make accurate, informed, and educated decisions regarding treatment (Ganz, 2011).

At present CBCT is unable to achieve an accurate representation of the occlusal surfaces of the teeth and the interocclusal relationship which is essential for any virtual predictive surgical planning (Nakasima *et al.,* 2005; Swennen *et al.,* 2009b; Swennen *et al.,* 2009c). Imaging patients with intra-oral metallic objects using CBCT will create streak artefacts.   These artefacts impair any virtual model by obliterating the occlusal surfaces of the teeth.   This is a major obstacle for occlusal registration and the fabrication of orthognathic wafers to

guide the surgical correction of dentofacial deformities (White and Pharoah, 2008b).

1.6 Constraints of cone beam CT

The wide spread use of CBCT has rapidly expanded within the field of dentistry and maxillofacial surgery; however CBCT technology has limitations in relation to the cone-beam projection geometry, detector sensitivity and contrast resolution. CBCT is affected by artefacts, noise and poor soft tissue contrast; this produces an image that lacks clarity or renders it almost useless (Scarfe and Farman, 2008; Schulze *et al.,* 2010).

1.6.1 Artefacts

In CT any systematic discrepancy between the CT numbers in the reconstructed image and the true attenuation coefficients of the subject being scanned is referred to as an artefact. CT and CBCT images are more susceptible to artefacts than conventional radiographs because the image is reconstructed from over a million independent detector measurements. Reconstruction techniques assume that all the measurements are consistent; therefore errors of measurement will reflect themselves as errors in the reconstructed image (Barrett and Keat, 2004).

Artefacts can be classified into four categories:

1. **Physics-based artefacts:** X-ray beams are composed of characteristic photons with an array of energies. As a beam penetrates an object the beam hardens meaning the energy increases, since low energy photons are absorbed more readily that high energy photons. The effect of this can be the formation of cupping artefacts and streaks or dark bands between dense objects in the image.
2. **Scanner-based artefacts:** If one or more detectors is faulty or incorrectly calibrated this will result in a consistently erroneous reading at each angular position resulting in the formation of circular artefacts.

3. **Helical and Multisection CT artefacts:** These artefacts occur when anatomical structures rapidly change in depth; these artefacts are accentuated at higher pitches.

4. **Patient-based artefacts:** Patient movement and metallic artefacts are potentially the most disruptive artefacts affecting the head and neck region. Patient motion will create misregistration artefacts which appear as shading or streaking in the reconstructed images. Careful patient positioning and the use of aids is usually sufficient to prevent voluntary movement in the majority of patients. However some involuntary motion may occur during the scanning procedure, any motion related artefacts can be minimised using scan modes and software correction features that are installed on most CBCT scanners.

1.6.2 Metallic streak artefacts

Imaging patients using CBCT who possess intraoral metallic objects (e.g. restorations, jewellery, implants or orthodontic appliances) will significantly impede the x-ray beam and cause severe streaking artefacts (De Man *et al.*, 2000). This occurs because the density of metal is outwith the normal range that can be processed by the CBCT computer, resulting in incomplete attenuation profiles (Barrett and Keat, 2004), Figure 1.3.

The destructive effects of metallic objects present in the head and neck region and the degradation of the images as a result of these objects has been extensively described in previous literature (Lemmens and Nuyts, 2008; Nakasima *et al.*, 2005; Swennen *et al.*, 2009b; Swennen *et al.*, 2009c; Uechi *et al.*, 2006).

Prior to any CBCT image being acquired from a patient, it is recommended that protocols are adhered to, minimising the likelihood of metallic streak artefact interference, these include:

- Patients should always be asked to remove any metallic object that are likely to be within the FOV.
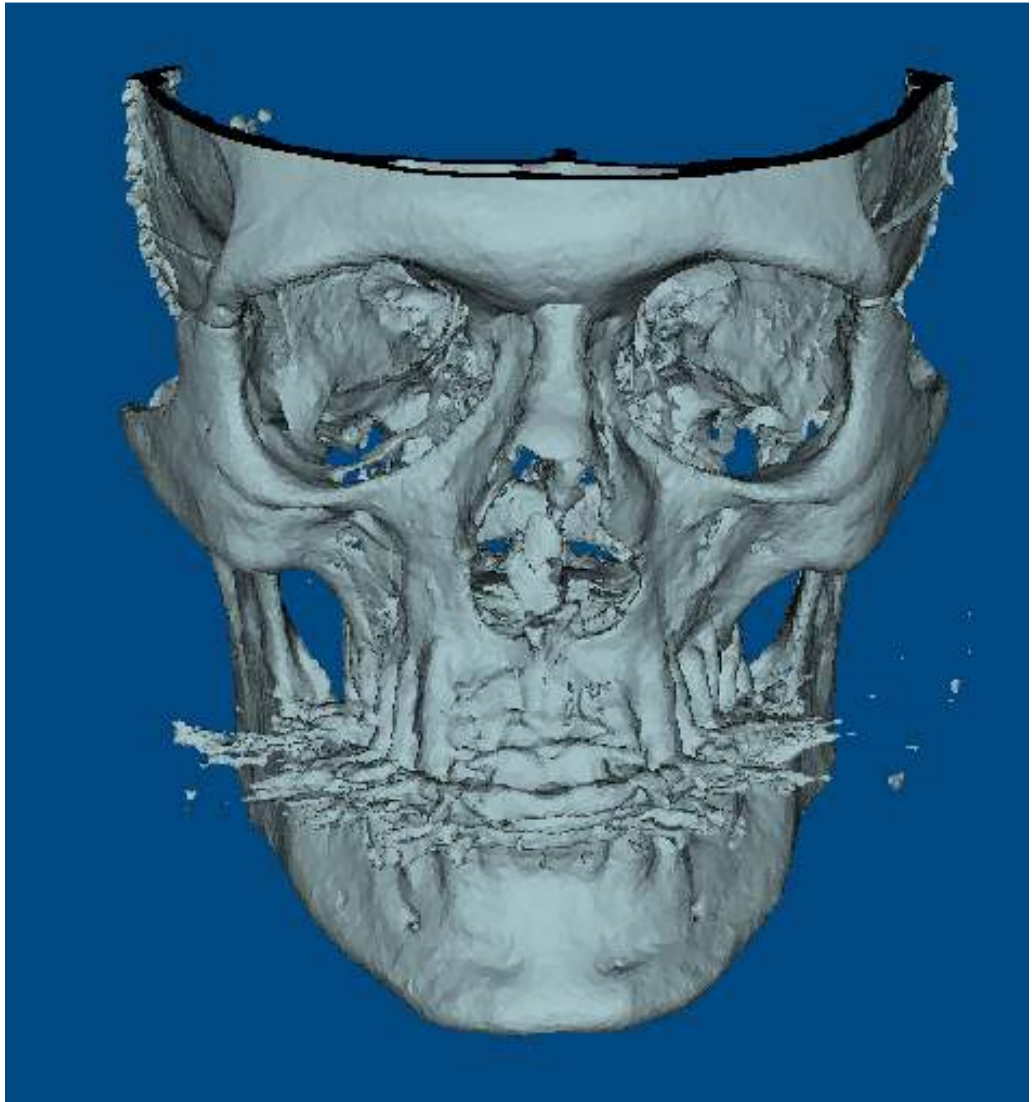
Figure 1.3   Image of a patient containing metallic restorations creating streak artifacts.

- If the metallic items cannot be removed ascertain whether or not a smaller FOV can be applied that may then limit the amount of metallic exposure.
- Increasing kilovoltage and applying settings that capture thinner sections may help penetrate objects; however this would result in exposing the patient to a higher dosage of harmful radiation.

The problem of metallic streak artefacts has been compounded by the fact that a greater number of people are retaining their natural dentition, with the assistance of metallic restorative materials (Odlum, 2001). Dental amalgam based filings and gold restorations are the most common form of material. Gold especially has a very high absorption of X-rays creating severe distortion of the CBCT images (Jakel and Reiss, 2007). The shape, size and density of the metal present has a significant influence on the severity of the artefacts (Lemmens and Nuyts, 2008).

1.6.3 Reduction / removal of metallic streak artefacts

A clean and accurate image of the dentition and the surrounding bone structures free from any artefacts is essential for the transition from current techniques of orthognathic planning and model surgery to a virtual environment, with the ultimate goal of producing an intermediate and final occlusal orthognathic wafer. In order to achieve this several techniques have been developed and can be categorised as:

- Metal artefact reduction (MAR) algorithms.
- Removal / masking metallic objects.
- Fusion of imaging techniques.

1.6.3.1 Metal artefact reduction (MAR) algorithms

The effects of metallic artefacts can be significantly reduced by applying specialised software correction or MAR algorithms (Abdoli *et al.,* 2010; Vannier *et al.,* 1997). These algorithms are computer adapted mathematical

calculations applied to raw data for the reconstruction of images and designed for the enhancement of soft tissue, bone and edge resolution.

Several studies have applied a variety of algorithms and techniques in order to reduce the degradation of images as a result of metallic objects present in the body (Bal and Spies, 2006; La Riviere and Billmire, 2005; Manglos *et al.,* 1995; Nakasima *et al.,* 2005; Zhang *et al.,* 2007).

A new technique of image conversion called the metal conversion method demonstrated through simulations that metal artefacts present in images could be reduced using the metal conversion method in conjunction with a MAR algorithm; however the current evaluation was limited to a visual analysis of a small set of simulations and measurements (Lemmens and Nuyts, 2008). A projection-correlation algorithm was developed that reduced the effects of metal artefacts by sequential substitution (MARSS). The corrupted portions of the projection data were substituted with corresponding portions from an unaffected adjacent slice. MARSS is conceptually simple, easy to implement and could effectively remove metal artefacts from the dental / maxillofacial region (Tohnak *et al.,* 2011).

An image that had been severely affected by metallic artefacts can have a maximum likelihood-expectation maximization (ML-EM) reconstruction algorithm applied. It was found that after 50 iterative correction cycles that only a few weak streak artefact images remained and the final image produced, depicted clear anatomical structures only marginally deviant from the original image without altering the size and shape (Kondo *et al.,* 2010).

Meilinger *et al.* (2009) presented a novel method for metallic artefact reduction for CBCT. They virtually replaced the metallic objects in the 3D volume with objects of identical geometry but with water like x-ray attenuation coefficient. They showed this technique significantly reduced the artefacts present in an image without loss of resolution, size or shape.

The final image that was produced with the application of MAR software and its variants were limited in that these algorithms made assumptions around the region of interest and could create other unwanted distortions (Park *et al.,*

2007), any streaking from metal present could be removed or suppressed this could result in an inevitable loss of detail around the metal-tissue interface (Barrett and Keat, 2004; Nkenke *et al.,* 2004b). Meaningful artefact reduction needs to have applied more sophisticated mathematical modelling of the physical image acquisition process rather than application of postprocessing of the erroneous results obtained from the algorithms currently in use (Schulze *et al.,* 2010).

1.6.3.2 Removal / masking metallic objects

A radical method of eliminating streak artefacts in CT-imaging of the head and neck region was tested by Odlum (2001). Six patients who were currently undergoing treatment for head and neck cancer and had previously been imaged with metal artefacts present on their images were selected. All metallic restorations present were removed and replaced with non-metallic composite resin restorations and the CT images recaptured, it was found that streak artefacts were completely eliminated in patients where a radiolucent composite material was used, however if a patient has metallic objects present such as retentive pins, stainless steel orthodontic brackets/wires and bone replacement implants this would be contra-indicated. It was suggested that head and neck cancer patients should be offered non-metallic restorations wherever possible. Replacing all metallic objects present would be the most effective and simplest technique to resolve the problem of metallic streak artefacts; however this is rarely possible or is impractical to achieve.

A study which aimed to reduce the effects of metallic objects by adding a silicone dental impression around the teeth was tested by Park *et al*. *(*2007). Four molar teeth were placed in two rows of two with a space of 50mm between the rows to simulate the average width of an adult male. In total six models were created, each with a different configuration of metallic bands, brackets and amalgams incorporated. Each model was CT scanned on a high resolution setting designed for bone. A standardised silicone dental shield was then added to each model around the teeth and the models were rescanned at the same settings. Any changes in the quality and quantity of artefacts was analysed using a picture archiving and communication system (PACS) software programme.

It was found that the models that were scanned without the shield created artefacts. The model with only orthodontic brackets added showed the least amount of distortion and the models containing amalgams produced larger and more severe artefacts. The addition of the silicone shield to the models successfully reduced the artefacts created. This was more apparent with the models containing amalgam.

The authors concluded that using a dental impression material to cover structures containing metallic objects could reduce the severity of artefacts created and this could have been the result of the transition between the metallic objects and air being less abrupt as a result of the density of the impression material. This technique could be useful in the reduction of artefacts, but it would be unlikely to produce an image of sufficient anatomical detail to be suitable for the production of an accurate dental surface.

1.6.3.3 Fusion of imaging techniques

None of the craniofacial imaging techniques currently available are capable of simultaneously capturing facial soft tissues, the facial skeleton and dentition at an optimal quality for use. This could only be achieved by the successful fusion of images made by different methods (Plooij *et al.*, 2011).

Image fusion is the process of generating a single image from multiple images using different imaging modalities and aligning them using a mathematical algorithm e.g. Iterative Closest Point or Iterative Corresponding Point (ICP). A more accurate depiction of an object can be obtained than would be possible from any single imaging modality.

It is possible to fuse three dimensional data using one of three methods:

- **Surface based matching:** Uses homologous geometric features, such as surfaces (Gabrani and Treiak, 1998).
- **Point based matching:** Involves identifying common landmarks between the images which superimpose the two images (Khambay *et al.*, 2002).
- **Voxel based matching:** Uses congruent voxels from a manually selected region (Plooij *et al.*, 2011).

1.6.3.4   Iterative closest point registration

Iterative Closest Point or Iterative Corresponding Point (ICP) is an accurate and reliable algorithm that has become the dominant method for aligning three dimensional models based purely on the geometry and sometimes the colour of meshes. The ICP algorithm is widely used for registering the output of 3D scanners, which typically only scan an object from one direction at any one time.

ICP starts with two meshes and an initial assumption of their relative rigid-body transformation and then iteratively (repeatedly) refines the transformation by repeatedly generating pairs of corresponding points on the meshes which are minimising any metric error. For each iteration, the ICP algorithm computes correspondences by finding their closest points, and then minimises the mean square error in the position between the correspondences. A good initial estimate of the transformation is required, and all the scene points are assumed to have correspondences on the model.

The ICP algorithm is of a very generic nature which leads to problems with convergence when the initial misalignment of the data is large (i.e. over 15 degrees). The impact of this limitation can be reduced through the use of pre-processing stages. Distinctive facial features such as the nose or the eyebrows can be accurately located and used to give a general estimate of that alignment (Ayoub *et al.,* 2007).

1.6.4 Fusion of dentition and the human skull

Several methods for replacing the virtual dentition acquired by CT, MSCT or CBCT to create a composite model have been described Table 1.1

Gateno *et al. (*2003) described a technique that incorporated an accurate representation of the dentition and merged it with a 3D model of the bone to create a composite virtual skull.

A single human skull with a complete dentition was selected and a radiolucent impression tray capable of acquiring upper and lower impressions simultaneously

Authors	Title of Paper	Registration Technique	Method of Analysis
E Nkeenke, S Zachow, M Benz, T Maier, K Veit, M Kramer, S Benz, G Hausler, F Wilhem Neukam & M Lell	Fusion of computed tomography data and optical 3D images of the dentition for streak artefact correction in the simulation of orthognathic surgery	Simple surface fusion	Absolute mean of corresponding data points
G.R.J. Swennen, W. Mollemans, C.D. Clercq, J. Abeloos, P. Lamoral, F. Lippens, N. Neyt, J. Casselman & F. Schutyser	A Cone-Beam computed tomography triple scan procedure to obtain a three-dimensional augmented virtual skull model appropriate for orthognathic surgery planning	CBCT triple scan	Euclidean distance between corresponding landmarks
J. Gateno, J. Xia, J.F. Teichgraeber & A. Rosen	A new technique for the creation of a computerized composite skull model	Extra-Oral Fiducial markers	Absolute mean between physical and virtual measurements
J. Gateno, J.J. Xia, J.F. Teichgraeber, A.M. Christensen, J.J. Lemoine, M.A.K. Liebshner M.J. Gliddon & M.E. Briggs	Clinical feasibility of computer-aided surgical simulation (CASS) in the treatment of complex cranio-maxillofacial deformities	Extra-Oral Fiducial markers	None
T. Sohmura, H. Hojoh, N. Kusumoto, M. Nishida, K. Wakabayashi & J. Takahashi	A novel method of removing artefacts because of metallic dental restorations in3-D images of jaw bone	Extra-Oral Fiducial markers	Absolute mean of misfit volume
J. Uechi, M. Okayama, T. Shibata, T. Muguruma, K. Hayashi, K. Endo & I. Mizoguchi	A novel method for the 3-dimensional simulation of orthognathic surgery by using a multimodal image-fusion technique	Extra-Oral Fiducial markers	Route mean squared distance between fiducial markers
F. Schutyser, G. Swennen & P. Suetens	Robust visualization of the dental occlusion by a double scan procedure	Intra-oral Fiducial markers	Absolute mean error of Euclidean distance
G.R.J. Swennen, E.L. Barth, C. Eulzer & F. Schutyser	The use of a new 3D splint and double CT scan procedure to obtain an accurate anatomic virtual augmented model of the skull	Intra-oral Fiducial markers	Absolute mean error using analysis of variance
G.R.J. Swennen, M.Y. Mommaerts, J. Abeloos, C. De Clercq, P. Lamoral, N. Neyt, J. Casselman, F. Schutyser	A cone-beam CT based technique to augment the 3D virtual skull model with a detailed dental Surface	Intra-oral Fiducial markers	Absolute mean error of Euclidean distance

Table 1.1   Image fusion registration techniques

was modified with the addition of four radiopaque markers. Impressions were taken of the upper and lower arches simultaneously. The impressions were then laser scanned and the resulting data was inverted to create a positive representation of the dental arches with the markers. The impression was then refitted onto the skull and rescanned. The teeth from the 3D CT skull were then virtually removed leaving the radiopaque markers. The laser scanned image of the teeth was then inserted into the 3D skull using the markers for alignment and the markers were then removed to create the final 3D skull.

The authors proved that it was possible to merge two different forms of image modality to create one accurate model that was an accurate representation of the bony structures and a detailed image of the dentition that would also be free from any form of metallic artefacts. All the measurements recorded supported the method of using markers as points of reference and this was regarded as highly accurate. This could mean that it is potentially possible to undertake presurgical planning on a PC without the need for gypsum based study models.

The technique was successful in accurately replacing the dentition; however this was essentially a case study and the technique had not been adapted for patient usage and it was apparent that the position of the radiopaque markers would be uncomfortable for the patient and would distort the surrounding soft tissues (Gateno *et al.,* 2003).

Gateno *et al*. (2007) adapted the technique for the clinical environment. Five patients with craniomaxillofacial deformities had their treatment planning predicted using Computer-Aided Surgical Simulation (CASS). This proved to be successful with the computer generated surgical splints and templates transferred to the patient in the operating room. However the modifications of the technique did not address the problem of patient comfort and soft tissue distortion.

Nkenke *et al*. (2004b) merged two different modalities of 3D imaging to eradicate streak artifacts in order to facilitate virtual osteotomy planning. Five upper and five lower gypsum dental casts were randomly selected. The models

were all scanned using a spiral CT scanner and the data recorded in stereolithographic format (STL). Using an optical 3D sensor the models were scanned and the data saved in an STL format. The casts then received occlusal amalgam restorations and were re-captured in 3D using the CT scanner and a 3D optical scanner. The CT scan and the 3D scan of the models with no restorations were initially aligned and then the alignment refined using the iterative closest point (ICP) algorithm *(Points were regarded as corresponding when the distance between the points was no greater than 1mm)*. This procedure was then repeated using the virtual models that had restorations present.

In the second part of the study a single patient received a CT scan of the maxilla and mandible and impressions of the teeth were taken and cast in gypsum. The models were scanned using the optical 3D scanner and the data was fused with the CT data and a virtual osteotomy was simulated.

The results of merging the two modalities of CT and 3D scan of the dental models ranged from:

- 6494.0 ± 1621.6 points with a mean distance of 0.1262mm ± 0.0301mm on the dentitions with no restorations. (*No statistical difference P =0.605*, **61%**).
- 6676.4 ± 1417.9 points with a mean distance of 0.2671mm ± 0.0580mm on the dentitions with restorations. (*Statistical difference P < 0.005*, **0.05%**).

Merging the two modalities of CT of the patient and 3D scan of the models:
- **Mandible** a mean error of 0.66mm ± 0.49mm *(44% below 0.5mm)*.
- **Maxilla** a mean error of 0.56mm ± 0.48mm *(54% below 0.5mm)*.

The authors demonstrated a technique that merged the two modalities of CT data and 3D sensor data; although the mean distance was significantly increased to 0.2671mm ± 0.0580mm with metallic restorations they believed that the accuracy was still acceptable to produce virtual planning of the post- operative occlusion, for training purposes, simulation of patient cases and the production of surgical splints and should therefore be regarded as a standard procedure in orthognathic surgery simulation.

It was initially determined that a 1mm discrepancy between the two imaging modalities was acceptable when applied to images with no metallic restorations present. This was then reduced to 0.5mm for an initial fine alignment of images that did possess restorations. This level of inaccuracy would not be considered as acceptable in a clinical environment (Ayoub *et al.,* 1998).

A study to remove the damaged dentition of jaw bone images and substitute it with dental cast models obtained by CT was devised by Sohmura *et al. (*2005). Four patients were recruited to participate in the study with varying dental anomalies. One patient had no metallic restorations present and the other three all possessed metallic restorations. Each of the four patients received CT scans with a devised interface in situ. The interface consisted of an acrylic resin impression or bite wafer that could be securely fitted in the patient's mouth with the addition of a gypsum marker plate. Impressions of the patient were acquired and cast to create study models, the interface was fitted to the models and this was then scanned using CT.

DICOM images produced were converted in to 3D images with the use of specialised software; the images of the marker plate in situ on the patients were fitted to the images of the marker plate on the dental casts. Any areas of the image that were affected by artefacts were removed and replaced with images of the dental casts and fused.

The position between the virtual dentition of the patient and the dental casts was examined in the patient that did not posses any metallic restorations. The accuracy of the registration was calculated and shown to have an error of 0.25mm and it was concluded that this would be acceptable for clinical application. The difference between the images of dental casts and the dentition of patients which contained metallic restorations and therefore streak artefacts was not acceptable due to the defective images.

The technique was successful in modifying CT images and replacing the distortions with dental casts through the use of a custom made interface. It is unclear why the authors regarded 0.25mm as a clinically acceptable value and only the case of the patient not having metallic restorations was used to

calculate the accuracy which may not accurately reflect the results of the cases that did posses metallic restorations. The size and positioning of the interface would be difficult to stabilise as well as any distortion of the surrounding soft tissue (Sohmura *et al.,* 2005).

A multi-scan CBCT procedure to enhance 3D virtual images was developed by Swennen *et al. (*2009b) to produce a virtual model with a more detailed representation of the occlusal surfaces and interdental data areas. Ten patients who were already attending for orthognathic appointments were recruited to participate. Each patient had measurements recorded of the height of the lower facial profile and the freeway space and a wax bite was taken in the centric position and measurements were again recorded to ensure that there was no change in the height of the lower facial profile and the freeway space. Impressions of the upper and lower arches were taken simultaneously followed be a triple scan procedure.

Scan 1: The patient was scanned in the sitting position using a CBCT scanner with the wax bite in position.

Scan 2: The impression tray was then re-inserted back into the patient's mouth and another scan using the CBCT was taken with a smaller field of view.

Scan 3: The impression was then removed and scanned on its own with CBCT at the highest resolution setting available and all three images were saved in a DICOM format.

Maxilim software was used to align all three images and the second and third scans were combined with the initial scan to create a detailed occlusal surface of the teeth with intercuspal data of the upper and lower arches.

The technique proved to be highly accurate, stable and comfortable for patients and relatively simple to apply, it was suggested that this should be applied for routine orthognathic surgery planning. However this technique exposes a patient to an increased dosage of harmful X-rays because of the necessity to receive two CBCT scans.

A double CBCT scan procedure with the introduction of a modified bite wafer to augment the 3D virtual skull model was described by Swennen *et al*. (2009). Ten patients who were already attending for orthognathic appointments were recruited to participate. Each patient had a modified wax bite wafer taken that recorded the dentition in a centric occlusion. The wafer was hardened intraorally and additional gutta percha markers were incorporated bucally for point based rigid registration purposes. Upper and lower impressions of the dentition were taken and the modified wafer was fitted back into the patient's mouth and a CBCT scan acquired.

The wafer was then removed and the impressions and the wafer were scanned using a CBCT on a higher resolution and the images of the patient, impressions and wafer were stored using a DICOM format. Virtual models were created from the impressions, and the tooth structures digitally extracted and occluded with the virtual image of the wafer using surface-based rigid registration and ICP. Then the virtual occluded arches aligned to the patient's skull by rigid-based registration at the centre of the virtual gutta percha markers.

The results of the study showed that it is possible to combine a CBCT scan of a patient with a CBCT of impressions of the upper and lower arches with a modified wax bite; however it was unclear how much working time was available before the wax wafer would distort in the patients mouth and a significant number of the gutta percha markers could not be used because they touched the patient teeth and were submerged in artefacts. Another significant disadvantage of this technique was the clinical workload and computing time to conduct each stage, this would be impractical and too time consuming for introduction into a clinical routine (Swennen *et al.,* 2007a; Swennen *et al.,* 2009; Swennen *et al.,* 2009c).

A double scan technique using a virtual 3D splint in order to obtain a detailed anatomic 3D virtual model of the skull was introduced by Swennen *et al*. (2007b). Ten human dry cadaver skulls with intact dentitions were obtained on which to conduct the experiments. Alginate impressions were taken of each dentition and gypsum dental casts produced. A rigid acrylic splint was fabricated for each skull with a pyramidal extension mounted anteriorly and

twelve spherical gutta percha markers were incorporated. The splints were firmly attached to each skull and a CT scan was acquired. The splints were then removed from the skulls and attached to their corresponding dental cast and a high resolution scan was acquired of each model. All scans were recorded in DICOM format and reconstructed using viewing software.

The virtual 3D splint was used for rigid registration to facilitate fusion of both CT datasets. An automatic rigid registration procedure was carried out on the gutta percha markers that were incorporated in the splint. This technique produced a 3D virtual augmented model of the skull with an accurate detailed dentition and interocclusal relationship.

The same procedure was used by Schutyser *et al*. (2005); however this technique had the significant disadvantage that soft tissue especially around the pyramidal extension would distort the surrounding soft tissues and depending on the severity of the artefacts present a significant number of the gutta percha markers which were likely to be submerged and unusable because of the nature of the horizontal streak artefacts (Swennen *et al*., 2007b; Swennen *et al*., 2009a).

A novel 3D simulation for planning orthognathic surgery, incorporating a multi-model image fusion technique was developed by Uechi *et al*. (2006). A virtual skull generated from CT was automatically integrated and fused with the corresponding dental casts scanned by laser. This was achieved using point-based rigid registration fiducial markers. Two female patients who had previously attended the Orthodontic Division, Dental Hospital, Health Sciences, University of Hokkaido and had received pre operative orthodontic treatment were recruited to participate in the study. Each had a horseshoe shaped reference splint constructed from a silicone impression material with three bucally placed ceramic balls attached as fiducial markers. The splints were fitted to the dentition of each patient and a CT scan acquired and stored in DICOM format. Alginate impressions were then taken of the upper and lower dentition in both patients and cast using a die stone. The splint was then fitted to the dental casts and laser scanned to capture the 3D images of the dental casts and splint. Both the images captured by CT and laser scanning were

reconstructed using 3D visualising software and the images of the skull and models were fused by point-based rigid registration on the fiducial markers.

The precision of fusion will always be dependent on the quality of the imaging modalities. The authors concluded that their technique could be used to precisely realise the presurgical and postsurgical occlusal relationships and the morphology of patients with severe skeletal deformities.

The major disadvantages of this technique was that it was extremely complicated and difficult to reproduce and the presence of the ceramic fiducial markers could distort the patients soft tissue and the markers would be obscured if severe streak artefacts were present (Uechi *et al.*, 2006).

1.6.4.1   Summary

Swennen *et al. (*2009) stated that current literature clearly indicates a paradigm shift towards 3D imaging and 3D fusion dominating the fields of orthodontics and maxillofacial predictive orthognathic surgery. This now enables the development of unprecedented virtual diagnosis, treatment planning, and evaluation of treatment outcomes for maxillofacial deformities.

Imaging patients, using CBCT, is complicated by intra-oral metallic objects which will create streak artefacts. These artefacts impair any virtual model by obliterating the occlusal surfaces of the teeth. This is a major obstacle for occlusal registration and the fabrication of orthognathic wafers to guide the surgical correction of dentofacial deformities. A new image fusion method is described and evaluated in this thesis that has been developed to replace the inaccurate occlusal surfaces of the teeth of the CBCT image with an accurate image utilising currently available dental materials, without any distortion of the surrounding soft tissues. It is inexpensive and does not expose the patient to any addition harmful radiation.

Chapter Two

Aims and Objectives

Aims

2.1 Aims

- To develop a method for the replacement of the distorted dentition from Cone Beam Computed Tomography (CBCT) scans with an accurate digital representation.

- To assess the accuracy and reproducibility of the developed method using cadaveric skulls.

- To assess the feasibility of the developed method for orthognathic surgery patients.

Chapter Three

Materials and Methods

Materials & Methods Part 1

3.1 Study design

The aims of part 1 of the study were to validate the accuracy of images captured using CBCT compared to those obtained by a laser scanner and ascertain whether or not they were interchangeable. This was followed by replacing the virtual dentition in dry cadaveric maxillae and mandibles with corresponding dentitions obtained from gypsum study casts with the aid of a custom made intra-oral reference device.

3.1.1 Laser scanning of mandibles

Six full dentate dried cadaver mandibles with no metallic restorations present in the dentition were obtained from the anatomy department at Glasgow University. Each mandible had wax (Anutex modelling wax, Bracon limited, East Sussex, UK) built-up around the labial, buccal and lingual aspect to replicate soft tissue, Figure 3.1.

Each mandible was scanned using a NextEngine desktop 3D scanner and Scanstudio software (NextEngine, California 90401). The scanner was accurate to 0.005mm. This was regarded as the gold standard for capturing a 3D image of the mandibles. Prior to each mandible being scanned the system was calibrated using the automated calibration process, in accordance with the manufacturer's instructions.

To reduce reflection each mandible was sprayed with an inert white powder (Ardrox 9D1B, Chemetall PLC, Bletchley, Milton Keynes). Each mandible was secured to the multidrive turntable and laser scanned using the Standard Definition (SD) setting, Figure 3.2. The images were then auto aligned and fused to create a single complete image, then exported as a binary Standard Tessellation Language (STL) file, Figure 3.3.

Figure 3.1   Labial/Buccal aspect of mandible with wax in position to replicate soft tissue.

Figure 3.2 Next Engine HD laser scanner and multidrive automated turntable with mandible attached.
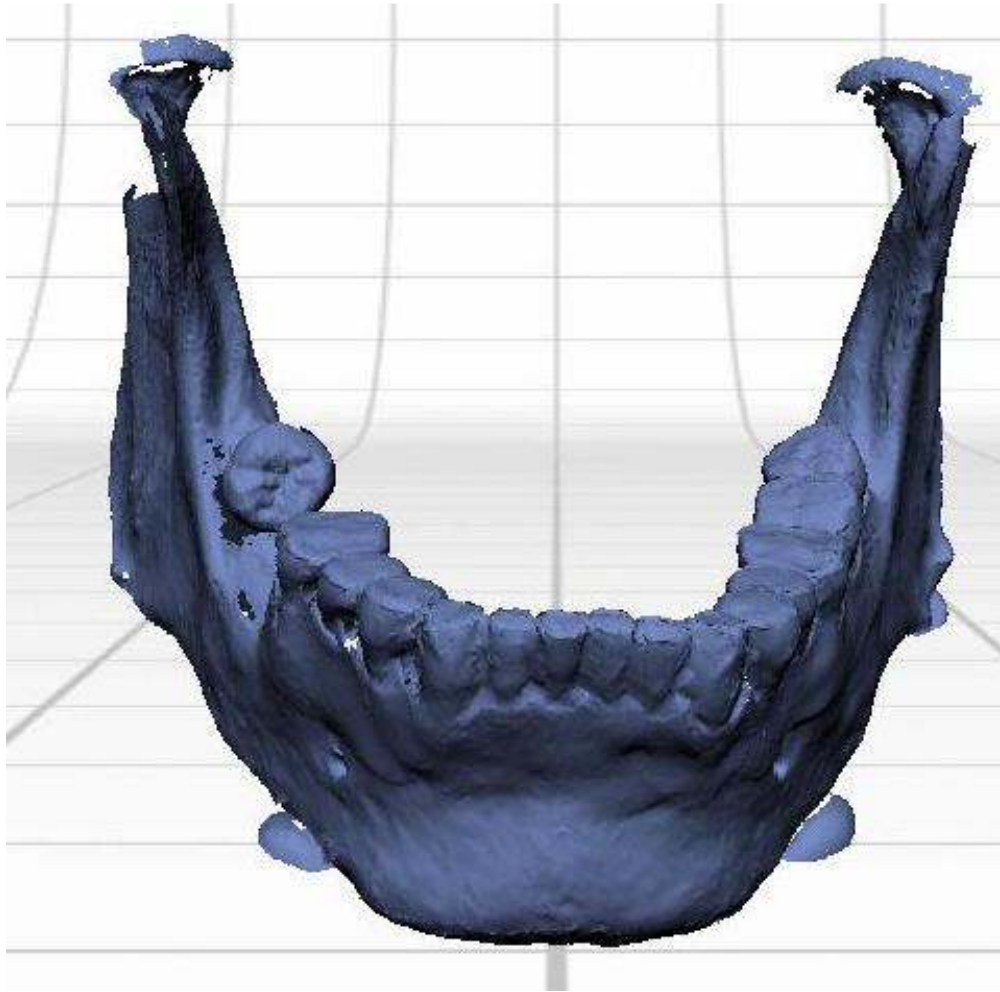
Figure 3.3   Auto aligned fused laser image of mandible.

3.1.2 CBCT scanning of mandibles

The Classic i-CAT Cone Beam 3-D imaging system (Imaging Sciences International, Warple Way, London) located within the radiology department of the University of Glasgow, Dental Hospital and School was used for acquiring CBCT images of the 6 mandibles.

Each mandible was positioned in the centre of the field of view (F.O.V.) and scanned on a radiolucent base, Figure 3.4. A 0.4mm isotropic voxel scan was acquired, producing a 10cm image which took 20 seconds to complete; this was the routine resolution for the acquisition of patient data. The images were exported in a Digital Communication in Medicine (DICOM) format.

3.1.3 CBCT image conversion

To enable the DICOM images to be manipulated within the software package VRMesh Studio (VirtualGrid, Seattle City, Washington) they were converted into a surface mesh using the imaging visualisation and processing software package MeVisLab (MeVis Medical Solutions AG, Bremen). An image processing pipeline was followed Figure 3.5, where each individual software module was connected as necessary to another to create an internal network which enabled the DICOM file to be transformed to a Binary STL file.

3.1.4 Comparison of laser and CBCT images of the mandible

Each of the mandible laser scanned images was imported into VRMesh software together with the corresponding CBCT using the common file format (STL), Figure 3.6. The images were initially registered manually by selecting landmarks present on both images using the following landmarks right mental foramen, left mental foramen and the mental protuberance. The registration process was further refined using the appropriate function within VRMesh; which relied upon the iterative closest point (ICP) algorithm. The distances between the two surface meshes were measured using the inspection between objects function. If they were perfectly aligned the distance between them would be zero and any deviations would be displayed in a histogram chart, Figure 3.7.

Figure 3.4   Mandible positioned within the centre of the
F.O.V.
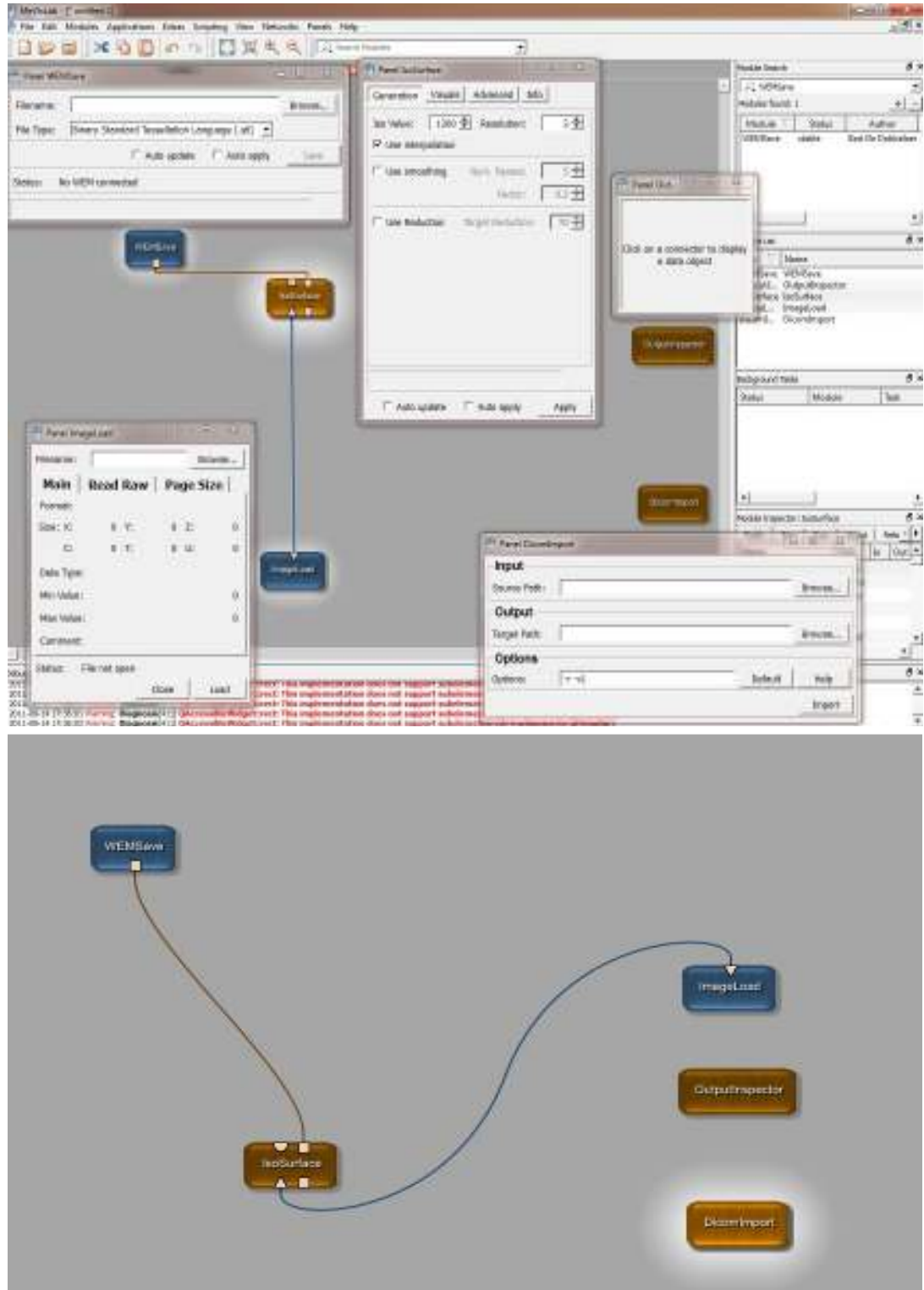
Figure 3.5   Image processing pipeline.

Figure 3.6   Laser image (Yellow) and CBCT Image (Red) imported into VRMesh.
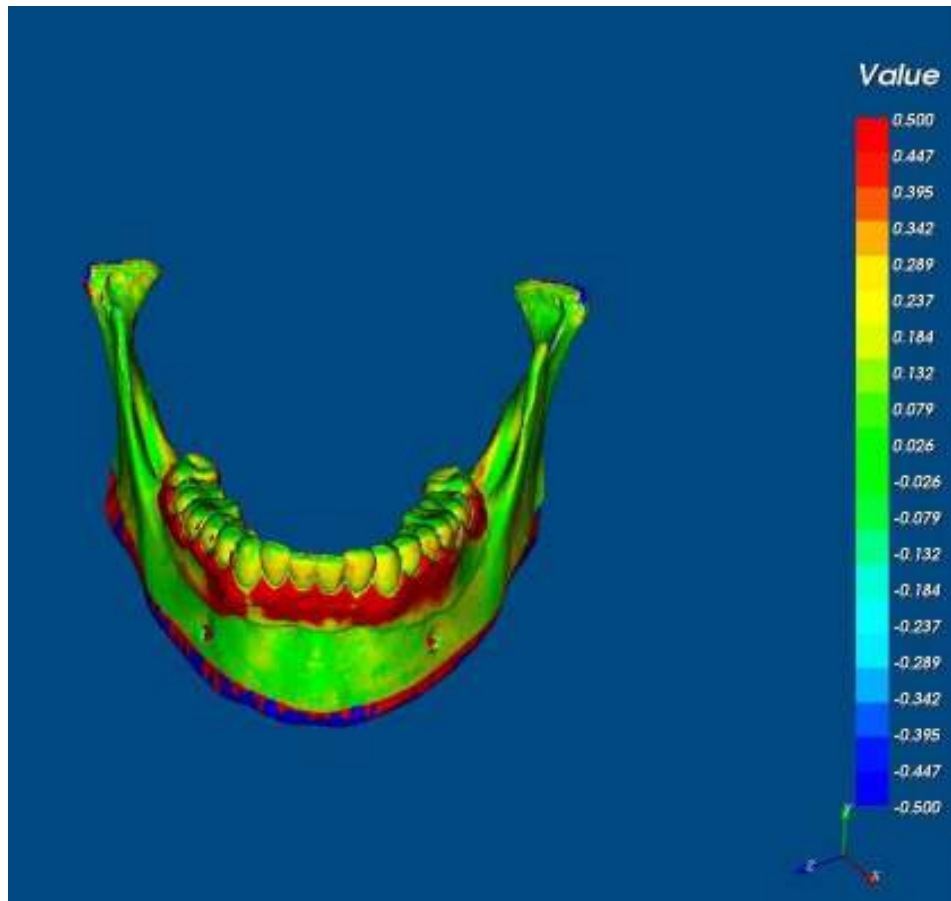
Figure 3.7   Colour error map displaying deviations between CBCT and laser meshes.

3.1.5 Comparison of laser and CBCT images of the mandibular dentition

To eliminate the influence of dentition in determining the accuracy of bone images acquired from laser scanning and CBCT at 0.4mm voxels, the dentition for each mandible was deleted from the CBCT scan image and the remaining "skeletal image" was saved as an individual STL file. In order to assess whether any distortion of the dentition had occurred during CBCT scanning the CBCT skeletal image was then re-imported into VRMesh and aligned with its corresponding laser scanned image, ensuring that the laser image was marked as the source object and the CBCT skeletal image was the target Figure 3.8. The images were then registered manually using specific landmarks present in both images including, right mental foramen, left mental foramen and the mental protuberance, Figure 3.9. The dentition was not present on the CBCT images and could therefore not be used during the alignment procedure. The CBCT skeletal image was then deleted and the original CBCT image with the dentition was imported. All information below 2-4 mm of the incisal edges and the first permanent molars was removed leaving only the incisal edges and occlusal surfaces of the CBCT and laser images Figure 3.10. The images were then analysed using the inspection between objects function and any deviations were displayed in the histogram chart. Figure 3.11.

3.2   Can the distorted dentition on a CBCT scan be accurately replaced?

3.2.1 Construction of the intra-oral transfer device

Alginate impressions of the dentition of the six dried cadaver mandibles were taken (Xantalgin, Heraeus Kulzer, GmbH, Hanua, Germany) using a standard impression stock tray (Orthocare, Bradford, West Yorkshire) Figure 3.12. Each impression was cast using a class III gypsum product (JW superyellow, John Winter &Co LTD, Halifax, England). The models produced were trimmed to create a working cast on which the acrylic appliances were constructed.
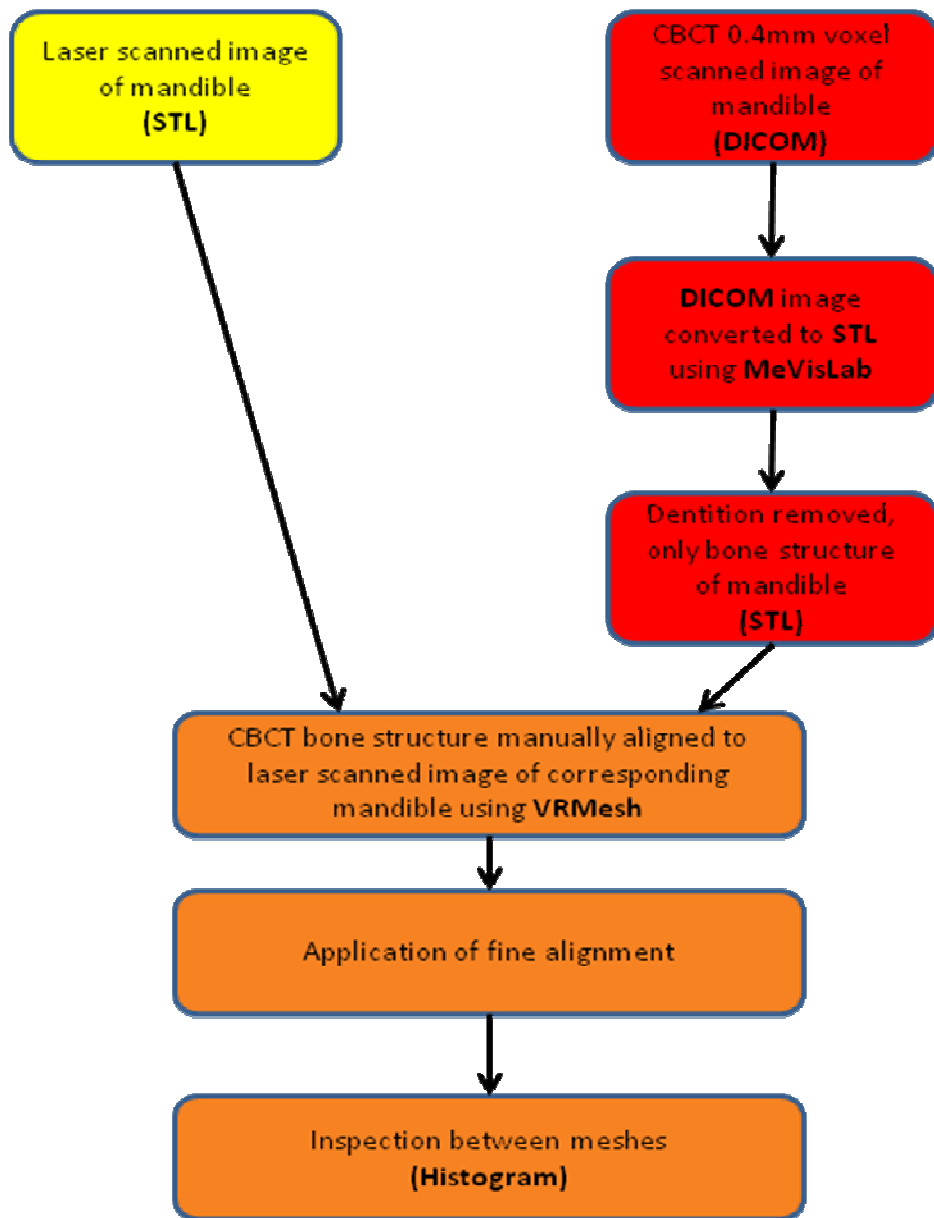
Figure 3.8 Bone structure acquired from laser scanning registered with the corresponding bone structure acquired from CBCT 0.4mm voxels.

Figure 3.9   Mandibular image with the dentition deleted and
anatomical points selected.
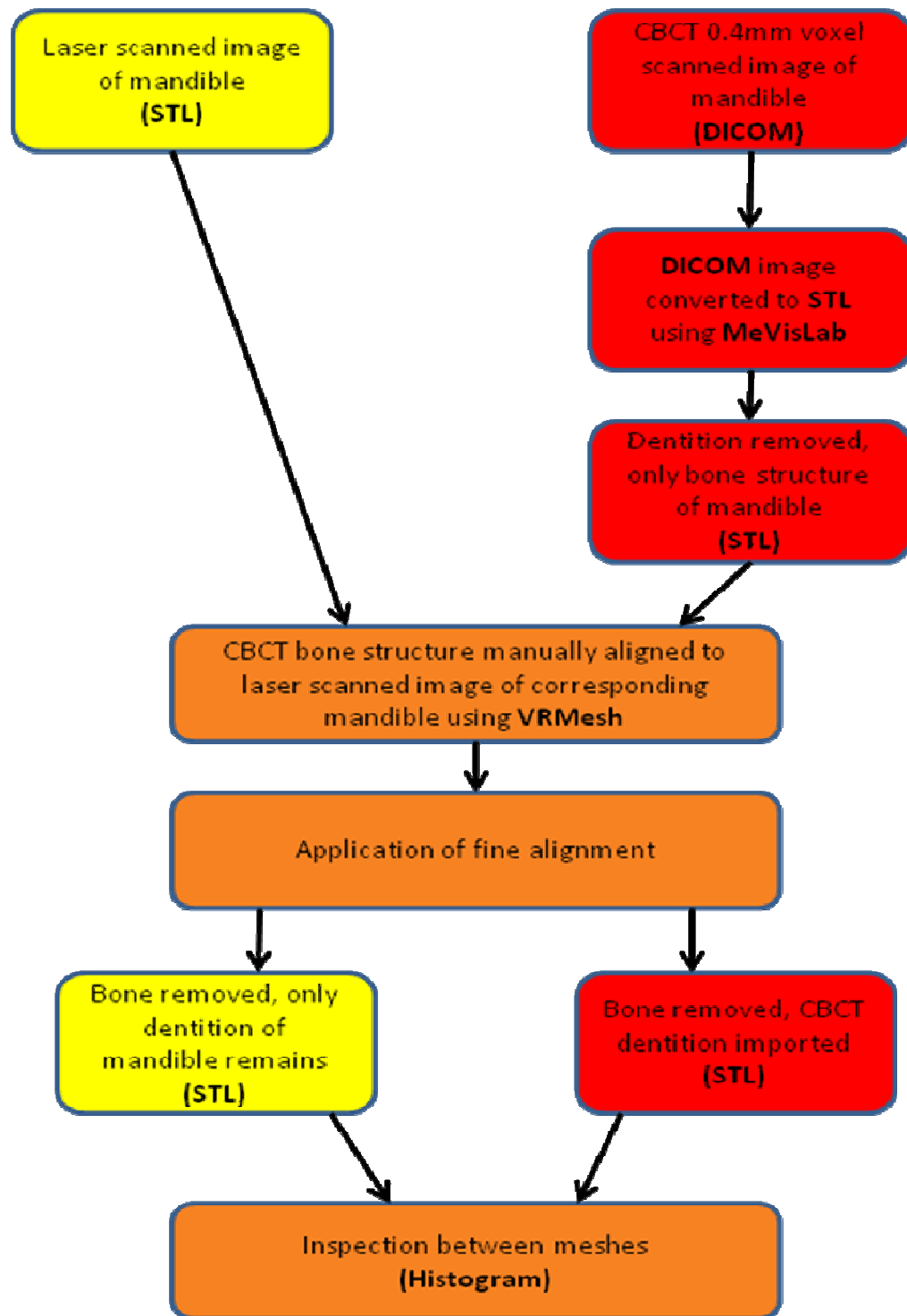
Figure 3.10 Pipeline to produce the positioning of the dentition as a result of bone structures, without the influence of the dentition.
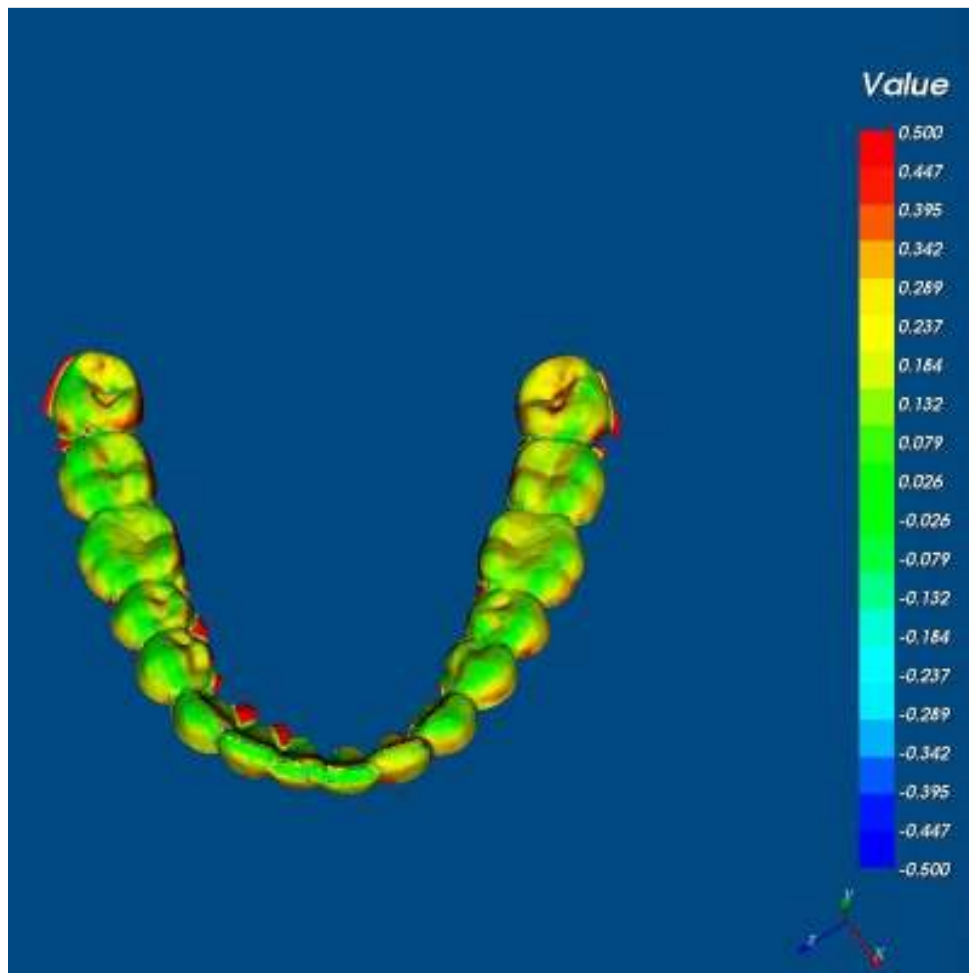
Figure 3.11 Colour error map displaying deviations between the meshes of the laser and CBCT images of the dentition aligning on only the skeletal structures.

Figure 3.12 Alginate impression of mandible.

A hexagonal die was hand crafted from modelling wax and was duplicated using silicone (Dublisil 15, Dreve Dentamid GmbH, Unna, Germany); this produced a master mould from which three hexagonal markers were produced for each of the acrylic appliances. The markers were cast using a grey super hard class IV stone (Sherahard-rock, John Winter &Co LTD, Halifax, England). Several colours were initially trialled and grey was found to be the most suitable in order for the laser scanner to capture the best detail.

The same working models were coated in a separation medium (Metrocryl plaster coating solution, Metrodent Limited, United Kingdom) and a lingual baseplate was constructed using orthodontic cold cure acrylic (MP2, Ortho-Care (UK) Ltd, Bradford, West Yorkshire). The acrylic was applied and processed in accordance with the manufacturer's instructions. The appliance was trimmed and polished so that acrylic would be tooth borne but not interfere with the occlusal or incisal detail of the dentition.

The three hexagonal plaster markers were then embedded into each of the upper and lower acrylic baseplates, Figure 3.13. For the lower appliance one marker was situated directly below the lower central incisors ensuring that it did not interfere with the lingual frenum. The other two markers were situated just below gingival margin of the first permanent molars on the left and right. The markers were then coated with a dental varnish (Copaliner, Dental A2Z Ltd, Blair Athol, Pitlochry, Perthshire) to seal them against the oral environment. The completed acrylic appliances were then securely attached to each of the cadaver mandibles. The mandibles were then laser scanned and CBCT scanned as described in section 3.1.1.

Figure 3.13 Gysum registration markers embedded in acrylic baseplate.

3.2.2 Comparison of laser and CBCT 0.4mm voxel scanned images of the hexagonal plaster markers

To establish the differences between images of the hexagonal plaster markers acquired using a laser scanner and a CBCT 0.4mm voxel scan. The STL image of each mandible with the acrylic appliance in-situ was captured by the laser scanner and imported into VRMesh. The three markers on each mandible were isolated and all other information were deleted Figure 3.14. The remaining image was saved as a new separate binary STL file. The process was repeated for each mandible with the appliance in situ and captured scanned using CBCT at 0.4 mm voxel. The image of the markers from the laser scan was then re-imported into VRMesh along with the images captured by the CBCT. The image captured at 0.4 mm voxel was manually aligned and then refined using ICP Figure 3.15. The distance between the meshes was displayed as before Figure 3.16.

3.2.3 Comparison between laser and CBCT 0.2mm voxel images of plaster dental models

Laser and CBCT 0.2mm voxel images of dental casts were compared. This was to assess if CBCT could reproduce accurate and detailed images comparable to laser scanned images.

Alginate impressions of the six mandibles with the intra-oral transfer device in situ were taken. These were cast using the class III gypsum product to create study casts with the transfer device in position. Each model was scanned using the Nextengine laser scanner and exported as a STL file.

The same models were then scanned using the CBCT at a resolution of 0.2mm voxel; these images were exported as a DICOM file then converted to a STL format using MeVisLab. Each virtual model captured using the laser scanner was imported in to VRMesh. Similarly those models acquired using CBCT were also imported using the same software Figure 3.17. Corresponding landmarks were identified on each image and manual rigid alignment was initially applied followed by fine alignment Fig 3.18.
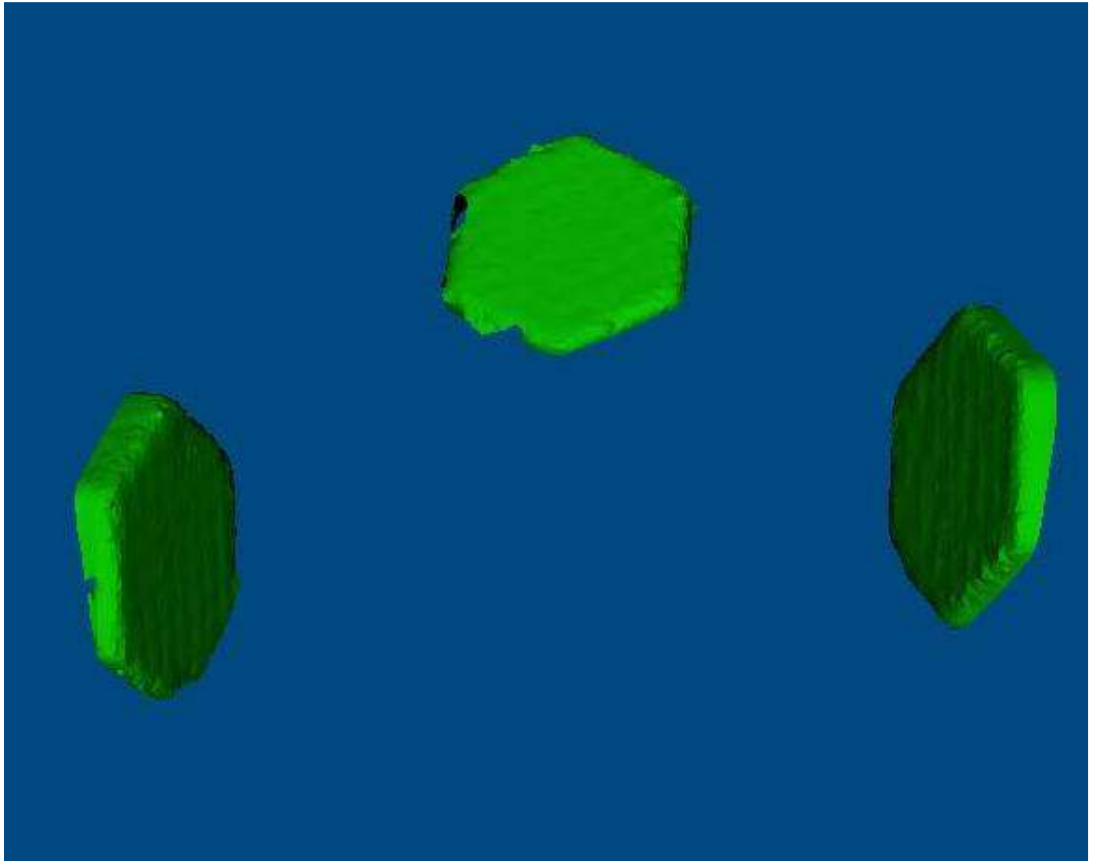
Figure 3.14 Hexagonal registration markers.
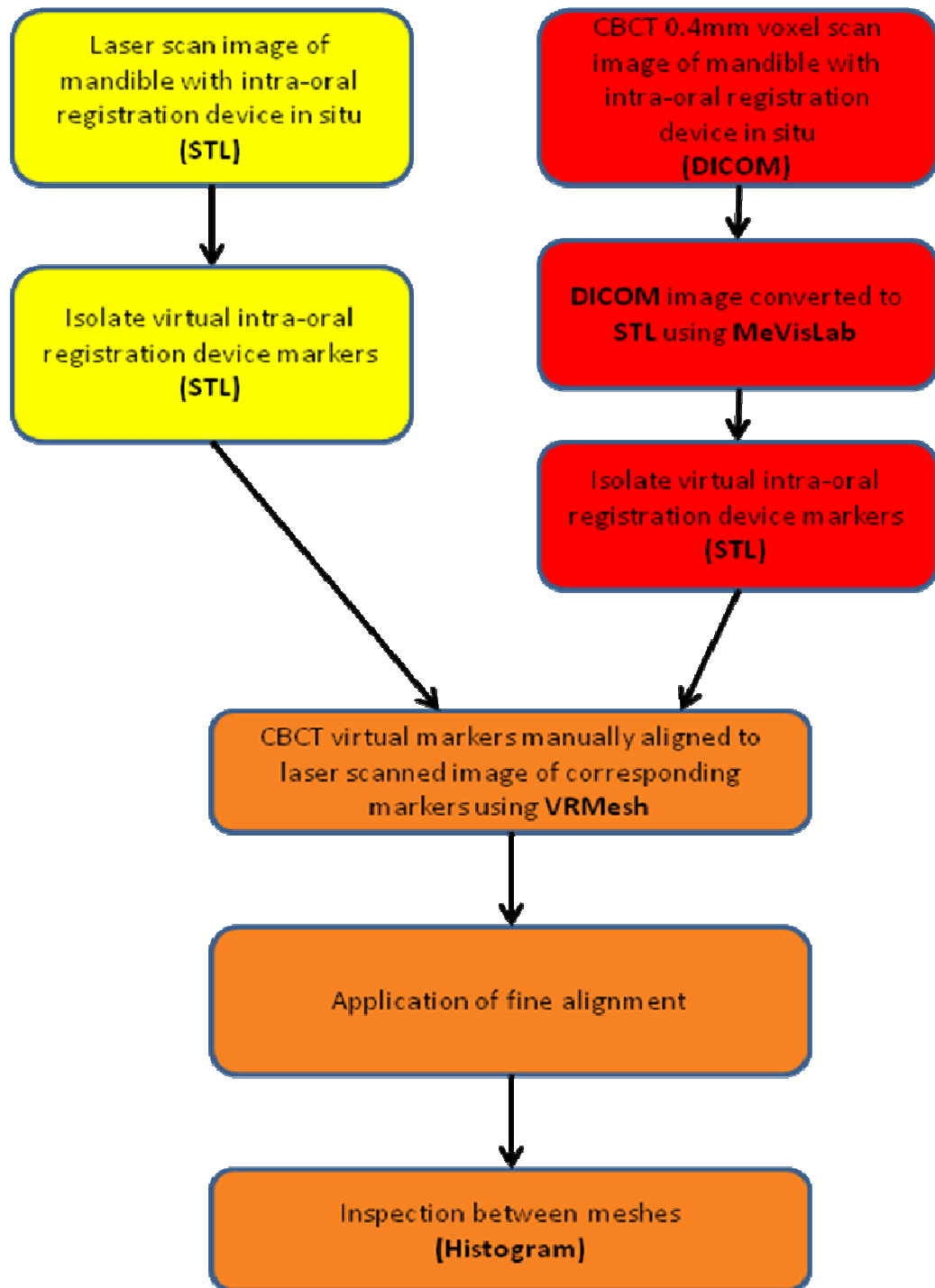
Figure 3.15 Pipeline to produce inspection of meshes between intra-oral markers acquired using a laser scanner and a CBCT 0.4mm voxel.
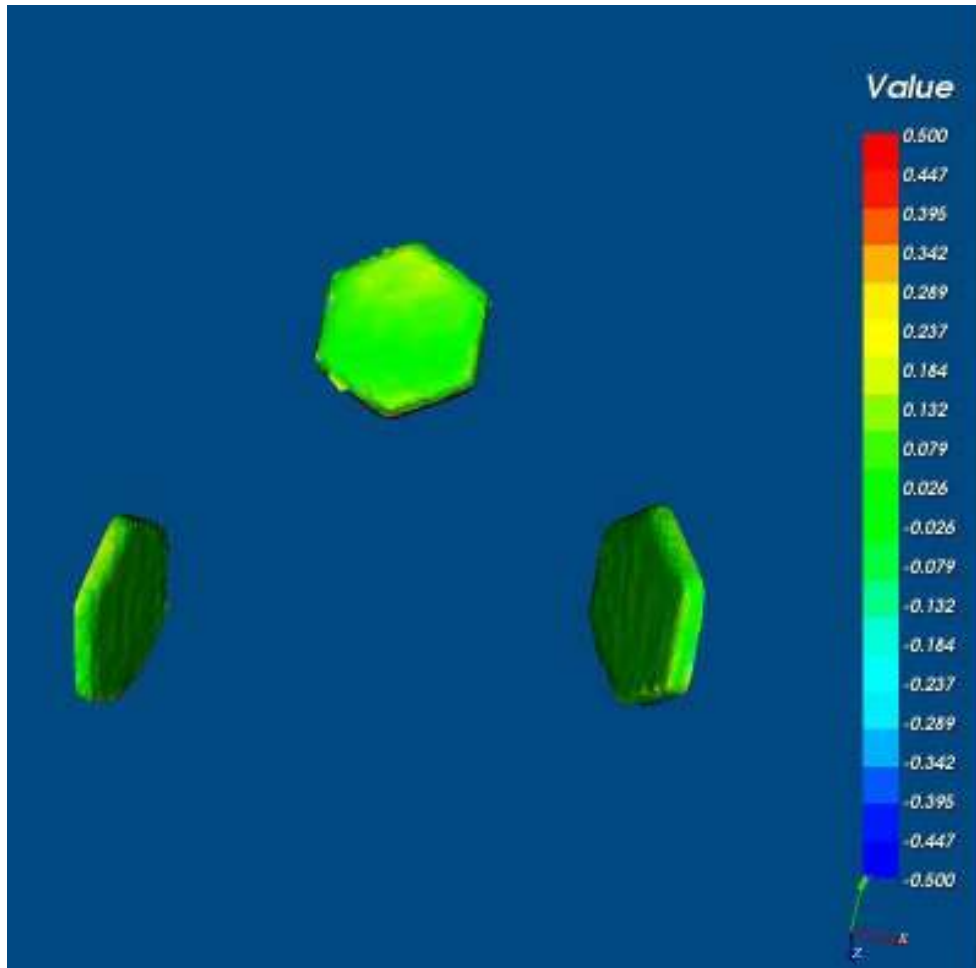
Figure 3.16 Colour error map displaying inspection between
meshes on registration markers.
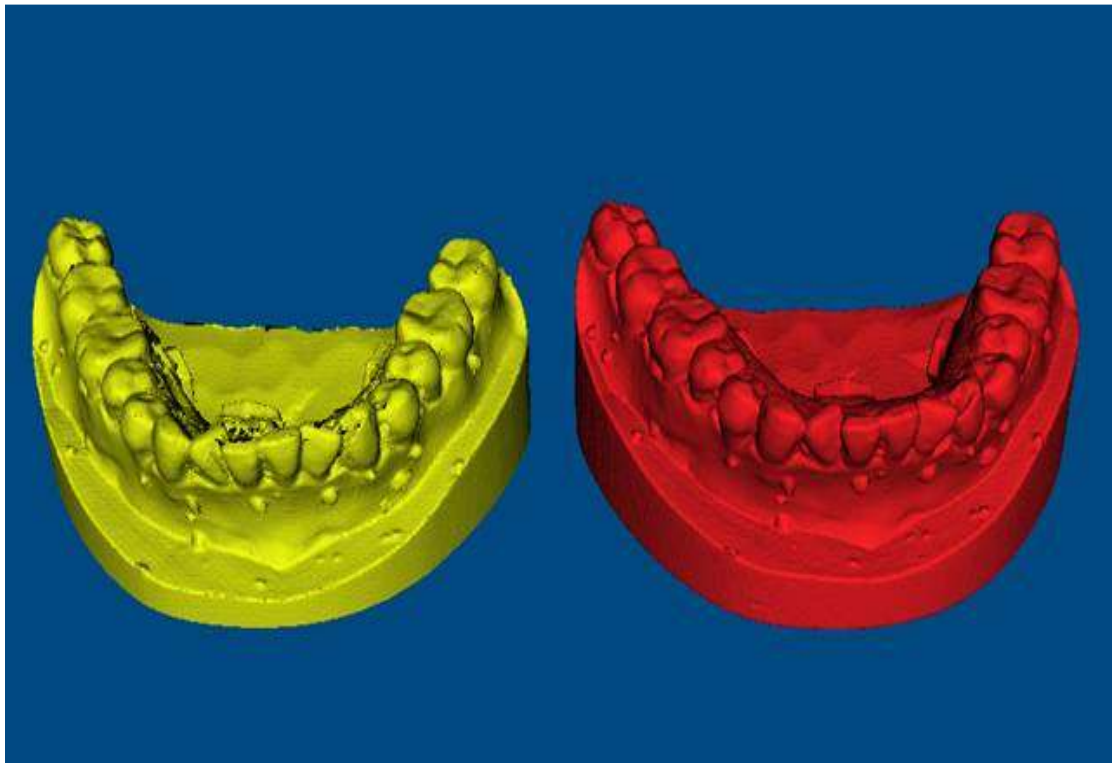
Figure 3.17 Laser scanned model (Yellow) and CBCT 0.2 voxel model (Red) prior to alignment.
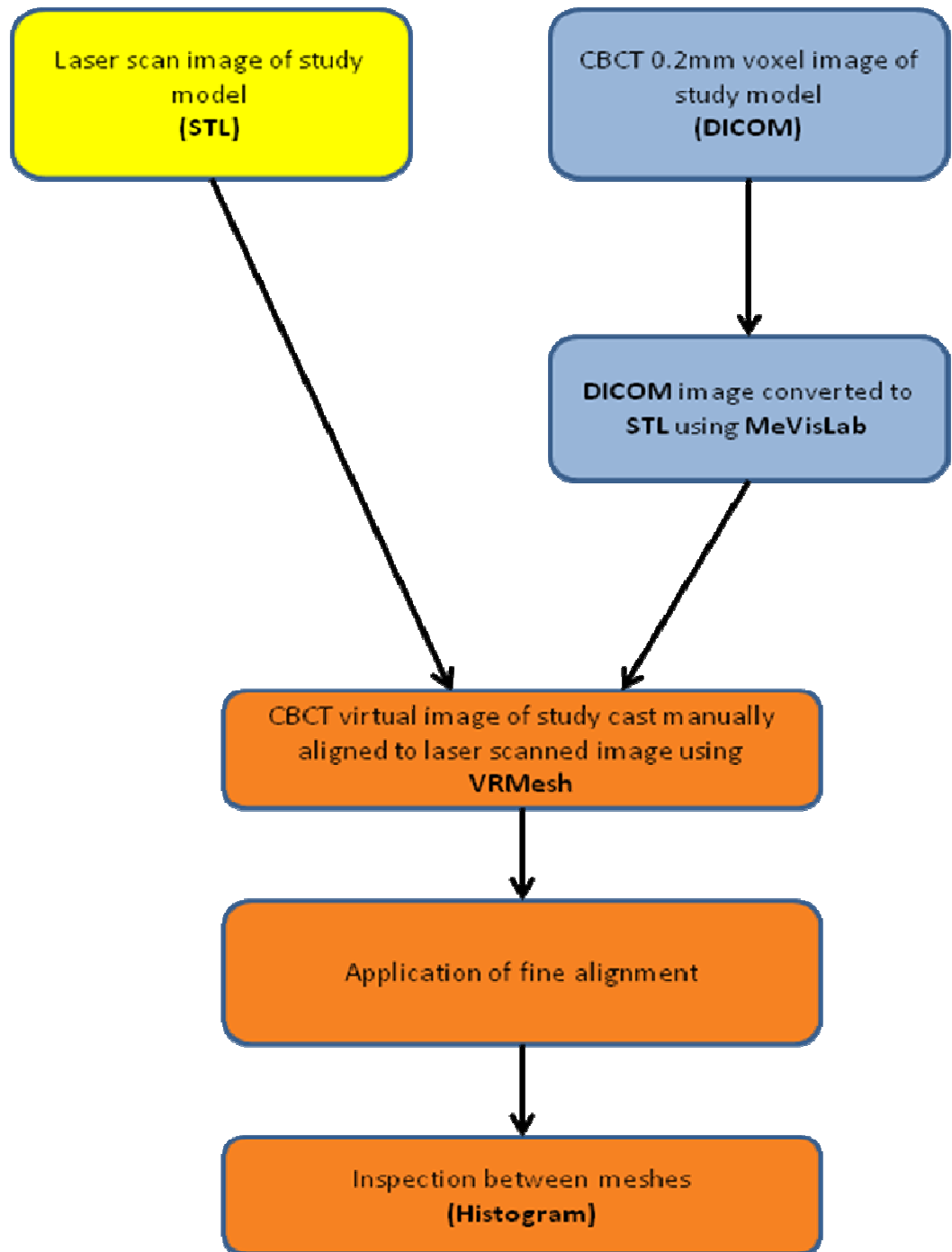
Figure 3.18 Pipeline to produce inspection of meshes between a study model acquired using a laser compared to the same model captured using CBCT 0.2mm voxel.

3.2.4 Validation of maxillary and mandibular dentition replacement

Six fully dentate dried cadaver skulls with no metallic restorations in the dentition were obtained from the anatomy department at Glasgow University. Each maxilla and mandible had wax applied around the labial, buccal and lingual aspect to replicate soft tissue as previously described (section 3.1.1)

The procedure to construct the acrylic appliances with markers for the mandibles was repeated on the maxillae. The only difference being that the markers were situated on the palatal aspect of the appliance. The completed appliances were then securely positioned on each maxilla and mandible, and all six complete skulls including mandibles and acrylic appliances with the markers in situ were CBCT scanned at 0.4 mm voxel.

3.2.5 Acquisition of the maxilla and mandibular dentition

Alginate impressions were taken for each of the six maxillae and six mandibles with the acrylic devices in situ. The impressions were then carefully removed from the teeth ensuring that the devices were also removed and remained secure and stable within the impression material. The impressions were then soaked in a disinfectant solution (Perform, Schülke & Mayr UK Ltd, Sheffield, UK). The impressions were then cast using the grey Sherahard-rock dental stone; this was trimmed to create a standard working model Fig 3.18. The models were then scanned using the CBCT at a resolution of 0.2 mm voxel in order to achieve maximum resolution.

Figure 3.19 Working model with acrylic appliance and markers in position.

3.2.6 Replacement of the dentition

The DICOM files for the cadaveric maxillae and mandibles and their corresponding study casts were all converted to STL files using MeVisLab, (section 3.1.3).

The STL image of the stone models were imported into VRMesh and the colour was changed to yellow for ease of recognition. The markers and dentition were isolated and all remaining information deleted and this was exported as a separate STL file. The same image was again imported but only the markers were isolated and a colour was allocated and the remaining part of the image deleted, the image of the markers was then exported as an STL file.

The STL file of only the markers was then imported into VRMesh; the corresponding file of either the mandible or maxilla with markers was also imported. The two images were then manually aligned on the markers, ensuring that the CBCT image of the maxilla or mandible was the source and the image of the markers was the target, fine alignment was then conducted Figure 3.19.

The image of the markers and dentition was then imported Figure 3.20. Approximately 2-4 mm below the occlusal surfaces and incisal edges of the dentition on both images were isolated and the remaining hard tissue information was then made invisible Figure 3.21. The two images of the dentition were then analysed using the inspection between objects function and any deviations displayed in the histogram chart Figure 3.22. The dentitions from the maxilla or mandible were deleted and the all remaining information were grouped together and merged to create a single file Figure 3.23. This produced a virtual image of the maxillae and mandibles with a replaced dentition.
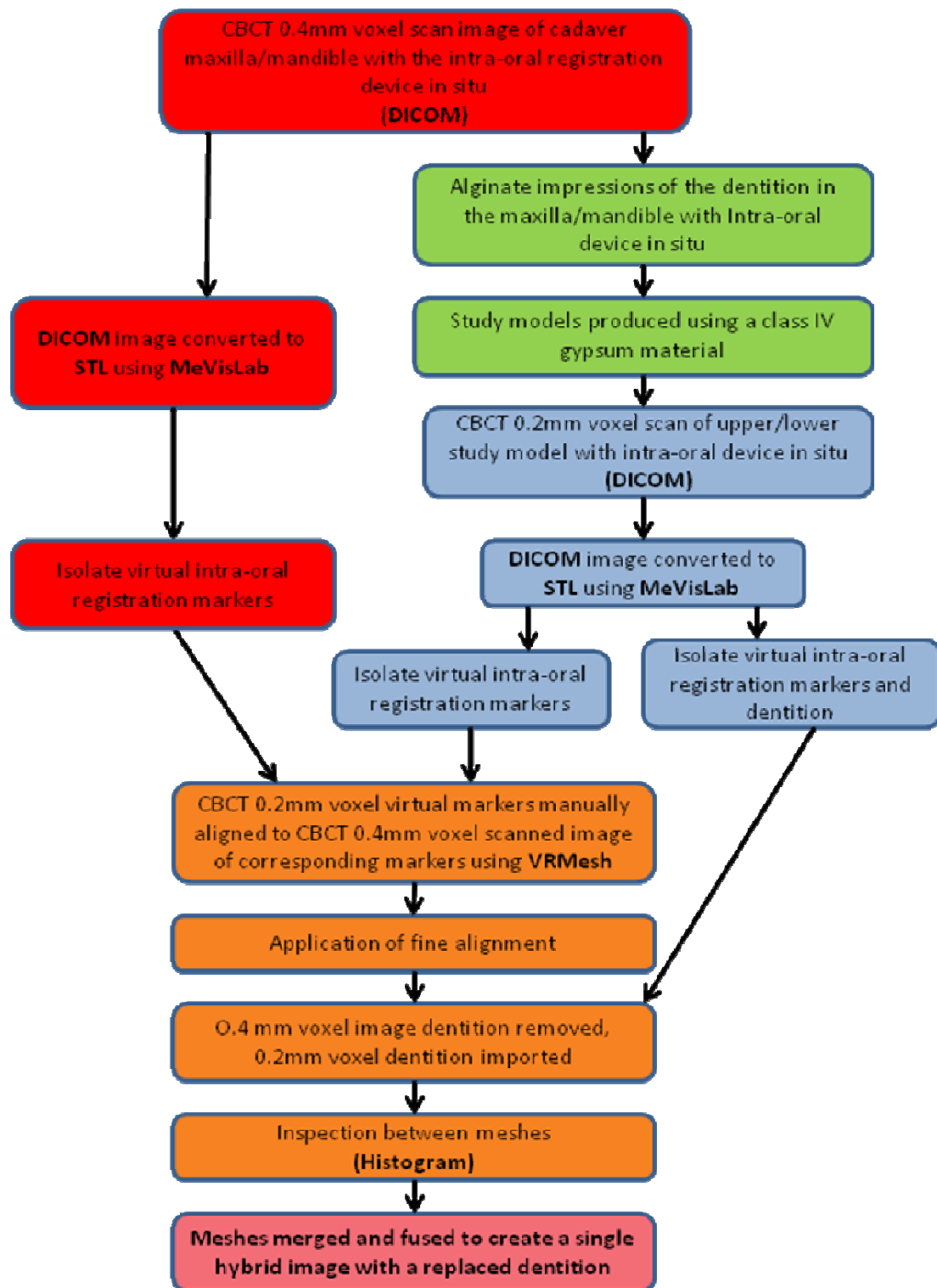
Figure 3.20 Pipeline to align virtual intra-oral marker images from CBCT 0.4 voxel to the corresponding markers acquired from a CBCT 0.2 voxel image.
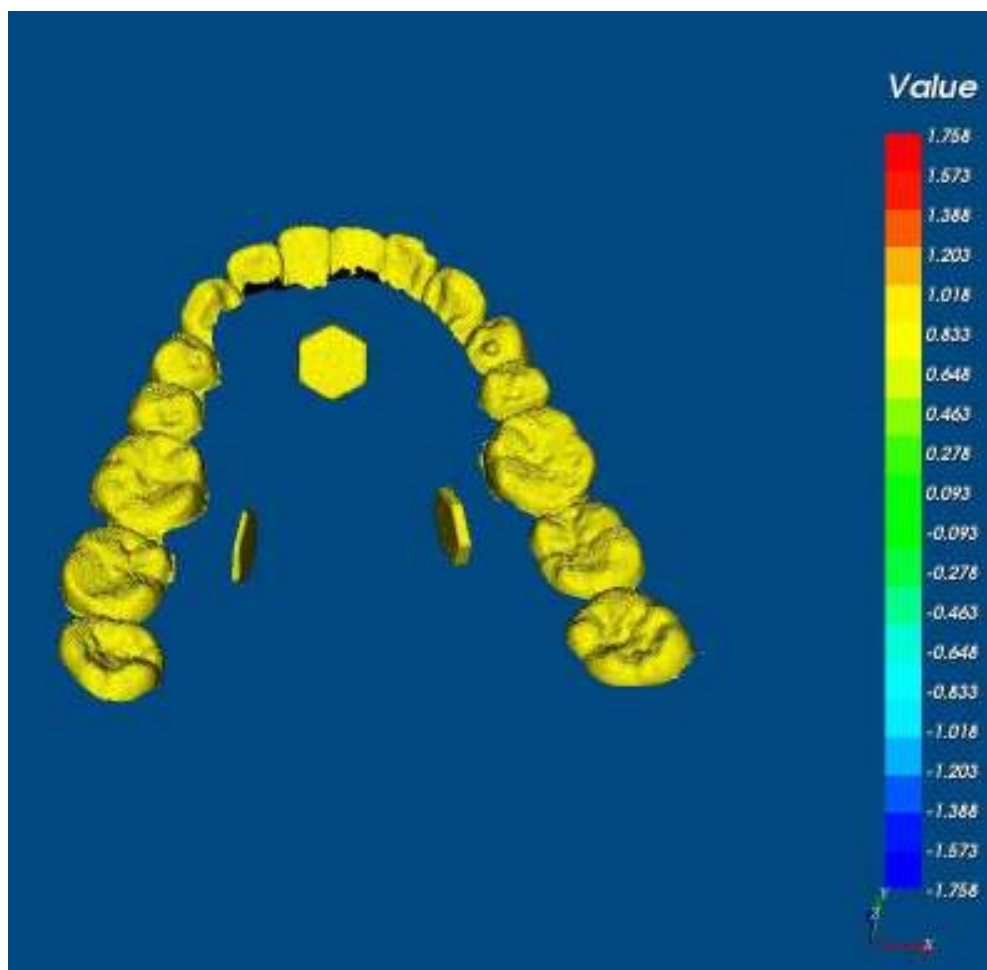
Figure 3.21 Imported dentition and registration markers.
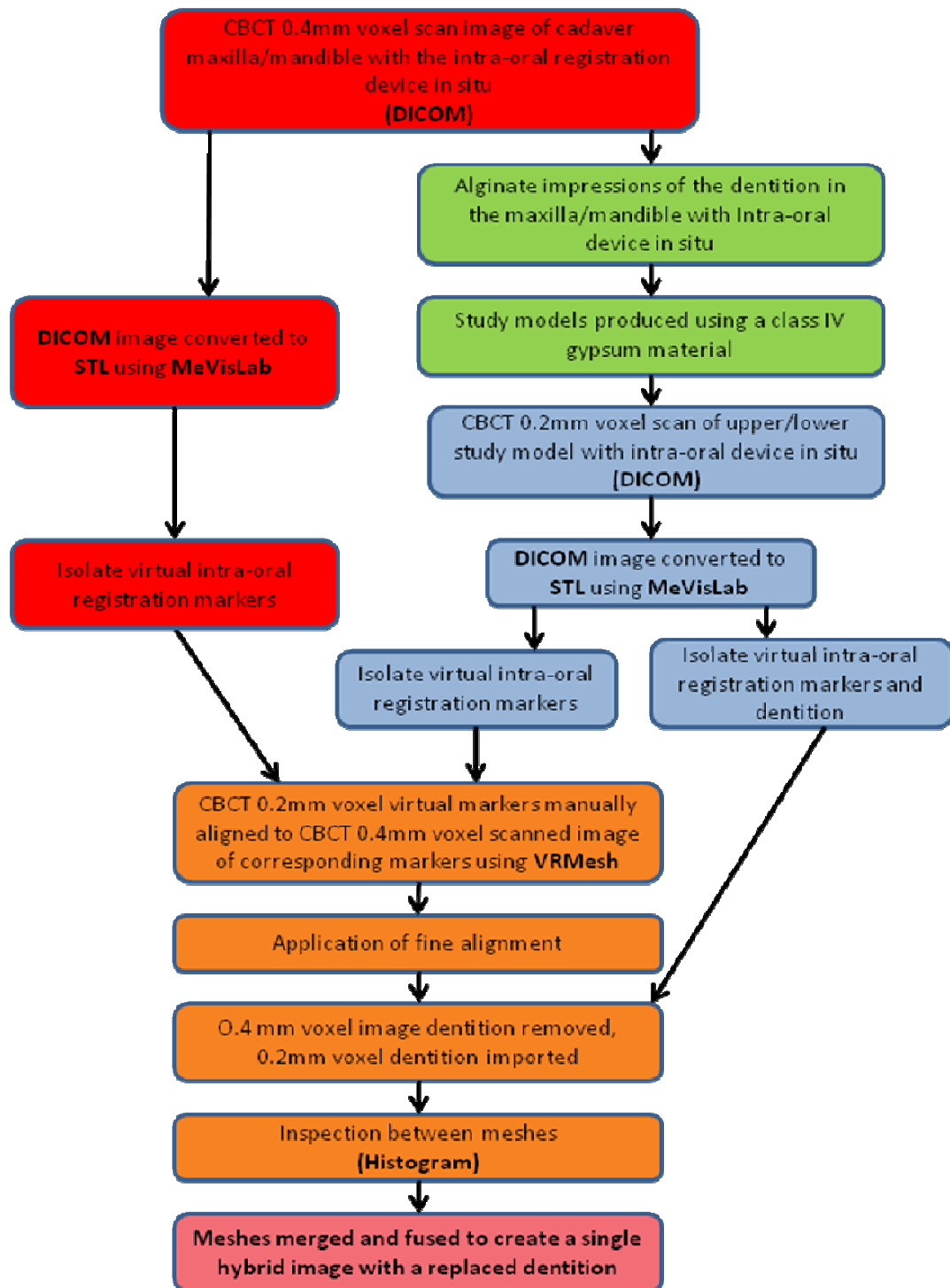
Figure 3.22 Pipeline to produce a hybrid virtual model with the existing dentition removed and replaced with the virtual dentition of a study cast.
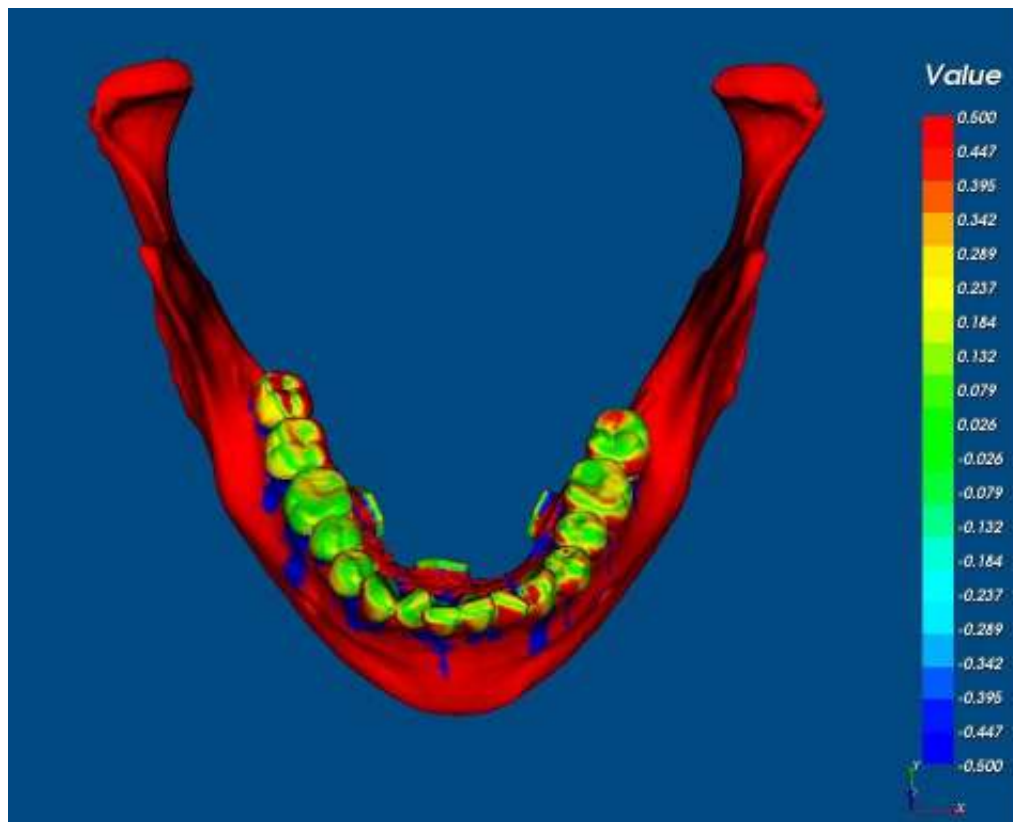
Figure 3.23 Colour error map displaying inspection between meshes for the replacement dentition.
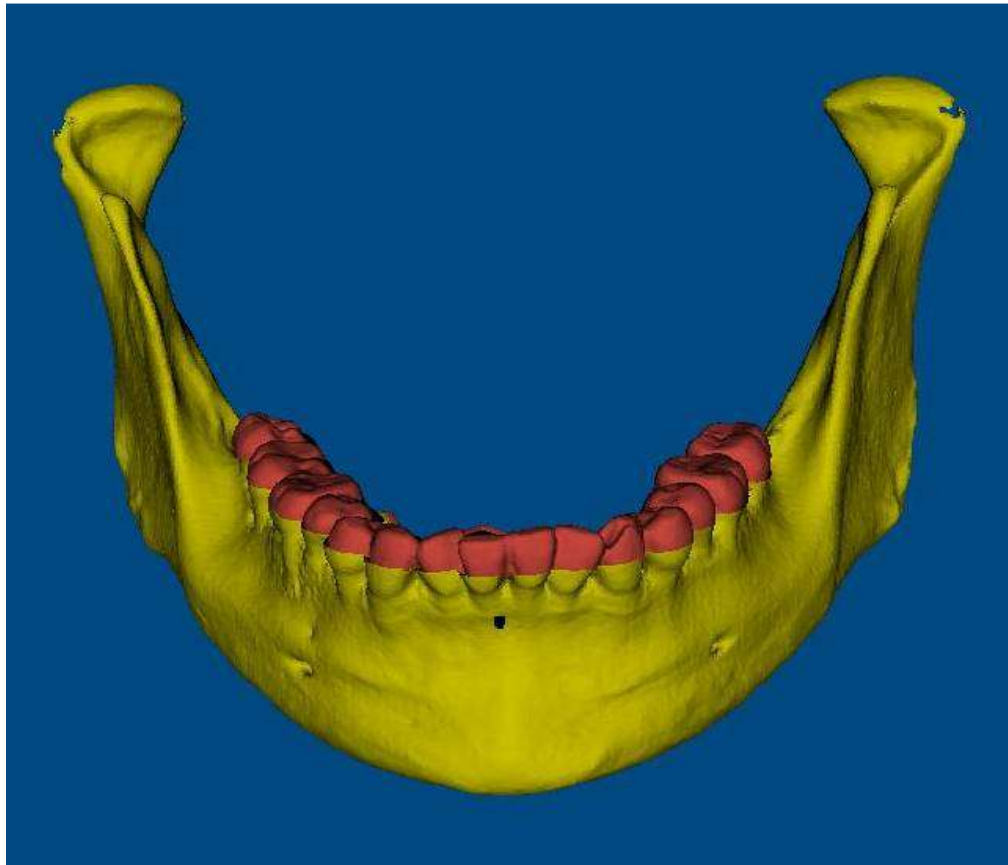
Figure 3.24 Single completed image with dentition replaced.

Materials & Methods Part II

3.3 Study design

The aim of part II of the study was to remove the virtual distorted dentition from the image of a patient acquired by CBCT and replace it with the dentition of the corresponding gypsum study model acquired through CBCT using the intra-oral transfer device.

No addition appointments or CBCT image acquisitions was required as a result of participation in the study. Ethical approval was obtained on the 18th March 2009 from the West Glasgow Ethics Committee, Acute services division, NHS Greater Glasgow and Clyde.

3.3.1 Recruitment of patients

Six patients were recruited from the orthognathic maxillofacial joint clinic at Glasgow Dental Hospital to participate in the study. All patients were currently attending the joint clinic for orthognathic assessment and planning between the period of January 2010 and May 2011.

3.3.1.1   Criteria

The inclusion criteria were as follows, the patient

- Should possess the majority of their own dentition.
- Scheduled for a routine CBCT scan prior to orthognathic surgery.
- Consented to take part in the study.

3.3.1.2   Study

Each patient was supplied with a patient information sheet and asked to read before agreeing to participate in the study.   When a patient agreed to participate in the study, they were requested to complete a patient consent form.

Upper and Lower alginate impressions were taken using a standard impression stock tray and disinfected using perform disinfectant and cast using a class III gypsum product and intra-oral transfer devices were constructed as previously described (section 3.1.6). An additional wax wafer was also constructed to ensure that the upper and lower dentitions were not in contact during the CBCT acquisition process, but the soft tissue was not distorted.

Participants were issued with an appointment requesting them to attend the radiology department at the Glasgow Dental Hospital, they were then contacted and requested to attend the orthodontic department prior to their radiology appointment.

An intra oral examination was conducted on each patient prior to attending the radiology department to ensure that no changes to the dentition had occurred since the previous appointment. The intra-oral transfer device was fitted to the upper and lower dentitions and checked for comfort and stability. Any transfer device that was deemed not to be secure was stabilised with the addition of small deposits of glass-ionomer luting cement (Aquacem, Dentsply, Konstanz, Germany) on the lingual and palatal aspects of the teeth.

Each patient was then seated in an upright position in the CBCT scanner with the intra-oral devices and wax wafer in position and their head securely positioned in accordance with manufacturers recommendations. Patients were then imaged using two 10cm FOV 0.4mm voxel scans to produce a 20cm image. The wax wafer was then removed and upper and lower alginate impressions were taken using modified impression trays with the intra-oral devices in situ and cast as previously described with the class IV grey stone. The same procedure for replacing the virtual dentitions in the cadaver skulls and mandibles was applied to the patients (section 3.1.12).

Chapter Four

Results

Results Part I

4.1 Are CBCT laser scanned images interchangeable?

Tables 4.1 - 4.3 of the results section analyses the experiments that were conducted to establish errors that occur when capturing hard tissue, dental structures and intra-oral markers on six cadaveric mandibles with a CBCT 0.4 voxel scan and comparing it to the same images that were acquired using a laser scanner. A correlation of 90% between the corresponding images was deemed to be reproducible and reliable, this would prevent outlying points negatively influencing the results (Kau *et al.,* 2006).

4.1.1 Differences between mandibular bone structure acquired from CBCT at 0.4mm voxel size and laser scanned images

Table 4.1 Shows the minimum, maximum and absolute mean distances between 90% of the mesh overlap for each of the six laser scanned and CBCT mandibular images. The maximum distance between the two superimposed surfaces for 90% of the mesh ranged from 0.24mm to 0.72mm. The absolute mean difference between the two surfaces representing the mandibular bone surface for 90% of the mesh ranged from 0.11 to 0.30mm.

The overall mean absolute distance between the laser scanned and CBCT mandibular images for 90% of the mesh was 0.16mm ± 0.07mm. Figure 4.1 shows the area of bone acquired with the CBCT registered and aligned with the laser scan red image. The differences between the two meshes are displayed in the form of a colour error map with the tolerance levels set at ± 0.5mm.

Table 4.1 The distance between the meshes of the mandibular bone structure acquired by CBCT (0.4mm voxel) and laser scanning following superimposition.

	Minimum distance between meshes (mm)	Maximum distance between 90% of mesh overlap (mm)	Absolute mean distance between 90% of mesh overlap (mm)	Standard Deviation
Cadaver Mandible 1	0	0.28	0.15	0.08
Cadaver Mandible 2	0	0.27	0.15	0.07
Cadaver Mandible 3	0	0.24	0.12	0.08
Cadaver Mandible 4	0	0.24	0.12	0.10
Cadaver Mandible 5	0	0.72	0.30	0.20
Cadaver Mandible 6	0	0.24	0.11	0.06
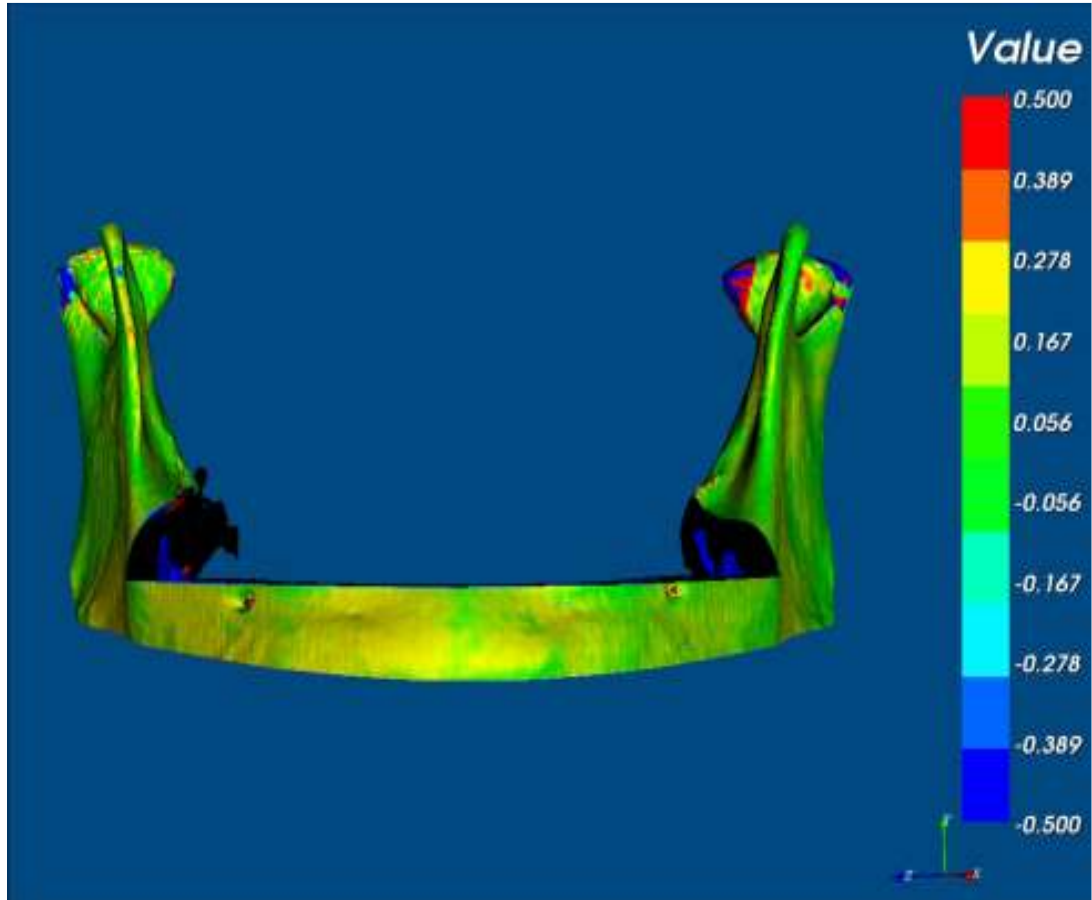
Figure 4.1 Colour error map showing differences between cadaveric mandible bone acquired from CBCT at 0.4mm voxels and laser scanned image.

4.1.2 Discrepancy between the occlusal surfaces of mandibles acquired by CBCT 0.4mm voxel and laser scanned images.

The position of the occlusal surfaces and the differences between meshes and magnification errors as a result of superimposing the CBCT 0.4 voxel image on the bone structure of a laser image are shown in Figure 4.2. The tolerance levels were set at ± 0.5mm and this is displayed as a colour error map Figure 4.3.

Maximum, minimum and absolute mean distances for 90% of the occlusal surfaces as a result of registration on bone structures acquired from the CBCT at 0.4 voxel and laser scanned images of six mandibles are displayed in table 4.2. This shows that the maximum distance of overlapping meshes between the surfaces had a variation ranging from 1.25mm to 0.32mm, with the absolute mean distances between the meshes ranging from 0.53mm to 0.14mm.

The overall mean absolute distance between the occlusal surfaces obtained from CBCT and laser scanning for 90% of the mesh was 0.25mm ± 0.14mm.

Figure 4.2   Demonstrates the magnification and positional errors that occur when capturing the dentition with CBCT and registering with a laser scanned image.
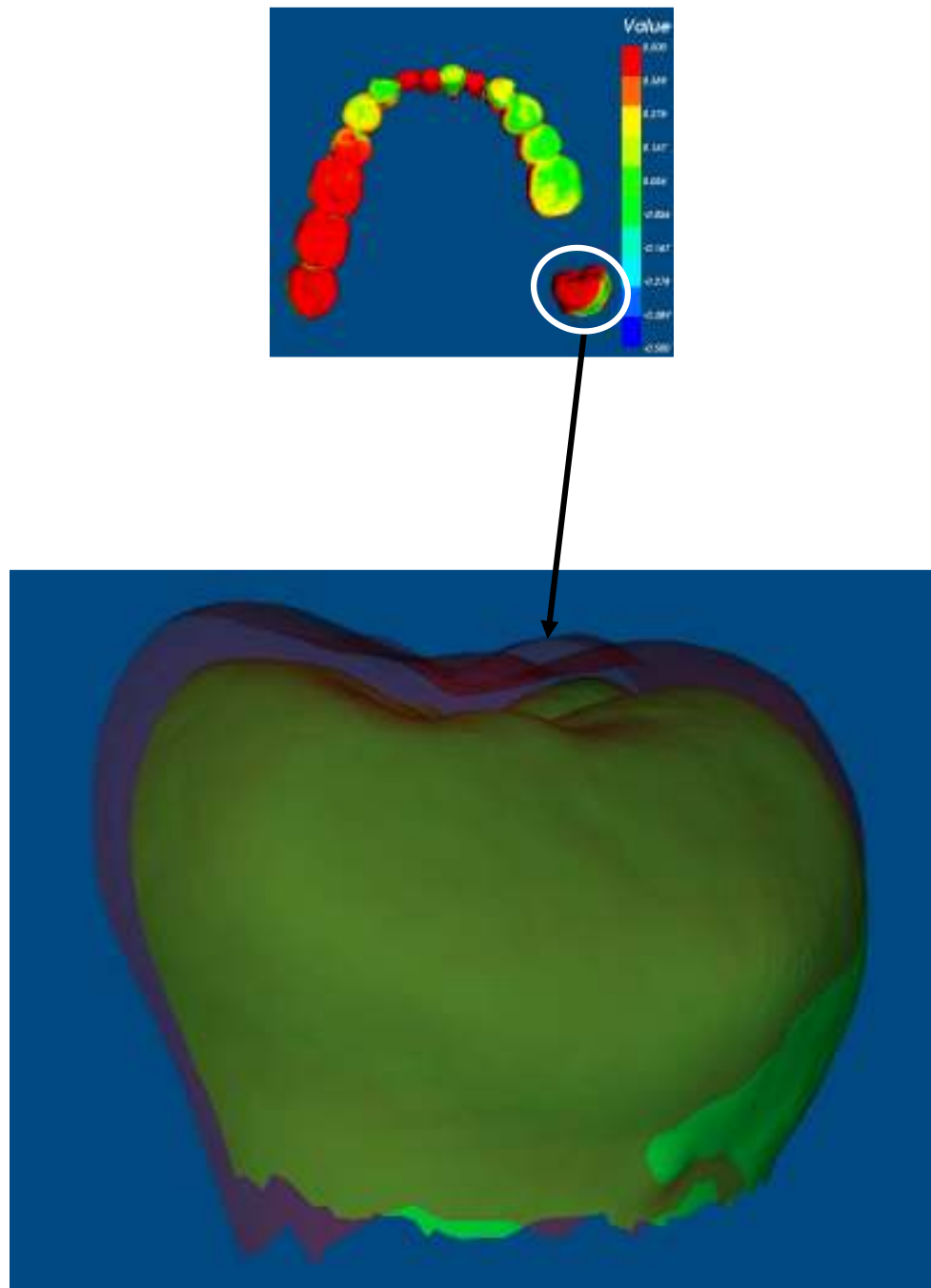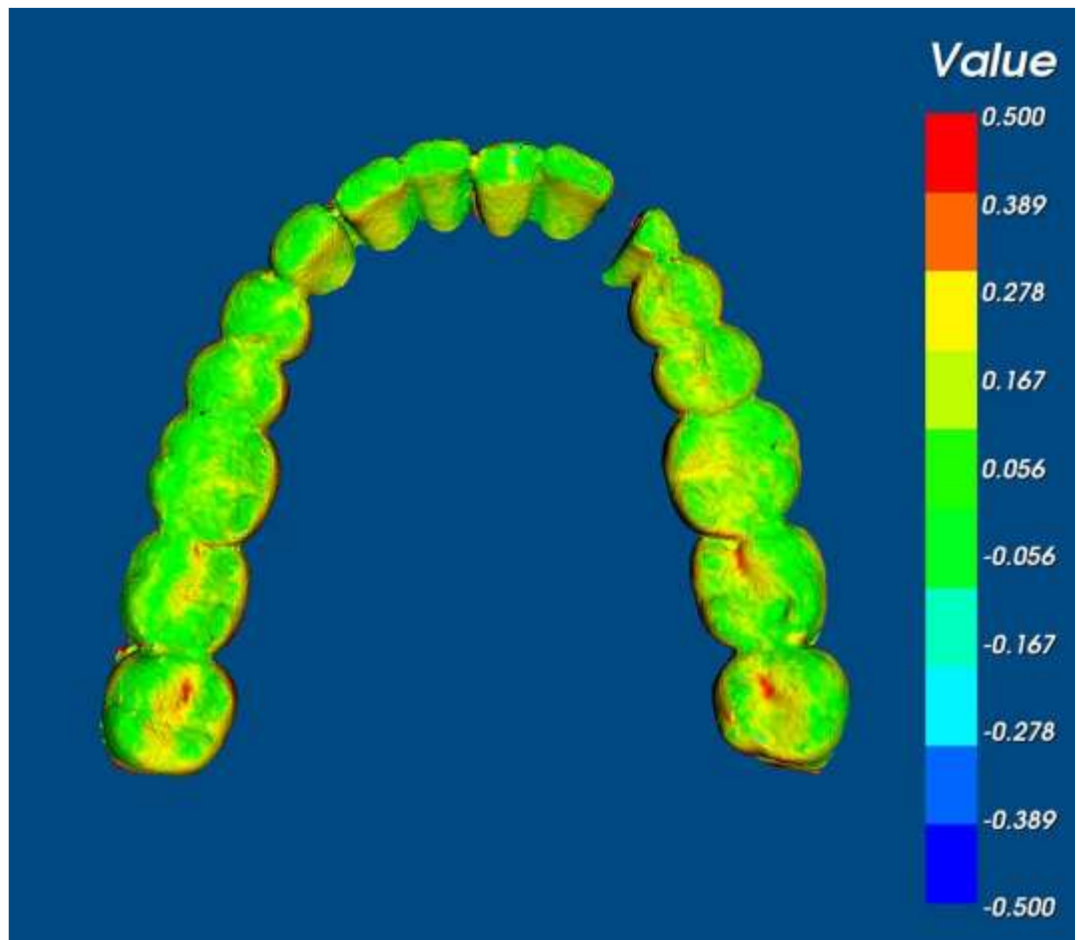
Figure 4.3   Colour error map showing differences between occlusal surfaces acquired by CBCT at 0.4mm voxels and laser scanned images.

Table 4.2   Differences in distance between the meshes of the occlusal surfaces when images are aligned on mandibular bone only.

	Minimum distance between meshes (mm)	Maximum distance between 90% of mesh overlap (mm)	Absolute mean distance between 90% of mesh overlap (mm)	Standard Deviation
Cadaver Mandible 1	0	0.36	0.20	0.10
Cadaver Mandible 2	0	0.32	0.14	0.09
Cadaver Mandible 3	0	0.39	0.23	0.09
Cadaver Mandible 4	0	0.35	0.21	0.09
Cadaver Mandible 5	0	1.25	0.53	0.43
Cadaver Mandible 6	0	0.35	0.18	0.09

4.1.3 Discrepancies between intra-oral registration device markers acquired from CBCT at 0.4mm voxels and laser scanned images

The results of the comparison between the intra-oral registration markers obtained through CBCT at 0.4 voxel and those acquired with the use of a laser scanner are shown in Table 4.3. The table shows the minimum, maximum and absolute mean distances between 100% of the mesh and 90% of the mesh overlap for the six CBCT and laser scanned images of the markers.

Comparing 90% of the mesh the maximum distance between the two registered surfaces had a range from 0.21mm to 0.11mm. The absolute mean difference between the two surfaces of the markers ranged from 0.10mm to 0.04mm. The overall mean absolute distance between the markers obtained from CBCT and laser scanning for 90% of the mesh was 0.08mm ± 0.02mm. Figure 4.4 displays the alignment of the two surfaces as a colour error map with the tolerance levels defined at ± 0.5mm.

Table 4.3   Distances between the meshes for the intra-oral registration device markers acquired using CBCT at 0.4mm voxels and laser scanned images.

	Minimum distance between meshes (mm)	Maximum distance between 90% of mesh overlap (mm)	Absolute mean distance between 90% of mesh overlap (mm)	Standard Deviation
Cadaver Mandible 1	0	0.20	0.08	0.05
Cadaver Mandible 2	0	0.17	0.08	0.05
Cadaver Mandible 3	0	0.19	0.07	0.05
Cadaver Mandible 4	0	0.21	0.09	0.07
Cadaver Mandible 5	0	0.19	0.10	0.05
Cadaver Mandible 6	0	0.11	0.04	0.03
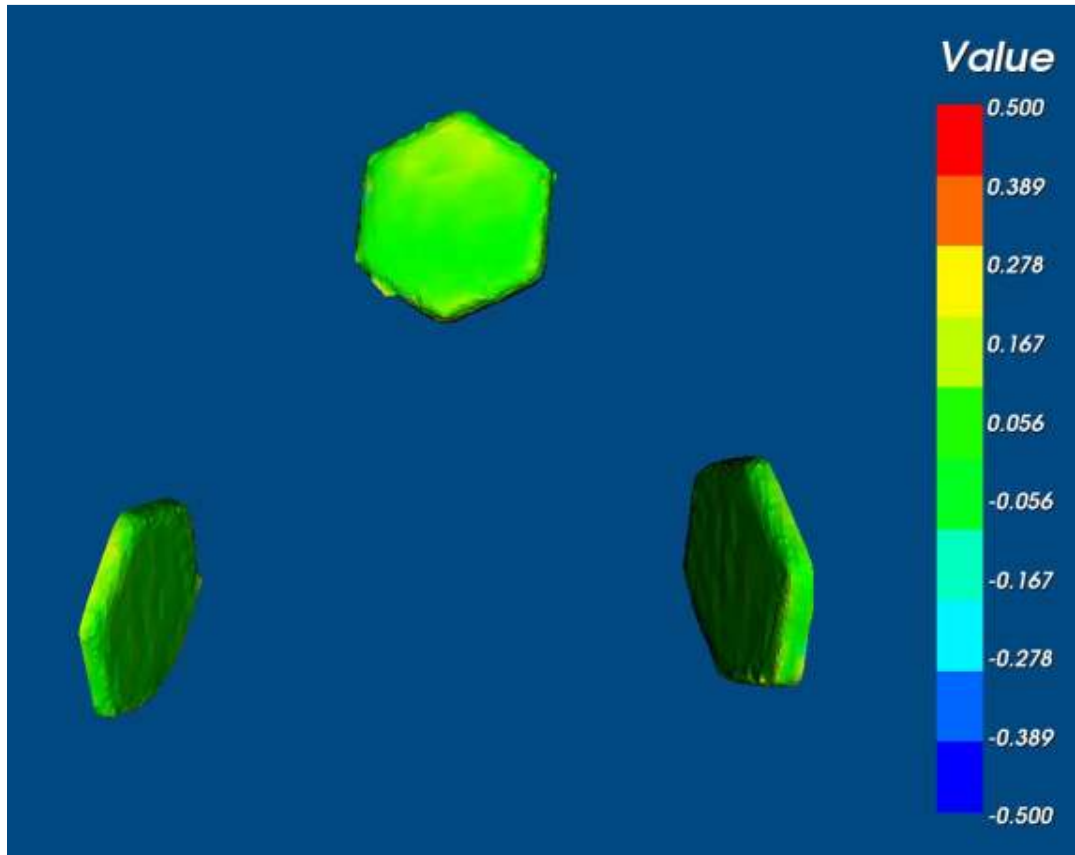
Figure 4.4   Colour error map showing discrepancies between intra-oral registration device markers acquired from CBCT at 0.4mm voxels and laser scanned images.

4.2 Study of images acquired using CBCT 0.2mm voxel resolution versus laser scanning.

Table 4.4 of the results section analysis a study that was conducted to establish errors that occur when 3D data of a study cast is acquired from a CBCT at the highest resolution against the same image scanned with the use of a laser scanner.

4.2.1 Differences between the model data acquired from a CBCT 0.2 voxel image and a laser scanned image.

The differences between the meshes as a result of superimposition of the study model image acquired from CBCT 0.2mm voxel resolution over the mesh acquired from laser scanning with the tolerance levels established at ± 0.5mm is shown as a colour error map in Figure 4.5.

For 90% of the two superimposed images the maximum distance between the mesh ranged from 0.17mm to 0.14mm. The absolute mean difference between the two surfaces of the study casts ranged from 0.06mm to 0.05mm.The overall mean absolute distance between the two images was 0.06mm ± 0.01mm.
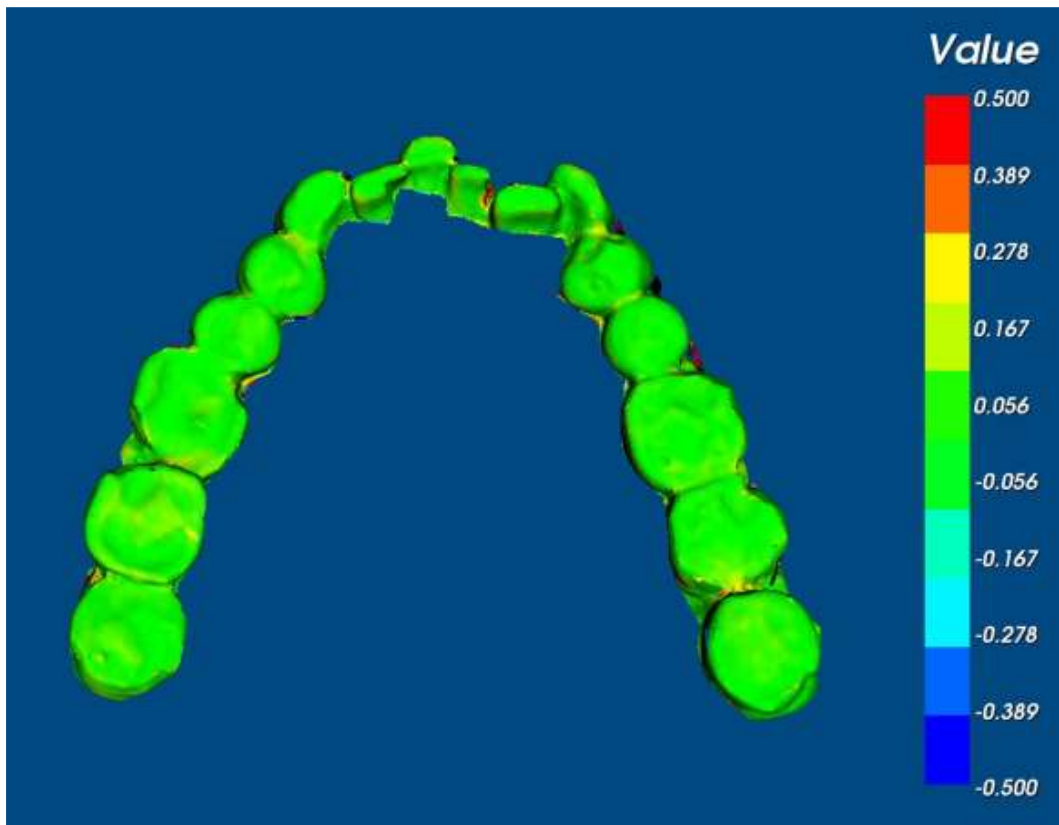
Figure 4.5   Colour error map showing differences between model data acquired from a CBCT 0.2 vox image and a laser scanned image.

Table 4.4 Differences between model data acquired from a CBCT 0.2 vox image and a laser scanned image

	Minimum distance between meshes (mm)	Maximum distance between 90% of mesh overlap (mm)	Absolute mean distance between 90% of mesh overlap (mm)	Standard Deviation
Model 1	0	0.14	0.05	0.04
Model 2	0	0.15	0.05	0.04
Model 3	0	0.17	0.06	0.04
Model 4	0	0.16	0.06	0.04
Model 5	0	0.16	0.06	0.05
Model 6	0	0.15	0.05	0.04

4.2.2 Discrepancies between markers acquired from a CBCT 0.4mm voxel scan and CBCT 0.2mm scan.

Cone Beam CT 0.4mm voxel scans were acquired with the intra-oral registration devices in situ on the maxillae and mandibular skulls. The corresponding study casts were then scanned by CBCT at a setting of 0.2mm voxel. The virtual markers from the 0.4mm scans were then isolated and registered with the 0.2mm scans. The discrepancies between the virtual markers are displayed as colour error maps with a tolerance setting of ± 0.5mm Figure 4.6 and Figure 4.7.

The maximum, minimum and absolute mean distances of 90% of the position of the markers acquired at 0.2mm as a result of registration on the 0.4mm markers is shown in Table 4.5 for the mandibles and Table 4.6 for the maxillae. The tables show that the maximum distance of overlapping meshes ranged from 0.30mm to 0.17mm in the mandibles, with the absolute mean distances varying from 0.10mm to 0.07mm. In the maxillae the maximum distance of overlapping meshes ranged from 0.17mm to 0.30mm, with the absolute mean distances varying from 0.13mm to 0.07mm.

The overall mean absolute distances between the markers obtained from CBCT 0.4mm voxel scans and 0.2mm voxel scans for 90% of the mesh in the mandibles was 0.09mm ± 0.01mm. In the maxillae the overall mean absolute distances between the markers was 0.09mm ± 0.01mm.

Table 4.5 Discrepancies between markers in the dry cadaveric mandibles acquired from a CBCT 0.4 vox scan in situ and CBCT 0.2 vox scanned images of the markers on a dental cast.

	Minimum distance between meshes (mm)	Maximum distance between 90% of mesh overlap (mm)	Absolute mean distance between 90% of mesh overlap (mm)	Standard Deviation
Mandible 1	0	0.20	0.08	0.06
Mandible 2	0	0.22	0.08	0.06
Mandible 3	0	0.24	0.10	0.08
Mandible 4	0	0.17	0.07	0.05
Mandible 5	0	0.29	0.10	0.09
Mandible 6	0	0.30	0.09	0.10
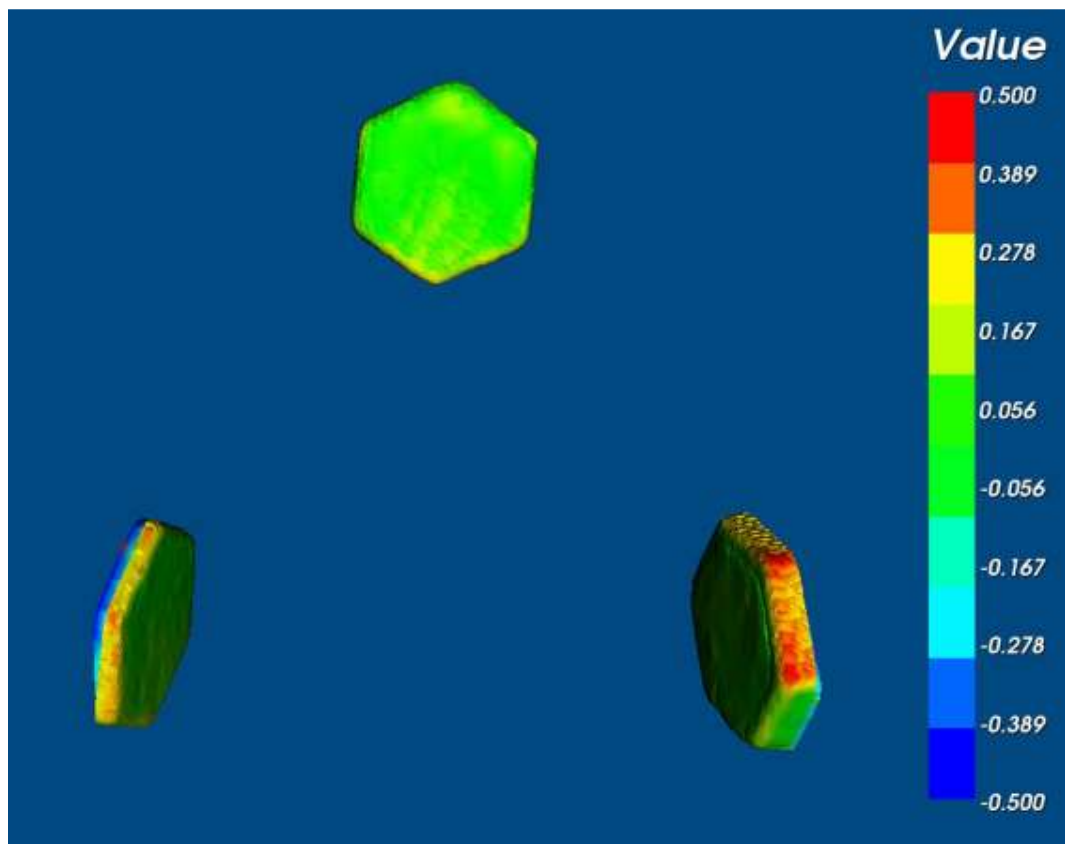
Figure 4.6   Colour error map showing discrepancies between markers in the dry cadaveric mandibles acquired from a CBCT 0.4 vox scan in situ and CBCT 0.2 vox scanned images of the markers in situ on the dental cast.

Table 4.6   Discrepancies between markers in the dry cadaveric maxillas acquired from a CBCT 0.4 vox scan in situ and CBCT 0.2 vox scanned images of the markers on a dental cast.

	Minimum distance between meshes (mm)	Maximum distance between 90% of mesh overlap (mm)	Absolute mean distance between 90% of mesh overlap (mm)	Standard Deviation
Maxilla 1	0	0.17	0.07	0.05
Maxilla 2	0	0.30	0.13	0.07
Maxilla 3	0	0.19	0.07	0.06
Maxilla 4	0	0.30	0.12	0.09
Maxilla 5	0	0.22	0.11	0.06
Maxilla 6	0	0.23	0.10	0.07
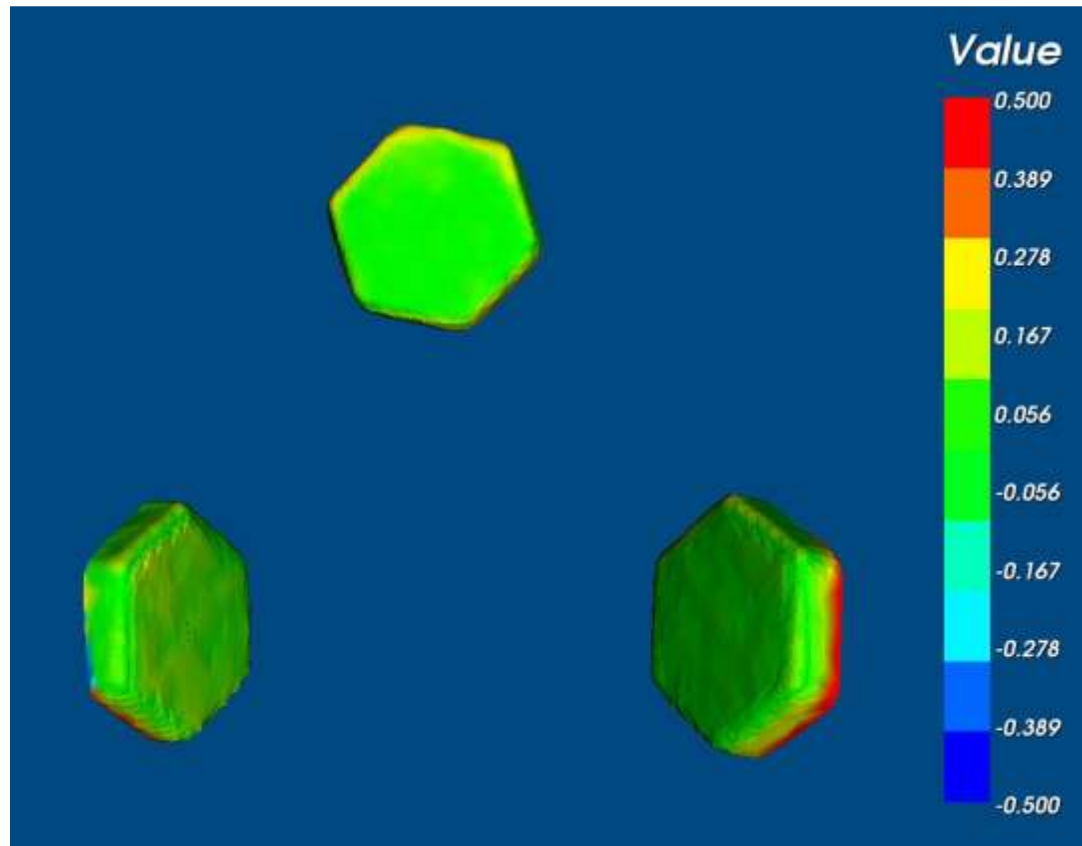
Figure 4.7   Colour error map showing discrepancies between markers in the dry cadaveric mandibles acquired from a CBCT 0.4 vox scan in situ and CBCT 0.2 vox scanned images of the markers on a dental cast.

4.2.3 Differences between the occlusal surfaces of virtual dentitions when registered on intra-oral markers with corresponding markers from study cast s (No metallic restorations present).

The occlusal surfaces of the dentitions of the maxillae and mandibles that were acquired from the CBCT at 0.4mm voxel were removed and replaced with the virtual occlusal surfaces of the corresponding study casts using the markers as the point of registration as previously described in section 4.2.1. The differences between the occlusal surfaces are shown in the histograms in Figure 4.8 for the maxillae and Figure 4.9 for the mandibles at a tolerance level of ± 0.5mm.

Table 4.7 shows the minimum, maximum and absolute mean distances for 90% of the mesh between the occlusal surfaces of the mandibles and the mesh of the corresponding study casts. For 90% of the mesh the two surfaces maximum range of overlap varied from 0.37mm to 1.05mm, with the absolute mean distance ranging from 0.12mm to 0.44mm. The overall mean absolute distance between the occlusal surface acquired from the mandibles by CBCT at 0.4mm voxels and the virtual surfaces of the study casts was 0.26mm ± 0.11mm for 90% of the mesh.

Table 4.8 shows the minimum, maximum and absolute mean distances for 90% of the mesh between the occlusal surfaces of the maxillae and the mesh of the corresponding study casts. For the mesh between the two superimposed surfaces the maximum distance of overlap ranged from 0.26mm to 0.71mm, with the absolute mean distance ranging from 0.10mm to 0.28mm. The overall mean absolute distance between the occlusal surface acquired from the maxillae by CBCT at 0.4mm voxel and the virtual surfaces of the study casts was 0.22mm ± 0.07mm for 90 % of the mesh.

Table 4.7 Differences between the positions of the dentitions as a result of registering the virtual intra-oral markers from the mandibles with the scans of the corresponding virtual markers from the study casts (No metallic restorations present).

	Minimum distance between meshes (mm)	Maximum distance between 90% of mesh overlap (mm)	Absolute mean distance between 90% of mesh overlap (mm)	Standard Deviation
Mandible 1	0	0.37	0.12	0.10
Mandible 2	0	0.50	0.20	0.15
Mandible 3	0	0.83	0.30	0.26
Mandible 4	0	0.48	0.18	0.13
Mandible 5	0	0.69	0.30	0.20
Mandible 6	0	1.05	0.44	0.34
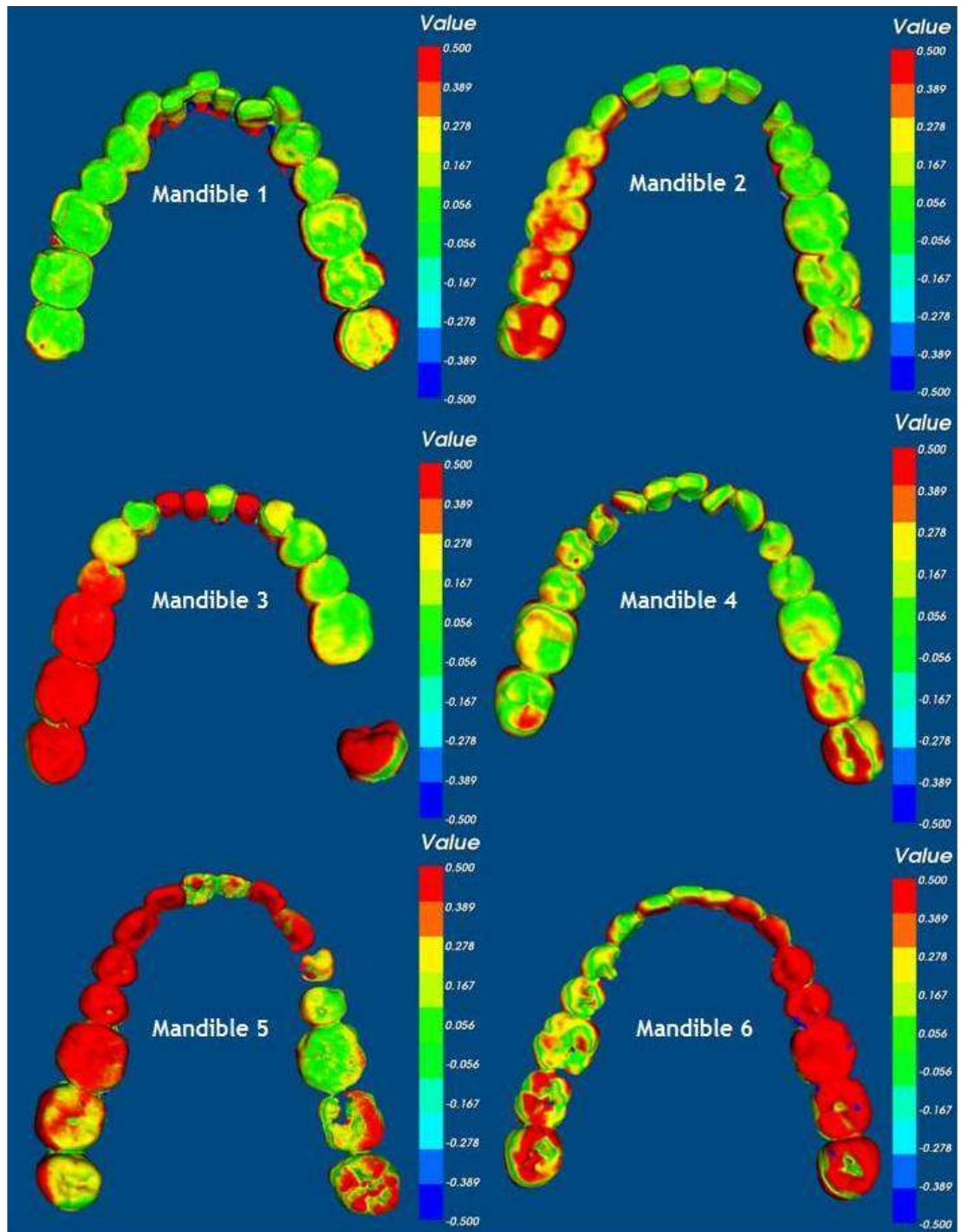
Figure 4.8 Colour error map showing differences between the positions of the dentitions as a result of registering the virtual intra-oral markers from the mandibles with the scans of the corresponding virtual markers from the study casts (No metallic restorations present).

Table 4.8   Differences between the positions of the dentitions as a result of registering the virtual intra-oral markers from the maxillae with the scans of the corresponding virtual markers from the study casts (No metallic restorations present).

	Minimum distance between meshes (mm)	Maximum distance between 90% of mesh overlap (mm)	Absolute mean distance between 90% of mesh overlap (mm)	Standard Deviation
Maxilla 1	0	0.57	0.18	0.15
Maxilla 2	0	0.62	0.28	0.19
Maxilla 3	0	0.67	0.27	0.21
Maxilla 4	0	0.60	0.25	0.19
Maxilla 5	0	0.71	0.26	0.23
Maxilla 6	0	0.26	0.10	0.07
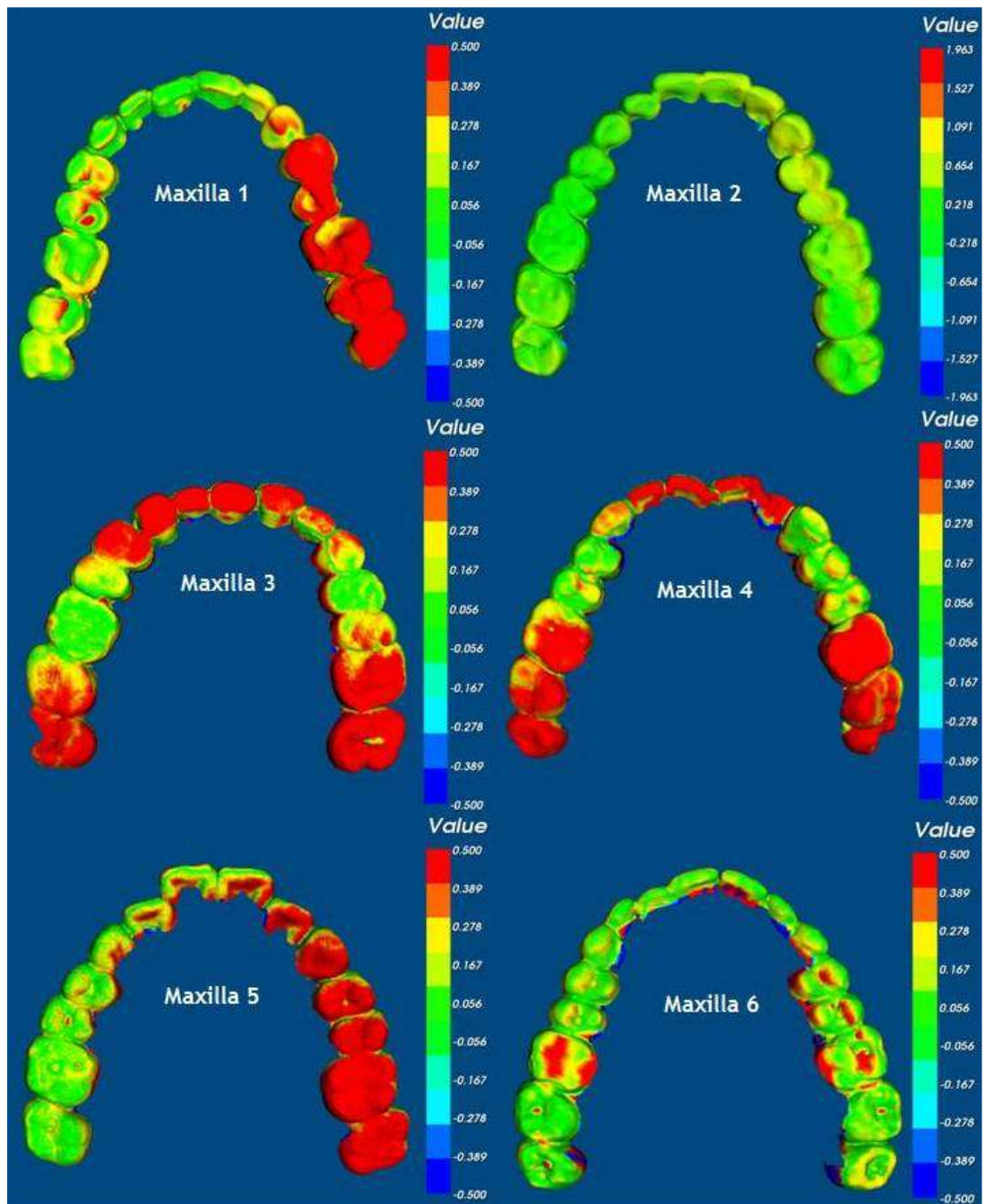
Figure 4.9 Colour error map showing differences between the positions of the dentitions as a result of registering the virtual intra-oral markers from the maxillae with the scans of the corresponding virtual markers from the study casts (No metallic restorations present).

Results Part II

4.3 In vivo discrepancies

4.3.1 Discrepancies between markers acquired from a CBCT 0.4mm voxel scan of patients and CBCT 0.2mm scan of corresponding study casts.

CBCT 0.4mm voxel scans were acquired with the intra-oral registration devices in situ on 6 patients who were attending the orthognathic joint clinic at Glasgow dental hospital. Corresponding study casts were then scanned by CBCT at a setting of 0.2mm voxel. The virtual markers from the patient's scans were then isolated and registered with the virtual scans of the study cast. The discrepancies between the virtual markers are displayed as a colour error map with a tolerance setting of ± 0.5mm Figure 4.10 and Figure 4.11.

The maximum, minimum and absolute mean distances of 90% of the position of the markers acquired from the study casts as a result of registration on the markers obtained from the patients is shown in Table 4.9 for the maxillae and Table 4.10 for the mandibular markers. The tables show that the maximum distance of overlapping meshes for 90% of the overlapping meshes ranged from 0.47mm to 0.32mm in the mandibles with the absolute mean distances ranging from 0.20mm to 0.13mm. In the maxillae the overlapping meshes for 90% ranged from 0.42mm to 0.24mm, with the absolute mean distances varying from 0.18mm to 0.09mm.

The overall mean absolute distances between the markers obtained from CBCT 0.4mm voxel scans of patients and 0.2mm voxel scans of study casts for 90% of the mesh was 0.16mm ± 0.02mm. In the maxillae the overall mean absolute distances between the markers was 0.12mm ± 0.04mm.

Table 4.9   Discrepancies between markers in patient's mandible acquired from a CBCT 0.4 vox scan in situ and CBCT 0.2 vox scanned images of their dental cast.

|	Minimum distance between meshes (mm)	Maximum distance between 100% of mesh overlap (mm)	Absolute mean distance between 100% of mesh overlap (mm)	Standard Deviation	Maximum distance between 90% of mesh overlap (mm)	Absolute mean distance between 90% of mesh overlap (mm)	Standard Deviation
Mandible 1	0	0.76	0.17	0.13	0.36	0.14	0.12
Mandible 2	0	0.51	0.18	0.12	0.34	0.16	0.10
Mandible 3	0	0.76	0.18	0.13	0.37	0.15	0.11
Mandible 4	0	0.80	0.20	0.17	0.47	0.16	0.16
Mandible 5	0	0.72	0.16	0.12	0.32	0.13	0.09
Mandible 6	0	0.72	0.23	0.16	0.45	0.20	0.16
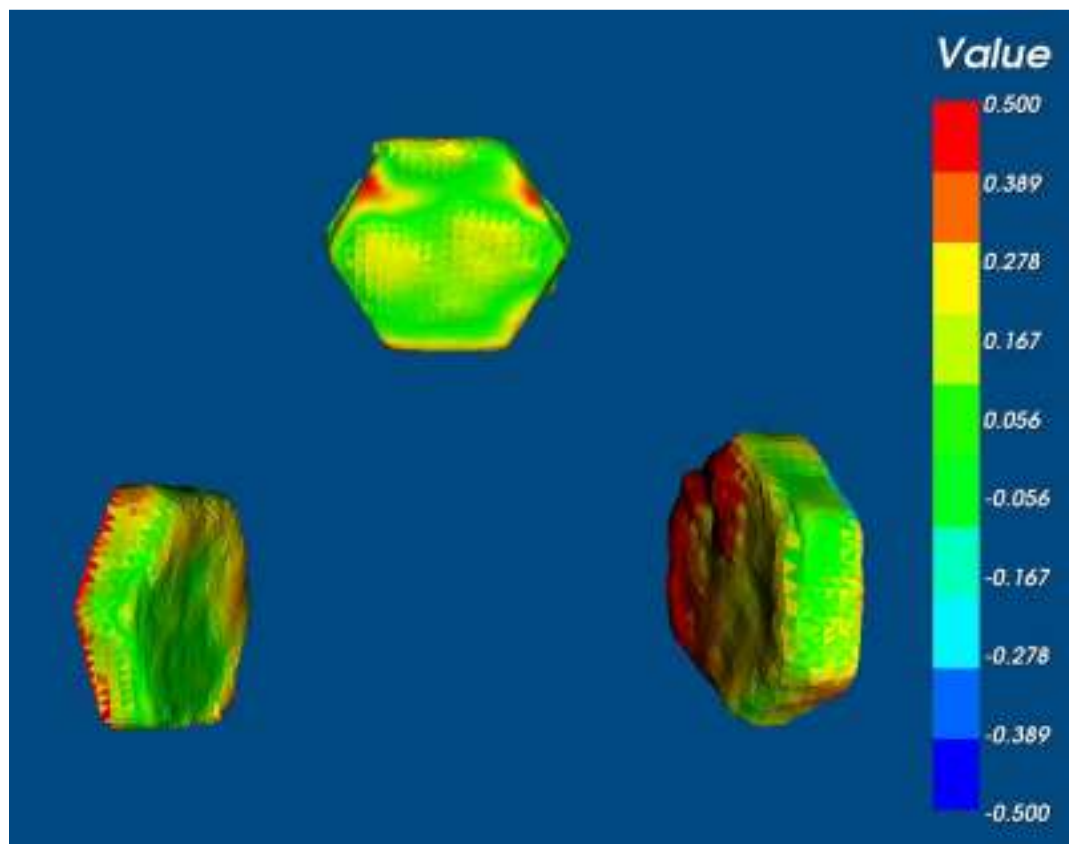
Figure 4.10 Colour error map showing differences between Markers in patient's mandible acquired from a CBCT 0.4 vox scan in situ and CBCT 0.2 vox scanned images of their dental cast.

Table 4.10 Discrepancies between markers in patient's maxillae acquired from a CBCT 0.4 vox scan in situ and CBCT 0.2 vox scanned images of their dental cast.

	Minimum distance between meshes (mm)	Maximum distance between 90% of mesh overlap (mm)	Absolute mean distance between 90% of mesh overlap (mm)	Standard Deviation
Maxilla 1	0	0.31	0.13	0.09
Maxilla 2	0	0.26	0.09	0.07
Maxilla 3	0	0.24	0.09	0.07
Maxilla 4	0	0.30	0.15	0.09
Maxilla 5	0	0.42	0.18	0.12
Maxilla 6	0	0.31	0.10	0.09
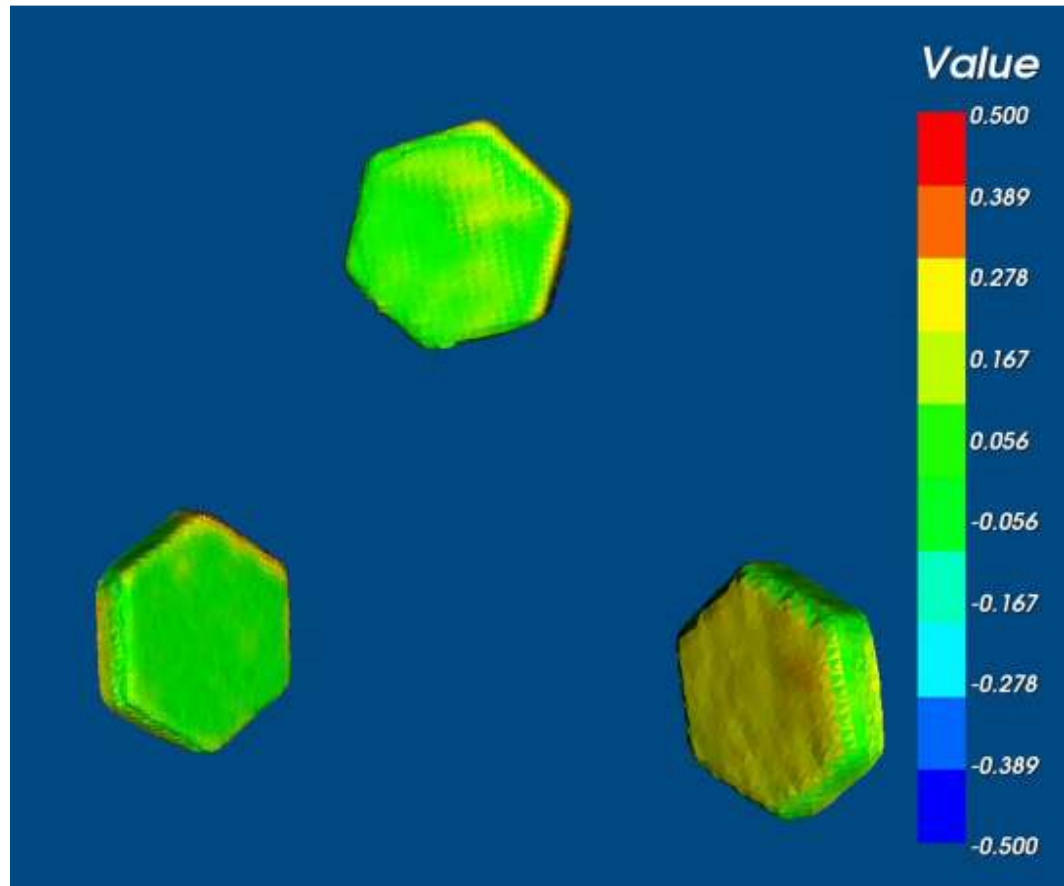
Figure 4.11 Colour error map showing differences between Markers in patient's mandible acquired from a CBCT 0.4 vox scan in situ and CBCT 0.2 vox scanned images of their dental cast.

Chapter Five

Discussion

Discussion Part I

5.1 CBCT imaging

Cone Beam CT is rapidly evolving as the routine imaging modality specifically designed for the maxillofacial region allowing users to view and interact with virtual images in the three planes of space. This offers a significant advancement in the diagnosis and planning of orthognathic surgery and assists patients in their understanding of how their facial appearance is likely to change following orthognathic surgery for the correction of maxillofacial abnormalities (Nkenke *et al.,* 2004).

An accurate representation of the occlusal surfaces of the teeth in radiographic images is essential. Current CBCT technologies produce images of insufficient accuracy and resolution (Gateno *et al.,* 2003). The presence of metallic objects creates streak artefacts, significantly impairing the accuracy of a virtual model by obliterating the occlusal surfaces of the teeth. This is a major obstacle for occlusal registration which interferes with the fabrication of orthognathic wafers to guide the surgical correction of dentofacial deformities.

The possibility of obtaining a CBCT image without streak artefacts can be achieved if all metallic objects within the oral environment are removed (Odlum, 2001). However to introduce this as routine clinical practice would neither be possible or practical. Removal of orthodontic brackets would be extremely time consuming, expensive and destabilising to the dentition.

In a study by Park *et al.* (2007) silicone impression materials were used to cover the areas of metal present in the oral environment, although this was successful in reducing the severity of the artefacts, no details were provided on the optimum thickness, consistency or density of the material. The addition of impression material in the buccal and labial segments prior to a CBCT scan would be likely to cause distortion of patient's soft tissues and the resultant images would not be of the clarity and quality required.

Metal artefact reduction (MAR) algorithms have been developed to improve the quality of images. The MAR algorithms reduce the severity of artefacts by adapting mathematical calculations to replace the areas of distortion. However as yet, no algorithm has been developed or validated to a level of accuracy that could produce images of suitable clarity and this could introduce further distortions (Park *et al.,* 2007). Advancements and further developments in MAR software may produce images of suitable quality; however this has not yet been achieved.

The only techniques currently available that can produce an accurate representation of the dentition are those that apply image fusion. The creation of a composite model is possible by merging two or more virtual images together. Current methods include simple fusion, triple scans, extra-oral fiducial markers and intra-oral fiducial markers.

Simple fusion is a technique that merges two different modalities of 3D imaging to replace a distorted image with a more accurate image free from streak artefacts. It is relatively easy to achieve, reproducible and does not distort the soft tissues (Nkenke *et al.,* 2004). In this method CT scans and dental casts are imaged using an optical scanner. Corresponding anatomical points are selected on the occlusal surfaces of the images and aligned using the iterative closest point (ICP) algorithm. When applied to dentitions with no metallic restorations there was a mean error of 0.13mm ± 0.03mm at the corresponding data points which were reported. In cases with restored dentitions, the mean error increased to 0.27mm ± 0.06mm but no reason was given for this increase in error.

In a single clinical case report, a mean error of 0.66mm ± 0.49mm *(44% below 0.5mm)* in the mandible and a mean error of 0.56mm ± 0.48mm *(54% below 0.5mm)* for the maxilla was reported (Nkenke *et al.,* 2004). The study concluded that a simple fusion method should be the standard technique for orthognathic surgery simulation, however this technique should be undertaken with caution as the method was only tested on a single patient and the use of optical scanning required specialist training, this may be too financially inhibitive to apply in practice. It is important to note that optical scanned dentition images were

registered on the original CT scan which contained inaccuracies. If streak artefacts in the CT image completely obliterate the occlusal surfaces of the dentition, this method would be impossible.

5.1.1 Cone beam CT triple scan

The Cone Beam CT triple scan is a method that involves the acquisition of three CBCT scans *(two of the patients and one of the dental impressions)*. The technique was designed to enhance a 3D virtual image by producing a composite model with a more detailed representation of the occlusal surfaces and interdental data without deformation of the patient's soft tissues.

This method has been applied to a synthetic skull and the technique was found to be highly accurate with a mean distance 0.08mm ± 0.03mm (ranging from 0.04mm to 0.11mm) when voxel-based registration was applied (Swennen *et al.*, 2009a). The method was applied to ten patients who reported no discomfort from the technique, therefore it was suggested that it should be applied to routine orthognathic planning.

The major disadvantage of this technique was that patients were subjected to two CBCT scans, this would be difficult to justify with current national guidelines on radiation exposure (Department of Health., 2000). Previous publications have assessed the accuracy of dentition replacement by comparing the undistorted dental image to the image of the teeth on the CBCT image. It should be noted that the CBCT image of the teeth is distorted and inaccurate. Therefore it is impossible to determine the validity of the method (Gateno *et al.*, 2003; Swennen *et al.*, 2009a; Uechi *et al.*, 2006).

5.1.2 Extra-oral fiducial markers

Several studies replaced existing virtual dentitions of patients with the use of extra oral fiducial markers (Sohmura *et al.*, 2005; Uechi *et al.*, 2006; Gateno *et al.*, 2003; Gateno *et al.*, 2007).The fiducial markers have been constructed from radiolucent materials in the form of a plate constructed from gypsum (Sohmura *et al.*, 2005), spherical balls manufactured from titanium or ceramic (Gateno *et*

al., 2003; Gateno *et al.,* 2007; Uechi *et al.,* 2006), or from gutta percha (Schutyser *et al.,* 2005).

Each of the methods required a custom manufactured transfer device positioned intra-orally during the CT scan. Impressions were obtained and either laser scanned with the fiducial markers in position (Gateno *et al.,* 2003; Gateno *et al.,* 2007), or gypsum study casts were produced on to which the transfer device was positioned (Uechi *et al.,* 2006) and CT scanned or laser scanned (Sohmura *et al.,* 2005). The distorted dentitions on the initial CT scans were removed leaving only the bone structures of the maxilla and mandible and the virtual fiducial markers. The corresponding virtual fiducial markers with the replacement dentition were then registered on to the original fiducial markers and fused to create a composite skull.

Gateno *et al.* (2003) used titanium fiducial markers as the points of registration on a cadaver skull and the tooth-to-tooth relationship showed a high level of accuracy with a mean difference of 0.1mm. However the technique in its current format could not be applied to patients as the markers were attached to rods and positioned horizontal to the buccal and mesial aspects of the dentition and this would distort patient's soft tissue. The technique was modified by relocating the markers to a more anterior position, protruding beyond the lips and this was trialled on five patients (Gateno *et al.,* 2007). The authors concluded that the replacement dentition was accurate to 0.15mm. It was not possible to establish the validity of the results since the method of analysis was not described.

The findings from Gateno *et al.* (2003) are comparable to those of Uechi *et al,* (2006) who found that their technique had a mean difference of 0.1mm for the tooth difference in analysed point measurements. The validity of these results is difficult to establish as the replacement dentition was compared to the original distorted CBCT dentition. In the method developed by Sohmura *et al.* (2005) the authors stated that the registration of the alveolar process on the virtual dental cast compared to that on the patient's actual alveolar bone had an error of 0.25 mm and concluded that this would be satisfactory for clinical applications. The author was obviously aware that it was not possible to measure the tooth-to-

tooth relationships as the dental images were defective and the dentition had been obliterated due to the presence of metallic artefact.

In the technique described by Schutyser *et al.* (2005) an acrylic occlusal registration device with extra-oral gutta percha spherical markers embedded was developed. This method was validated on ten cadaver skulls and the results showed that when the virtual markers were registered there was a mean error of 0.14mm ± 0.03mm, this was comparable to previous studies (Gateno *et al.*, 2003; Gateno *et al.,* 2007; Uechi *et al.,* 2006). This level of accuracy was considered to be acceptably accurate for the purposes of 3D planning. However the authors reported that it was impossible to register corresponding points on several of the virtual gutta percha markers as several were obliterated by streak artefacts. It was also noted that the optimum size for markers was 1.5mm, any larger markers suffered from a streaking effect similar to that experienced with metallic objects. The technique was then trialled on seven patients and the results showed that the markers were aligned with a mean error 0.16mm ± 0.03mm.

The method of replacing a defective dentition using extra-oral fiducial markers significantly distorts the patients surrounding soft tissues. Some devices opened the patient's bite making it impossible to determine the patient's natural centric occlusion. The previous methods describe the use of a CT scanner for capturing images; this would expose a patient to an increase in radiation compared to a CBCT scan.

5.1.3 Intra-oral fiducial markers

Intra-oral fiducial markers work on the same principal as the extra-oral markers previously described. However the intra-oral fiducial markers are designed to minimise the level of soft tissue deformation (Swennen *et al.,* 2009b).The transfer device is predominantly constructed in wax, which may be prone to distortion if left within the oral cavity for any length of time. The intra-oral gutta percha fiducial markers can also be obliterated by the streak artefacts and inconsistencies in the size of the markers may introduce further errors during the registration process.

The method has been evaluated on ten patients each with a wax bite registration device with radiolucent gutta percha markers embedded and an extension positioned in the palatal vault for the purposes of registration similar to the method described by Schutyser *et al.* (2005). Results showed a registration error ranging from 0.04mm to 0.53mm on the markers, with a mean registration error of 0.18mm ± 0.10mm. Although the results were considered to be clinically acceptable by Swennen *et al.* (2009b) there is no evidence supporting the conclusion that the dentition would be replaced to the same level of accuracy, as previously described this is impossible to achieve.

A major disadvantage of this technique is its implementation into the clinical environment. The method described is very time consuming, specialist computing expertise and hardware are required and the need for multiple point-based registration is likely to introduce unwanted errors.

5.2 Methodology of a new innovative intra-oral registration device

The aim of this pilot study was to develop a new method of replacing inaccurate images of the dentition using the positive attributes of the techniques previously discussed and by overcoming the shortcomings associated with each method.

5.2.1 Evolution of a new intra-oral registration device

To establish the final design of the new registration device several prototypes had to be developed and tested prior to establishing the final design Figure 5.1. Each new design overcame the problems of its predecessor until it evolved into the final design that was introduced into the clinical environment.

The first attempt design "A" was an intra-oral registration device that used fiducial markers positioned bucally and labially. The design was immediately discarded. The fiducial markers would distort soft tissues and be too complex to manufacture, this was supported by previous studies (Gateno *et al.,* 2003; Gateno *et al.,* 2007; Schutyser *et al.,* 2005; Sohmura *et al.,* 2005; Uechi *et al.,* 2006).
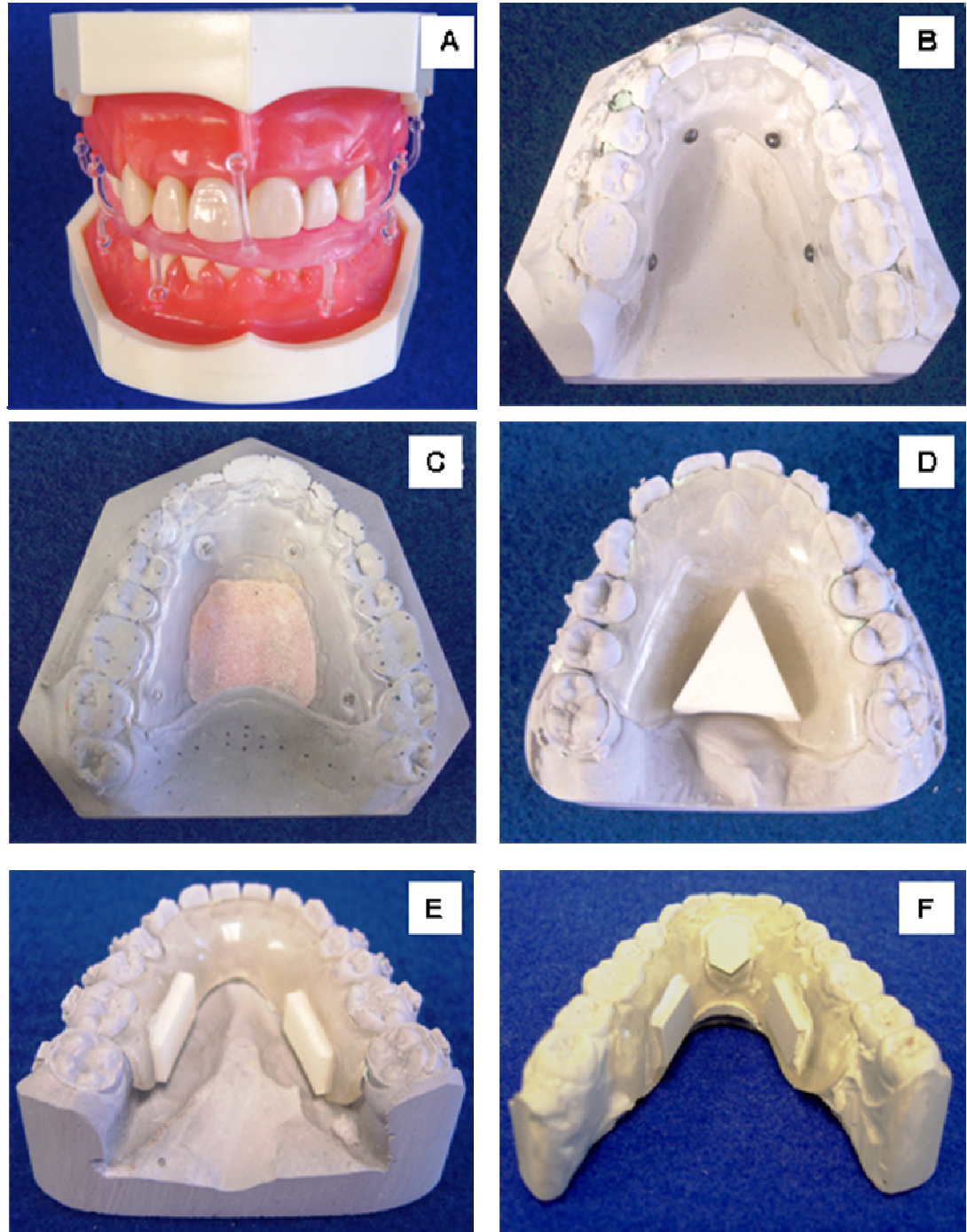
Figure 5.1 Prototype intra-oral registration devices

Design "B" introduced a new and untried technique that positioned markers above and below the level of the clinical crowns on the palatal and lingual aspects of the jaws, this prevented the markers from being obliterated by streak artefacts which had been a problem identified by Swennen *et al.* (2009b). The design also prevented any unwanted distortion of the soft tissues that had affected previous studies (Gateno *et al.,* 2003; Gateno *et al.,* 2007; Schutyser *et al.,* 2005; Sohmura *et al.,* 2005; Uechi *et al.,* 2006). Initial testing was encouraging with the appliance being stable on the dental casts; however when the appliance was fitted on a dry cadaver skull and scanned using CBCT, It was found that the images of the spherical titanium markers caused streak artefacts changing the shape and dimensions of the markers. The size of the virtual images of the markers was too small to apply the semi-automated ICP algorithm. This has not been previously reported and may have been due to the type of CT scanner, i.e. CBCT or the software algorithm used in image segmentation, even though the technique had been previously used (Gateno *et al.,* 2003; Gateno *et al.,* 2007; Uechi *et al.,* 2006).

Given the fact that the titanium markers surface area was too small to align the two images a patch of barium was placed in the palatal vault, design "C". This patch was designed to create a radiopaque area that would allow application of the semi-automated ICP on the corresponding virtual images (Nkenke *et al.,* 2004; Schutyser *et al.,* 2005; Swennen *et al.,* 2009b). Titanium markers were still included to create points that could be easily identified on both images for rigid registration (Gateno *et al.,* 2003; Gateno *et al.,* 2007). The radiopaque barium was easily identified on the CBCT scan, but unfortunately the barium patch was flush with the palatal aspect of the intra-oral device and would therefore not appear on the surface laser scan. This would prevent image registration.

The titanium markers were discarded in designs "D" and "E" as they were no longer required, the 3D markers provided enough visual information for the initial registration and were constructed from a combination of barium and MP2 orthodontic acrylic. The markers were constructed of a sufficient size that would allow the application of ICP (Nkenke *et al.,* 2004; Schutyser *et al.,* 2005; Swennen *et al.,* 2009b). The 3D markers were partially embedded into the

acrylic baseplate with two thirds standing proud. This allowed laser scanning to capture a 3D representation of the markers in order to overcome the deficiencies of the previous prototypes. A major disadvantage of the method was the denser areas of barium created artefacts; this caused more problems and the quality of CBCT image varied depending on the concentration of barium within each marker. This rendered the use of barium markers useless since they were extremely difficult to consistently reproduce.

In design "F" the material for constructing the markers was changed to a class IV dental stone similar in its properties and density to ceramic (Sohmura *et al.,* 2005; Uechi *et al.,* 2006). The fundamental design of the registration device remained the same as devices "D" and "E"; however the size and shape of the markers were uncomfortable for patients; therefore it was modified in the final design.

5.2.2 Intra-oral registration device

The intra-oral registration device shown in Figure 5.2 has been designed to overcoming the shortcomings of previous devices. The baseplate was constructed of a bio-compatible self-curing orthodontic acrylic routinely used for the construction of removable and functional orthodontic appliances (Swennen *et al.,* 2007). The baseplate material was dimensionally stable, and did not distort from heat within the oral cavity, which affected previous methods (Swennen *et al.,* 2009b). The acrylic was easily segmented from virtual images because of the large differential in HU values between bone, teeth and acrylic (Gateno *et al.,* 2003; Gateno *et al.,* 2007; Schutyser *et al.,* 2005; Sohmura *et al.,* 2005; Swennen *et al.,*2009a; Swennen *et al.,* 2009b; Uechi *et al.,* 2006).

Incorporating the markers into the baseplate was a straight forward procedure. The gypsum material used was already in everyday use making the technique cost effective. The appliance was designed to be comfortable, non-invasive and securely positioned on the palatal and lingual aspects of the maxilla and mandible. The markers were below the level of the clinical crowns preventing any occlusal interference or deformation of the facial soft tissues which had

Figure 5.2   Intra-oral registration device.

occurred in previous studies (Gateno *et al.,* 2003; Gateno *et al.,* 2007; Schutyser *et al.,* 2005; Sohmura *et al.,* 2005; Swennen *et al.,* 2007; Uechi *et al.,* 2006).

The device was easily fitted to patients with very little additional clinical time required. No additional CBCT scans were required (Swennen *et al.,* 2009a). Alginate impressions were taken of the patients with the appliances in situ and cast in dental stone which were scanned using the CBCT scanner; therefore no additional scanning hardware required to be purchased (Gateno *et al.,* 2003; Gateno *et al.,* 2007; Sohmura *et al.,* 2005; Uechi *et al.,* 2006). The option of laser scanning the dental casts was also available, but the present study showed that the accuracy of laser scanning and CBCT of the dental models was very similar and not clinically significant.

The images produced from the CBCT were converted into the common file format STL and decimated, thus significantly reducing the amount of computing power required than had been required with previous methods (Swennen *et al.,* 2009b). The virtual images of the markers were clear and showed no signs of the distortion that had been previously reported (Schutyser *et al.,* 2005; Swennen *et al.,* 2009b). The images were of sufficient size so that the ICP algorithm could be applied, allowing the technique to be predominantly computer automated and removing operator variability (Swennen *et al.,* 2007).

Discussion Part II

5.3   The clinical situation

The accuracy of replacement of the distorted dentition with the corresponding virtual dental models on the dried skulls was assessed by measuring the distances between corresponding points on the mesh surfaces. Depending on the orientation and overlap of the meshes both negative and positive distances could result, if the conventional mean values were used the negative and positive values would cancel each other out underestimating the error. For this reason the absolute mean value, regardless of sign, was used to calculate the error of replacement. Previous studies have also used a similar method of assessment called the root mean square error (Swennen *et al.,* 2009a). The problem with this method is that any outlying points will positively bias the results and may overestimate the error. When superimposing meshes it is inevitable that a small part of one mesh may be missing, this will result in an outlier in the measurement since a corresponding point cannot be found on the second mesh. In order to resolve this only 90% of the superimposed mesh points were used (Kau *et al.,* 2006).

The present method of replacing the distorted dentition relies on an intra-oral device with intra-oral markers that align accurately.   Accordingly a mean absolute superimposition error of around 0.09mm was recorded between the marker surfaces of the dried skull (0.4mm voxel CBCT) and the markers on the plaster dentition (0.2mm voxel CBCT). Ideally the dried skull should have been scanned at the higher resolution of 0.2mm voxel. This could have produced even less error in the superimposition but this could not be transferred into the clinical arena since 0.4mm voxel CBCT scans are the norm for patients. This magnitude of error is similar to previous studies (Swennen *et al.,* 2007; Schutyser *et al.,* 2005), where the results found an error of about 0.14mm.

The mean absolute error of the superimposed markers based on the dried skull was in the region of 0.09mm therefore it could be assumed that when the dentition was reintroduced the error between the CBCT image of the dentition

and the replacement images would be similar. However when the images of the dentitions were compared the absolute mean distances between the meshes was around 0.26mm in the mandible and 0.22mm in the maxilla. Therefore 0.1mm of the 0.26mm and 0.2mm mean absolute error could be attributed to magnification of the CBCT image of the dried skull dentition.

This error was not unexpected as previous work by Al-Rawi *et al*. (2010) stated that the presence of enamel in the body degrades the x-ray beam resulting in beam hardening. This makes it impossible to keep the beam completely uniform and may account for some of the increase in error between the dentitions due to magnification. This was confirmed by acquiring and registering images of a dried mandible by both CBCT scanning (0.4mm voxels) and laser scanning. The discrepancies on bone of the aligned images were in the region of 0.16mm. However when the dentition from both images was reintroduced and analysed the magnitude of error increased on average by 0.10mm to 0.25mm.

The increase in error between the markers on marker (0.9mm) and bone on bone (0.16 mm) may be accounted for as positional error, this would mean that the meshes from the virtual images do not perfectly align and introduce small discrepancy. The fiducial markers are uniform three dimensional structures with a constant density, whereas bone varies in size, density and shape. This can affect the 0.4mm voxel CBCT x-ray beam and the software that reconstructs the images; however the increase in error was only 0.07mm which would be regarded as an acceptable level of alignment. Reviewing current literature and the methods comparable to this study, no other author appears to have accounted for these errors.

In an attempt to determine if the CBCT 0.4mm voxel scanned fiducial markers had distorted during scanning the markers were also imaged by laser scanning and aligned, the errors were in the region of 0.08mm ± 0.02mm. This supported the findings that 0.4mm voxel CBCT images of the fiducial markers could be registered onto laser scanned images with a high degree of accuracy. A potential shortcoming of this technique was the requirement of additional hardware for laser images i.e. the laser scanner. Cone Beam CT 0.2mm voxel scans were taken of gypsum study casts and registered and compared with the laser scans of

the same models. This proved to be very encouraging; there was an error of 0.06 mm between the CBCT and the laser images. The error was determined as clinically insignificant and CBCT 0.2mm voxel was established as the preferred technique for imaging study casts with the fiducial markers.

Having initially validated the methodology in vitro the process was transferred into the clinical arena. A 0.09mm discrepancy between the image of the markers from the patient and the image of the markers from the study casts would have been expected to be similar to the findings on the dried cadaver skulls. However the mean absolute error between meshes increased to 0.16mm for the mandible and 0.12mm for the maxilla, which was very similar to the findings by Swennen *et al.,* (2008) who recorded a marker on marker error of about 0.18mm in ten patient cases. The most likely cause for this increase in error is the introduction of soft tissue; the previous trials had all been conducted on dry models and skulls. Overall the increase in error was in the region of 0.05mm and was regarded as clinically insignificant. Table 5.1 shows the absolute mean distance of error between each technique of registering two virtual images of the markers and the standard deviation.

The stages that were applied to replace the dentition on the dried cadaver images were followed for the patient cases. Since the magnitude of error in registering the two corresponding images of markers had increased, it can be assumed that the same magnitude of error would be likely to occur with the dentition; however as Sohmura *et al.* (2005) had already stated if images contain metallic streak artefacts then the ability to assess discrepancies between the old and new replacement virtual dentition is not possible. If it is assumed that the increase in error is consistent then the new dentition would be registered in the region of 0.29mm which would be regarded as clinically satisfactory. Table 5.2 shows the absolute mean distance of error for each experiment conducted with their corresponding standard deviation.

Table 5.1   Absolute mean distance of error between techniques for registering virtual images of markers.

	Absolute mean distance between 90% of mesh overlap (mm)	Standard Deviation
CBCT & laser scanned markers superimposed	0.08	0.02
0.4mm voxel CBCT mandible markers & 0.2mm voxel CBCT plaster model markers superimposed	0.09	0.01
0.4mm voxel CBCT maxilla markers & 0.2mm voxel CBCT plaster model markers superimposed	0.10	0.03
CBCT patient markers for mandible & markers on CBCT plaster models superimposed	0.16	0.02
CBCT patient markers for maxilla & markers on CBCT plaster models superimposed	0.12	0.04

Table 5.2   Absolute mean distance of error for each experiment conducted.

	Absolute mean distance between 90% of mesh overlap (mm)	Standard Deviation
CBCT & laser scanned mandibles superimposed bone only	0.16	0.07
CBCT & laser scanned mandibles superimposed on bone to determine tooth magnification	0.25	0.14
CBCT & laser scanned markers superimposed	0.08	0.02
CBCT & laser scanned plaster dental models superimposed	0.06	0.01
0.4mm voxel CBCT mandible markers & 0.2mm voxel CBCT plaster model markers superimposed	0.09	0.01
0.4mm voxel CBCT maxilla markers & 0.2mm voxel CBCT plaster model markers superimposed	0.10	0.03
CBCT dried mandibular dentition superimposed on CBCT plaster models using markers only	0.26	0.11
CBCT dried maxillary dentition superimposed on CBCT plaster models using markers only	0.22	0.07
CBCT patient markers for mandible & markers on CBCT plaster models superimposed	0.16	0.02
CBCT patient markers for maxilla & markers on CBCT plaster models superimposed	0.12	0.04

Although no direct comparisons could be made with some of the previous publications Nkenke *et al*. (2004) noted errors in the region of 0.56mm for the replacement of dentition in patients, which was regarded to be of sufficient accuracy to act as the standard protocol for orthognathic surgery simulation. The methods by Uechi *et al*. (2006) and Swennen *et al*. (2009a) used the root mean square (RMS) error to assess the discrepancies between centres of the fiducial markers when aligning using three stages of registration, it has already been noted that using the RMS method will positively bias results and overestimate the results.

5.3.1 Specific statistical considerations

Due to the small sample size of six cases, it was not appropriate to apply statistical tests to see if there was a statistical difference between laser scanned and CBCT recorded images. The accuracy of the two techniques in recording 3D surface morphology of the dental casts was within a tenth of a millimetre which provided clinical confidence in the technology. If we were using a larger sample size and a different imaging modality it would be appropriate to conduct more sophisticated statistics to highlight the significance of the findings. The use of a surface mesh is a comprehensive method of evaluating the accuracy of recording morphological characteristics. This was fully exploited in this study rather than using individual landmarks which may not represent the underlying morphology as comprehensively as surface meshes.

5.3.2 Future work

Currently the only methods capable of creating an accurate virtual representation of the dentition create a composite skull through image fusion. However these techniques can only replace the dentition with limited accuracy. The intra-oral device presented in the current study has been successfully used in overcoming a number of the problems associated with the previous methods; however there are areas of the technique that require further assessment.

The aim of this pilot study was to replace the existing dentition of an image acquired by 0.4mm voxel CBCT and validate the technique. The reason why the

method could not be validated on patients was that there was no currently available method to directly capture the patients dentition and intra-oral devices simultaneously. This obviously was readily available on dried skulls. The CBCT image of the dentition could not be used as the "gold standard" since it was magnified and distorted. The method was validated on cadaver skulls with an error of 0.24mm. Future work could involve the use of intra-oral scanners. These scanners are able to record the dentition in a 3D digital format; this would negate the requirement for obtaining impressions of the dentition from the maxilla and mandible. Obvious advantages of acquiring the digital information directly would be the shortened time required to record the dentition, errors occurring during the impression taking and casting process would be eliminated and the inherent errors of CBCT at 0.2mm Voxel and the conversion from a DICOM format to the common file format STL would be removed.

Intra-oral cameras that are currently available capture the dentition by emitting some form of light or by acquiring 3D photographic images. The limitations of current systems are that they have been primarily designed for scanning individual teeth or quadrants and are unable to image structures in the palatal and lingual vaults. Future advancements of intra-oral systems would allow the capture of full dental arches and the fiducial markers required for the registration of the replacement images. If this were to be successful it might be possible to design a technique that would validate this method.

An immediate improvement to the new registration device would be CBCT imaging of the mandibular and maxillary impressions with the registration devices in situ. This is currently being evaluated and preliminary results have shown that it is possible to invert the image of the impressions to create a virtual study model with the fiducial markers in position, if this procedure proves comparable to the existing method of casting impressions in gypsum then this approach would significantly improve the efficiency of the overall process removing errors associated with model casting.

The use of metallic restorations is decreasing these being replaced with composite alternatives and plastic brackets are available for a limited number of orthodontic cases. These materials are less dense than their metallic

counterparts, this allows the x-ray beam to penetrate deeper by reducing beam hardening. Further studies should be undertaken to evaluate the advantages of non metallic restorations and devices in an oral environment.

Cone Beam CT 0.4mm voxel images do not provide high resolution images of the dentition, but advancements in CBCT scanners and MAR algorithms may allow patients to be imaged at higher resolutions without increasing the exposure to radiation. As new and innovative ways of obtaining 3D images of the hard tissues are being developed it may become possible to image patients without exposing them to x-rays. MRI is the most promising imaging modality that could achieve this and is currently regarded as the gold standard for acquiring soft tissue images (Lewis *et al.,* 2008). Future developments in MRI may adapt this imaging technique to hard tissue.

5.3.3 Future orthognathic planning

Commercially available software packages are now available allowing users to interact with the virtual environment. The use of 3D imaging is revolutionising the prediction and planning of orthognathic surgery and how it is assessed.

The eventual goal for 3D orthognathic planning is the production of an orthognathic wafer. This wafer would be designed using 3D computer aided software and manufactured through rapid prototyping. The computer aided manufacturing systems that are likely to produce these wafers are 3D stereo lithography printing or 3D milling. Both of these methods are currently used in the manufacturing industry; however there are a number of issues associated with 3D wafer production that future developments will hopefully overcome. The wafer produced can only ever be as accurate as the information from which it is designed. This intra-oral registration device is a significant advance in the creation of a composite skull; however no technique is capable of creating the hybrid skull with absolute precision, any errors associated with each stage will be transferred to the virtual and physical wafer.

Interestingly Gateno *et al*. (2003) showed that stereolithographic surgical wafers were comparable to conventionally produced wafers regarding fit. Further work

is required to establish a gold standard of 3D wafer production, the criterion on which this will be measured will be related to cost, bio-compatibility, ease of production, speed of production, reproducibility, strength, durability and accuracy. Only when these standards have been determined should the paradigm shift to 3D wafer production be considered.

Chapter Six

Conclusions

Conclusions

6.1 Conclusions

- This study was successful in developing a method that could replace the distorted dentition acquired from a CBCT scan with an accurate digital representation.

- The technique showed satisfactory results for the accuracy and reproducibility of the method using cadaveric skulls.

- The feasibility of the method was successfully implemented into the clinical environment.

This study did not assess the level of accuracy with which the distorted dentition could be replaced in patients. This was because no current method is capable of capturing the dentition without distortion.

The recommendation is that this method should be utilised for clinical applications on orthognathic surgery patients. It would facilitate comprehensive analysis in the model surgery planning.

Chapter Seven

Appendices

Appendices

7.1   Appendix I   Ethical approval letter

Acute Services Division

NHS
Greater Glasgow and Clyde

West Glasgow Ethics Committee 2
Western Infirmary
Dumbarton Road
Glasgow
G11 6NT

Telephone: 0141 211 620
Facsimile: 0141 211 1920

18 March 2009

Mr Neil Nairn
Glasgow Dental Hospital & School
378 Sauchiehall Street
Glasgow
G2 3JZ

Dear Mr Nairn

Full title of study:	A study aimed to assess the accuracy with which digital study models can replace dental structures on low dose cone beam CT scanned images.
REC reference number:	09/S0709/24

The Research Ethics Committee reviewed the above application at the meeting held on 17 March 2009. Thank you for attending to discuss the study.

Ethical opinion

The committee reviewed the above submission and had no ethical issues with this.

The committee did however require the undernoted minor amendments to the Information Sheet:

a) Page 2 – "What are the benefits of taking part etc" - amend "would" to read "may".
   Page 2 - 3rd line - "will" should read "may"
b) Page 2 – "Who is funding the study" - should be amended
c) The independent contact person on page 7 of the submission should be added to the PIS.

The above minor amendments should come back to the secretary for checking and filing

The members of the Committee present gave a favourable ethical opinion of the above research on the basis described in the application form, protocol and supporting documentation, subject to the conditions specified below.

Ethical review of research sites

The Committee agreed that all sites in this study should be exempt from site-specific assessment (SSA). There is no need to submit the Site-Specific Information Form to any Research Ethics Committee. The favourable opinion for the study applies to all sites involved in the research.

Delivering better health

www.nhsggc.org.uk

42369

Conditions of the favourable opinion

The favourable opinion is subject to the following conditions being met prior to the start of the study.

Management permission or approval must be obtained from each host organisation prior to the start of the study at the site concerned.

Management permission at NHS sites ("R&D approval") should be obtained from the relevant care organisation(s) in accordance with NHS research governance arrangements. Guidance on applying for NHS permission is available in the Integrated Research Application System or at http://www.rdforum.nhs.uk.

Approved documents

The documents reviewed and approved at the meeting were:

Document	Version	Date
Supervisor CV		27 February 2009
Participant Consent Form	1.0	27 February 2009
Participant Information Sheet	1.0	27 February 2009
Covering Letter		27 February 2009
Protocol	1.0	27 February 2009
Investigator CV		27 February 2009
Application	2.0	27 February 2009

Membership of the Committee

The members of the Ethics Committee who were present at the meeting are listed on the attached sheet.

Statement of compliance

The Committee is constituted in accordance with the Governance Arrangements for Research Ethics Committees (July 2001) and complies fully with the Standard Operating Procedures for Research Ethics Committees in the UK.

After ethical review

Now that you have completed the application process please visit the National Research Ethics Website > After Review

You are invited to give your view of the service that you have received from the National Research Ethics Service and the application procedure. If you wish to make your views known please use the feedback form available on the website.

The attached document "After ethical review – guidance for researchers" gives detailed guidance on reporting requirements for studies with a favourable opinion, including:

- Notifying substantial amendments
- Progress and safety reports
- Notifying the end of the study

The NRES website also provides guidance on these topics, which is updated in the light of changes in reporting requirements or procedures.

We would also like to inform you that we consult regularly with stakeholders to improve our service. If you would like to join our Reference Group please email referencegroup@nres.npsa.nhs.uk.

09/S0709/24	Please quote this number on all correspondence

With the Committee's best wishes for the success of this project

Yours sincerely

Ancha A Torrie
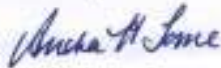
Dr S Langridge
Chair

Email: andrea.torrie@ggc.scot.nhs.uk

Enclosures: List of names and professions of members who were present at the meeting and those who submitted written comments
"After ethical review – guidance for researchers" SL-AR2

Copy to: Dr Melissa McBride

Dr Balvinder Khambay, University of Glasgow

144

7.2   Appendix II   Patient Information

Patient Information Sheet

Title of study

A study aimed to assess the accuracy with which digital study models can replace dental structures on low dose cone beam CT scanned images.

You have been invited to take part in a research study. Before you decide whether or not to take part, it is important for you to understand why the research is being done and what it will involve. Please take time to read the following information carefully and discuss it with others, if you wish. Ask us if there is anything that is not clear, or if you would like more information. Take time to decide whether or not you wish to take part.

Thank you for reading this information.

What is the purpose of the study?

You have been seen on numerous occasions by the Clinical Team in order to prepare you for surgical correction of your facial appearance. The routine final planning stages involve a low dose CT scan of your head, including your teeth. Unfortunately the metal brace and fillings on your teeth cause distortion of the CT image, which interfere with planning your operation.   The aim of this investigation is to assess whether it is possible to remove the distorted parts of the image and replace them with the correct images.

Why you have been invited to take part in this study.

You are about to undergo surgical correction of your facial appearance.

Do I have to take part in the study?

It is up to you to decide whether or not you would like to take part in this study. If you decide to take part in this investigation, you will be given this information sheet to keep and you will be asked to sign a consent form.

What will happen if I decide to take part in the study?

If you consent to take part in this investigation, you would be asked to attend your pre-planning clinics as normal. The only addition would be that when the routine CT scan is taken at the Glasgow Dental Hospital & School you will be asked to wear a small removal brace which would have been made previously on moulds for your teeth. The CT scan is routine and will take place regardless of whether you consent to the study.

What are the side effects of this imaging?

There are no risks or side effects from these removable braces.

What are the benefits of taking part in the study?

You may not have a direct benefit in contributing to this study; however, it may provide us with useful information regarding future planning of patients similar to yourself. Based on the findings, the surgical techniques may be fine-tuned and we may be able to provide realistic information regarding the anticipated result of this surgery for future patients.

Will my information be kept confidential?

All the information that is collected in this study will be kept strictly confidential. Any information that may leave the hospital for further analysis at the Statistics Department will have the names and addresses removed so that they cannot be recognised.

What will happen to the results of the research study?

We intend to publish our findings in the medical press. Your image will not be able to be identified from the article. If you are interested, we can provide you with a copy when it is published.

Who is funding the research?

This study is being funded by the Biotechnology and Craniofacial Section of the Glasgow Dental School & Hospital.

Who has reviewed the study?

The study has been reviewed and approved by Greater Glasgow West Research Ethics Committee.

If you need more information or you wish to ask questions before you decide whether you will take part in this investigation, please contact Dr Balvinder Khambay, Glasgow Dental Hospital & School or Mr Philip Benington, Glasgow Dental Hospital & School.

7.3 Appendix III Consent Form

NHS
Greater
Glasgow

North Glasgow University Hospitals Division

Patient Consent Form (Adult)

Pilot study: A study aimed to assess the accuracy with which digital study models can replace dental structures on low dose cone beam CT scanned images.

Patient's name:
_____

Date of birth:
_____

		Yes
	No	
1.	Have you read the information sheet?	☐
	☐	
2.	Do you understand the study?	☐
	☐	
3.	Did we answer all of your questions?	☐
	☐	
4.	Do you want to take part in this study?	☐
	☐	
5.	Are you happy for your captured image to be used for publication?	☐

Who have you spoken to?

Dr/Mr/Mrs/Prof.
_____

Do you understand that you can change your mind at any time? **Yes** ☐ **No** ☐

Signed:
_____

Name (print):
_____

Signature of witness:
_____

Name (print):
_____

Chapter Eight

References

References

Abdoli, M., Ay, M.R., Ahmadian, A., Dierckx, R.A., & Zaidi, H. Reduction of dental filling metallic artifacts in CT-based attenuation correction of PET data using weighted virtual sinograms optimized by a genetic algorithm. *Medical Physics* 2010; **37**: 6166-6177

Akizuki, H., Yoshida, H., & Michi, K. Ultrasonographic evaluation during reduction of zygomatic arch fractures. *Journal of Cranio-Maxillo-Facial Surgery*; 1990; **18**: 263-266

AL-RAWI, B., HASSA, B., VANDENBERGE, B., & JACOBS, R. Accuracy asessment of three-dimensional surface reconstructions of teeth from Cone Beam Computed Tomography scans. *Journal of Oral Rehabilitation*; 2010; **37**: 1-7

Arai, Y., Tammisalo, E., Iwai, K., Hashimoto, K., & Shinoda, K. Development of a compact computed tomographic apparatus for dental use. *Dento-Maxillo-Facial Radiology*; 1999; **28**: 245-8

Arridge, S., Moss, J.P., Linney, A.D., & James, D.R. Three dimensional digitization of the face and skull. *Journal of Maxillofacial Surgery*; 1985; **13**: 136-143

Asquith, J., Gillgrass, T., & Mossey, P. Three-dimensional imaging of orthodontic models: a pilot study. *European Journal of Orthodontics*; 2007; **29**: 517-522

Ayoub, A.F., Wray, D., Moos, K.F., Jin, J., Niblett, T.B., Urquhart, C., Mowforth, P., & Siebert, P. A three-dimensional imaging system for archiving dental study casts: a preliminary report. *International Journal of Adult Orthodontics and Orthognathic Surgery*; 1997: **12**: 79-84

Ayoub, A.F., Siebert, P., Moos, K.F., Wray, D., Urquhart, C., & Niblett, T.B. A vision-based three-dimensional capture system for maxillofacial assessment and surgical planning. *British Journal of Oral and Maxillofacial Surgery*; 1998; **36**: 353-357

Ayoub, A.F., Garrahy, A., Hood, C., White, J., Bock, M., Siebert, J.P., Spencer, R., & Ray, A. Validation of a vision-based, three-dimensional facial imaging system. *Cleft Palate-Craniofacial Journal;* 2003; **40**: 523-529

Ayoub, A.F., Xiao, Y., Khambay, B., Siebert, J.P., & Hadley, D. Towards building a photo-realistic virtual human face for craniomaxillofacial diagnosis and treatment planning. *International Journal of Oral and Maxillofacial Surgery;* 2007; **36**: 423-428

Bal, M. & Spies, L. Metal artifact reduction in CT using tissue-class modeling and adaptive prefiltering. *Medical Physics*; 2006; **33**: 2852-2859

Bamber, M.A., Harris, M., & Nacher, C. A validation of two orthognathic model surgery techniques. *Journal of Orthodontics*; 2001; **28**: 135-142

Bamber, M.A. & Vachiramon, A. Surgical wafers: a comparative study. *Journal of Contemporary Dental Practice;* 2005; **6**: 99-106

Barbenel, J.C., Paul, P.E., Khambay, B.S., Walker, F.S., Moos, K.F., & Ayoub, A.F. Errors in orthognathic surgery planning: the effect of inaccurate study model orientation. *International Journal of Oral and Maxillofacial Surgery*; 2010; **39**: 1103-1108

Barrett, J.F. & Keat, N. Artifacts in CT: recognition and avoidance. *Radiographics*; 2004; **24**: 1679-1691

Bearcroft, P.W. Imaging modalities in the evaluation of soft tissue complaints. *Best Practice and Research in Clinical Rheumatology*; 2007; **21**: 245-259

Bell, A., Ayoub, A.F., & Siebert, P. Assessment of the accuracy of a three-dimensional imaging system for archiving dental study models. *Journal of Orthodontics*; 2003; **30**: 219-223

Bishara, S.E., Treder, J.E., & Jakobsen, J.R. Facial and dental changes in adulthood. *American Journal of Orthodontics and Dentofacial Orthopedics*; 1994; **106**: 175-186

Bowley, J.F., Michaels, G.C., Lai, T.W., & Lin, P.P. Reliability of a facebow transfer procedure. *The Journal of Prosthetic Dentistry*; 1992; **67**: 491-498

Broadbent, B.H. A new x-ray technique and its application to orthodontia. *The Angle Orthodontist*; 1931; **1**: 45-66

Burke, P.H. & Beard, L.F.H. Stereophotogrammetry of the face : A preliminary investigation into the accuracy of a simplified system evolved for contour mapping by photography. *American Journal of Orthodontics*; 1967; **53**: 769-782

Burke, P.H., Banks, P., Beard, L.F., Tee, J.E., & Hughes, C. Stereophotographic measurement of change in facial soft tissue morphology following surgery. *British Journal of Oral Surgery*; 1983; **21**: 237-245

Commer, P., Bourauel, C., Maier, K., & Jager, A. Construction and testing of a computer-based intraoral laser scanner for determining tooth positions. *Medical Engineering and Physics*; 2000; **22**: 625-635

Da Silveira, A.C., Daw, J.L., Jr., Kusnoto, B., Evans, C., & Cohen, M. Craniofacial applications of three-dimensional laser surface scanning. *Journal of Craniofacial Surgery*; 2003; **14**: 449-456

De Man, B., Nuyts, J., Dupont, P., Marchal, G., & Suetens, P. Reduction of metal streak artifacts in X-ray computed tomography using a transmission maximum a posteriori algorithm. *Nuclear Science, IEEE Transactions on*; 2000; **47**: 977-981

Dean, D., Hans, M.G., Bookstein, F.L., & Subramanyan, K. Three-dimensional Bolton-brush growth study landmark data: Ontogeny and sexual dimorphism of the Bolton standards cohort. *Cleft Palate-Craniofacial Journal*; 2000; **37**: 145-156

Denisyuk, Y.N. On the reflection of optical properties of an objectin a wave field of light scattered by it. *Doklady Akademii Nauk SSSR*; 1962; **144**: 1275-1278

Eggers, G., Rieker, M., Kress, B., Fiebach, J., Dickhaus, H., & Hassfeld, S. Artefacts in magnetic resonance imaging caused by dental material. *Magma*; 2005; **18**: 103-111

Ellis III, E. Accuracy of model surgery: Evaluation of an old technique and introduction of a new one. *Journal of Oral and Maxillofacial Surgery*; 1990; **48**: 1161-1167

Ferrario, V.F., Sforza, C., Miani, A., Jr., & Serrao, G. A three-dimensional evaluation of human facial asymmetry. *Journal of Anatomy*; 1995; **186**: 103-10

Ferrario, V.F., Sforza, C., Poggio, C.E., & Serrao, G. Facial three-dimensional morphometry. *American Journal of Orthodontics and Dentofacial Orthopedics*; 1996; **109**: 86-93

Gabor, D. A new microscopic principle. *Nature*; 1948; **161**: 777

Gabrani, M. & Treiak, O. J. A novel interpolation problem: surface based matching; 1998; **1**: 793-797.

Ganz, S.D. Cone Beam Computed Tomography-assisted Treatment Planning Concepts. *Dental Clinics of North America*; 2011; **55**: 515-536

Gateno, J., Forrest, K.K., & Camp, B. A comparison of 3 methods of face-bow transfer recording: Implications for orthognathic surgery. *Journal of Oral and Maxillofacial Surgery*; 2001; **59**: 635-640

Gateno, J., Xia, J., Teichgraeber, J.F., & Rosen, A. A new technique for the creation of a computerized composite skull model. *Journal of Oral and Maxillofacial Surgery*; 2003; **61**: 222-7

Gateno, J., Xia, J.J., Teichgraeber, J.F., Christensen, A.M., Lemoine, J.J., Liebschner, M.A., Gliddon, M.J., & Briggs, M.E. Clinical feasibility of computer-aided surgical simulation (CASS) in the treatment of complex cranio-maxillofacial deformities. *Journal of Oral and Maxillofacial Surgery*; 2007; **65**: 728-734

Gold, B.R. & Setchell, D.J. An investigation of the reproducibility of face-bow transfers. *Journal of Oral Rehabilitation*; 1983; **10**: 495-503

Hajeer, M.Y., Ayoub, A.F., Millett, D.T., Bock, M., & Siebert, J.P. Three-dimensional imaging in orthognathic surgery: the clinical application of a new method. *International Journal of Adult Orthodontics and Orthognathic Surgery;* 2002; **17**: 318-30

Hajeer, M.Y., Millett, D.T., Ayoub, A.F., & Siebert, J.P. Applications of 3D imaging in orthodontics: part I. *Journal of Orthodontics:* 2004a: **31**: 62-70

Hajeer, M.Y., Millett, D.T., Ayoub, A.F., & Siebert, J.P. Applications of 3D imaging in orthodontics: part II. *Journal of Orthodontics*; 2004b; **31**: 154-62

Harradine, N., Suominen, R., Stephens, C., Hathorn, I., & Brown, I. Holograms as substitutes for orthodontic study casts: a pilot clinical trial. *American Journal of Orthodontics and Dentofacial Orthopedics*; 1990; **98**: 110-116

Harrell, W.E., Jr., Hatcher, D.C., & Bolt, R.L. In search of anatomic truth: 3-dimensional digital modeling and the future of orthodontics. *American Journal of Orthodontics and Dentofacial Orthopedics*; 2002; **122**: 325-330

Heike, C.L., Upson, K., Stuhaug, E., & Weinberg, S.M. 3D digital stereophotogrammetry: a practical guide to facial image acquisition. *Head and Face Medicine*; 2010; **6**: 18

Hell, B. 3D sonography. *International Journal of Oral and Maxillofacial Surgery*; 1995; **24**: 9

Hirogaki, Y., Sohmura, T., Satoh, H., Takahashi, J., & Takada, K. Complete 3-D reconstruction of dental cast shape using perceptual grouping. *IEEE Transactions on Medical Imaging*; 2001; **20**: 1093-1101

Jakel, O. & Reiss, P. The influence of metal artefacts on the range of ion beams. *Physics in Medicine and Biology*; 2007; **52**: 635-644

Kalender, W.A. X-ray computed tomography. *Physics in Medicine and Biology*; 2006; **51**: 29-43

Kau, C.H., Zhurov, A., Scheer, R., Bouwman, S., & Richmond, S. The feasibility of measuring three-dimensional facial morphology in children. *Orthodontics and Craniofacial Research*; 2004; **7**: 198-204

Kau, C.H., Zhurov, A., Bibb, R., Hunter, L., & Richmond, S. The investigation of the changing facial appearance of identical twins employing a three-dimensional laser imaging system. *Orthodontics and Craniofacial Research*; 2005; **8**: 85-90

Kau, C.H., Richmond, S., Savio, C., & Mallorie, C. Measuring Adult Facial Morphology in Three Dimensions. *The Angle Orthodontist*; 2006; **76:** 773-778

Keating, P.J., Parker, R.A., Keane, D., & Wright, L. The holographic storage of study models. *British Journal of Orthodontics*; 1984; **11**: 119-25

Keating, A.P., Knox, J., Bibb, R., & Zhurov, A.I. A comparison of plaster, digital and reconstructed study model accuracy. *Journal of Orthodontics*; 2008; **35**: 191-201

Khambay, B., Nebel, J.C., Bowman, J., Walker, F., Hadley, D.M., & Ayoub, A. 3D stereophotogrammetric image superimposition onto 3D CT scan images: the future of orthognathic surgery. A pilot study. *International Journal of Adult Orthodontics and Orthognathic Surgery*; 2002; **17**: 331-341

Khambay, B., Nairn, N., Bell, A., Miller, J., Bowman, A., & Ayoub, A.F. Validation and reproducibility of a high-resolution three-dimensional facial imaging system. *British Journal of Oral and Maxillofacial Surgery*; 2008: **46**: 27-32

Kondo, A., Hayakawa, Y., Dong, J., & Honda, A. Iterative correction applied to streak artifact reduction in an X-ray computed tomography image of the dento-alveolar region. *Oral Radiology*; 2010; **26**: 61-65

Kragskov, J., Bosch, C., Gyldensted, C., & Sindet-Pedersen, S. Comparison of the reliability of craniofacial anatomic landmarks based on cephalometric radiographs and three-dimensional CT scans. *Cleft Palate-Craniofacial Journal*; 1997; **34**: 111-6

Kusnoto, B. & Evans, C.A. Reliability of a 3D surface laser scanner for orthodontic applications. *American Journal of Orthodontics and Dentofacial Orthopedics*; 2002; **122**: 342-348

La Riviere, P.J. & Billmire, D.M. Reduction of noise-induced streak artifacts in X-ray computed tomography through spline-based penalized-likelihood sinogram smoothing. *Medical Imaging, IEEE Transactions on*; 2005; **24**: 105-111

Leith, E.N. & Upatnieks, J. Reconstructed Wavefronts and Communication Theory. *Journal of the Optical Society of America*; 1962; **52**: 1123-1130

Lemmens, C. & Nuyts, J. Metals in PET/CT: Causes and reduction of artifacts in PET images; 2008: 4184-4192

Lewis, E.L., Dolwick, M.F., Abramowicz, S., & Reeder, S.L. /20. Contemporary imaging of the temporomandibular joint. *Dental Clinics of North America*; 2008; **52**: 875-890

Liang, X., JACOBS, R., Hassan, B., Li, L., Pauwels, R., Corpas, L., Souza, P., Martens, W., Shahbazian, M., Alonso, A., & Lambrichts, I. A comparitive evaluation of Cone Beam Computed Tomography (CBCT) and Multi-Slice (MSCT). *European Journal of Radiology*: 2009; **75**: 270-274

Lu, P., Li, Z., Wang, Y., Chen, J., & Zhao, J. The research and development of noncontact 3-D laser dental model measuring and analyzing system. *Chinese Journal of Dental Research;* 2000; **3**: 7-14

Mah, J.K., Danforth, R.A., Bumann, A., & Hatcher, D. Radiation absorbed in maxillofacial imaging with a new dental computed tomography device. *Oral Surgery Oral Medicine Oral Pathology Oral Radiology and Endodontics;* 2003; **96**: 508-13

Mah, J. & Hatcher, D. Three-dimensional craniofacial imaging. *American Journal of Orthodontics and Dentofacial Orthopedics*; 2004; **126**: 308-309

Manglos, S.H., Gagne, G.M., Krol, A., Thomas, F.D., & Narayanaswamy, R. Transmission maximum-likelihood reconstruction with ordered subsets for cone beam CT. *Physics in Medicine and Biology*; 1995; **40**, 1225-1241

Martensson, B. & Ryden, H. The holodent system, a new technique for measurement and storage of dental casts. *American Journal of Orthodontics and Dentofacial Orthopedics*; 1992; **102**: 113-9

Matteson, S.R., Bechtold, W., Phillips, C., & Staab, E.V. A method for three-dimensional image reformation for quantitative cephalometric analysis. *Journal of Oral and Maxillofacial Surgery*; 1989; **47**: 1053-1061

Mayer R. Invention and Innovation from Canada's National Research Council. *Scientific Canadian*; 1999

McCance, A.M., Moss, J.P., Wright, W.R., Linney, A.D., & James, D.R. A three-dimensional soft tissue analysis of 16 skeletal class III patients following bimaxillary surgery. *British Journal of Oral and Maxillofacial Surgery*; 1992; **30**: 221-232

McCance, A.M., Moss, J.P., Fright, W.R., Linney, A.D., & James, D.R. Three-dimensional analysis techniques--Part 2: Laser scanning: a quantitative three-dimensional soft-tissue analysis using a color-coding system. *Cleft Palate-Craniofacial Journal*; 1997; **34**: 46-51

McCann, P.J., Brocklebank, L.M., & Ayoub, A.F. Assessment of zygomatico-orbital complex fractures using ultrasonography. *British Journal of Oral and Maxillofacial Surgery*; 2000; **38**: 525-529

Meilinger, M., Schmidgunst, C., Schultz, O., & Lang, E. W. Metal Artifact Reduction in CBCT Using Forward Projected Reconstruction Information and Mutual Information Realignment. *World Congress on Medical Physics and Biomedical Engineering*; 2009; **25**: 46-49

Mori, Y., Miyajima, T., Minami, K., & Sakuda, M. An accurate three-dimensional cephalometric system: a solution for the correction of cephalic malpositioning. *Journal of Orthodontics;* 2001; **28**: 143-9

Moss, J.P., Linney, A.D., Grindrod, S.R., Arridge, S.R., & Clifton, J.S. Three-dimensional visualization of the face and skull using computerized tomography and laser scanning techniques. *European Journal of Orthodontics*; 1987; **9**: 247-253

Motohashi, N. & Kuroda, T. A 3D computer-aided design system applied to diagnosis and treatment planning in orthodontics and orthognathic surgery. *European Journal of Orthodontics*; 1999: **21**: 263-274

Nakasima, A., Terajima, M., Mori, N., Hoshino, Y., Tokumori, K., Aoki, Y., & Hashimoto, S. Three-dimensional computer-generated head model reconstructed from cephalograms, facial photographs, and dental cast models. *American Journal of Orthodontics and Dentofacial Orthopedics*; 2005; **127**: 282-292

Nandini, S., Velmurugan, N., & Kandaswamy, D. Calcific healing of a crown root fracture of a maxillary central incisor evaluated with spiral computed tomography and hounsfield units: a case report. *Dental Traumatology*; 2008; **24**: 96-100

Nattestad, A. & Vedtofte, P. Pitfalls in orthognathic model surgery. The significance of using different reference lines and points during model surgery and operation. *International Journal of Oral and Maxillofacial Surgery*; 1994; **23**: 11-15

Nkenke, E., Zachow, S., Benz, M., Maier, T., Veit, K., Kramer, M., Benz, S., Hausler, G., Neukam, F.W., & Lell, M. Fusion of computed tomography data and optical 3D images of the dentition for streak artefact correction in the simulation of orthognathic surgery. *Dentomaxillofacial Radiology*; 2004a; **33**: 226-232

Nkenke, E., Zachow, S., Benz, M., Maier, T., Veit, K., Kramer, M., Benz, S., Hausler, G., Neukam, F.W., & Lell, M. Fusion of computed tomography data and optical 3D images of the dentition for streak artefact correction in the simulation of orthognathic surgery. *Dentomaxillofacial Radiology*; 2004b; **33**: 226-232

O'Grady, K.F. & Antonyshyn, O.M. Facial asymmetry: three-dimensional analysis using laser surface scanning. *Plastic and Reconstructive Surgery*; 1999; **104**: 928-937

O'Malley, A.M. & Milosevic, A. Comparison of three facebow/semi-adjustable articulator systems for planning orthognathic surgery. *British Journal of Oral and Maxillofacial Surgery*; 2000; **38**; 185-190

O'Neil, M., Khambay, B., Moos, K.F., Barbenel, J., Walker, F., & Ayoub, A. Validation of a new method for building a three-dimensional physical model of the skull and dentition. *British Journal of Oral and Maxillofacial Surgery*; 2010

Odlum, O. A method of eliminating streak artifacts from metallic dental restorations in CTs of head and neck cancer patients. *Special Care in Dentistry*; 2001; **21**: 72-74

Okumura, H., Chen, L.H., Tsutsumi, S., & Oka, M. Three-dimensional virtual imaging of facial skeleton and dental morphologic condition for treatment planning in orthognathic surgery. *American Journal of Orthodontics and Dentofacial Orthopedics*; 1999; **116**: 126-31

Olszewski, R. & Reychler, H. Limitations of orthognathic model surgery: theoretical and practical implications. *Revue de Stomatologie et de Chirurgie Maxillo-Faciale*; 2004; **105**: 165-169

Palomo, J.M., Kau, C.H., Palomo, L.B., & Hans, M.G. Three-dimensional cone beam computerized tomography in dentistry. *Dentistry Today*; 2006; **25**: 130, 132-5

Papadopoulos, M.A., Christou, P.K., Christou, P.K., Athanasiou, A.E., Boettcher, P., Zeilhofer, H.F., Sader, R., & Papadopulos, N.A. Three-dimensional craniofacial reconstruction imaging. *Oral Surgery Oral Medicine Oral Pathology Oral Radiology and Endodontics*; 2002; **93**: 382-393

Park, W.S., Kim, K.D., Shin, H.K., & Lee, S.H. Reduction of metal artifact in three-dimensional computed tomography (3D CT) with dental impression materials. *Conference Proceedings: Annual International Conference of the IEEE Engineering in Medicine and Biology Society*; 2007; 3496-3499

Persson, A., Andersson, M., Oden, A., & Sandborgh-Englund, G. A three-dimensional evaluation of a laser scanner and a touch-probe scanner. *Journal of Prosthetic Dentistry*; 2006; **95**: 194-200

Plooij, J.M., Maal, T.J.J., Haers, P., Borstlap, W.A., Kuijpers-Jagtman, A.M., & Berge, S.J. Digital three-dimensional image fusion processes for planning and evaluating orthodontics and orthognathic surgery. A systematic review. *International Journal of Oral and Maxillofacial Surgery*; 2011; **40**: 341-352

Popat, H. & Richmond, S. New developments in: three-dimensional planning for orthognathic surgery. *Journal of Orthodontics*; 2009; **37**: 62-71

Proffit, W.R. & White, R.P., Jr. Who needs surgical-orthodontic treatment? *International Journal of Adult Orthodontics and Orthognathic Surgery*; 1990; **5**: 81-89

Quimby, M.L., Vig, K.W., Rashid, R.G., & Firestone, A.R. The accuracy and reliability of measurements made on computer-based digital models. *Angle Orthodontist*; 2004; **74**: 298-303

Rabey Graham. Craniofacial Morphanalysis. *Proceedings of the Royal Society of Medicine*; 1971; **64**: 103-111

Rabey, G.P. Current principles of morphanalysis and their implications in oral surgical practice. *British Journal of Oral Surgery*; 1977; **15**: 97-109

Ras, F., Habets, L.L., van Ginkel, F.C., & Prahl-Andersen, B. Quantification of facial morphology using stereophotogrammetry demonstration of a new concept. *Journal of Dentistry*; 1996; **24**: 369-374

Renzi, G., Carboni, A., Perugini, M., & Becelli, R. Intraoperative measurement of maxillary repositioning in a series of 30 patients with maxillomandibular vertical asymmetries. *International Journal of Adult Orthodontics and Orthognathic Surgery*; 2002; **17**: 111-115

Romeo, A., Canal, F., Roma, M., de la Higuera, B., Ustrell, J.M., & von Arx, J.D. Holograms in orthodontics: a universal system for the production, development, and illumination of holograms for the storage and analysis of dental casts. *American journal of orthodontics and dentofacial orthopedics : Official Publication of the American Association of Orthodontists, its Constituent Societies, and the American Board of Orthodontics*; 1995; **108:** 443-447

Rossouw, P.E., Benatar, M., Stander, I., & Wynchank, S. A critical comparison of three methods for measuring dental models. *Journal of the Dental Association of South Africa*; 1991; **46**: 223-226

Santoro, M., Galkin, S., Teredesai, M., Nicolay, O.F., & Cangialosi, T.J. Comparison of measurements made on digital and plaster models. *American Journal of Orthodontics and Dentofacial Orthopedics*; 2003; **124**: 101-105

Savara, B.S. A method for measuring facial bone growth in three dimensions. *Human Biology*; 1965; **37**: 245-255

Scarfe, W.C. & Farman, A.G. What is cone-beam CT and how does it work? *Dental Clinics of North America*; 2008; **52**: 707-30

Schulze, R.K., Berndt, D., & d'Hoedt, B. On cone-beam computed tomography artifacts induced by titanium implants. *Clinical Oral Implants Research*; 2010; **21**: 100-107

Schutyser, F., Swennen, G., & Suetens, P. Robust visualization of the dental occlusion by a double scan procedure. *Medical Image Computing and Computer-Assisted Intervention*; 2005; **8**: 1-74

Sharifi, A., Jones, R., Ayoub, A., Moos, K., Walker, F., Khambay, B., & McHugh, S. How accurate is model planning for orthognathic surgery? *International Journal of Oral and Maxillofacial surgery*; 2008; **37**: 1089-1093

Sohmura, T., Hojoh, H., Kusumoto, N., Nishida, M., Wakabayashi, K., & Takahashi, J. A novel method of removing artifacts because of metallic dental restorations in 3-D CT images of jaw bone. *Clinical Oral Implants Research*; 2005; **16**: 728-35

Soncul, M. & Bamber, M.A. The optical surface scan as an alternative to the cephalograph for soft tissue analysis for orthognathic surgery. *International Journal of Adult Orthodontics and Orthognathic Surgery*; 1999; **14**: 277-283

Soncul, M. & Bamber, M.A. Evaluation of facial soft tissue changes with optical surface scan after surgical correction of Class III deformities. *Journal of Oral and Maxillofacial Surgery*; 2004; **62**: 1331-1340

Speculand, B., Butcher, G.W., & Stephens, C.D. Three-dimensional measurement: The accuracy and precision of the reflex metrograph. *British Journal of Oral and Maxillofacial Surgery*; 1988a; **26**: 265-275

Speculand, B., Butcher, G.W., & Stephens, C.D. Three-dimensional measurement: The accuracy and precision of the reflex microscope. *British Journal of Oral and Maxillofacial Surgery*; 1988b; **26**: 276-283

Spencer, R., Hathaway, R., & Speculand, B. 3D computer data capture and imaging applied to the face and jaws. *British Journal of Oral and Maxillofacial Surgery*; 1996; **34**: 118-123

Strauss, R.A. & Burgoyne, C.C. Diagnostic imaging and sleep medicine. *Dental Clinics of North America*; 2008; **52**: 891-915

Swennen, G.R., Mommaerts, M.Y., Abeloos, J., De, C.C., Lamoral, P., Neyt, N., Casselman, J., & Schutyser, F. The use of a wax bite wafer and a double computed tomography scan procedure to obtain a three-dimensional augmented virtual skull model. *Journal of Craniofacial Surgery*; 2007a; **18**: 533-539

Swennen, G.R.J., Barth, E.L., Eulzer, C., & Schutyser, F. The use of a new 3D splint and double CT scan procedure to obtain an accurate anatomic virtual augmented model of the skull. *International Journal of Oral and Maxillofacial Surgery*; 2007b; **36**: 146-152

Swennen, G.R., Mommaerts, M.Y., Abeloos, J., De, C.C., Lamoral, P., Neyt, N., Casselman, J., & Schutyser, F. A cone-beam CT based technique to augment the 3D virtual skull model with a detailed dental surface. *International Journal of Oral and Maxillofacial surgery*; 2009a; **38**: 48-57

Swennen, G.R.J., Mollemans, W., De Clercq, C., Abeloos, J., Lamoral, P., Lippens, F., Neyt, N., Casselman, J., & Schutyser, F. A cone-beam computed tomography triple scan procedure to obtain a three-dimensional augmented virtual skull model appropriate for orthognathic surgery planning. *Journal of Craniofacial Surgery*; 2009b; **20**: 297-307

Swennen, G.R.J., Mollemans, W., & Schutyser, F. Three-Dimensional Treatment Planning of Orthognathic Surgery in the Era of Virtual Imaging. *Journal of Oral and Maxillofacial Surgery*; 2009c; **67**: 2080-2092

Takada, K., Lowe, A.A., & DeCou, R. Operational performance of the Reflex Metrograph and its applicability to the three-dimensional analysis of dental casts. *American Journal of Orthodontics*; 1983; **83**: 195-199

Tasaki, M.M. & Westesson, P.L. Temporomandibular joint: diagnostic accuracy with sagittal and coronal MR imaging. *Radiology*; 1993; **186**: 723-729

Tohnak, S., Mehnert, A.J., Mahoney, M., & Crozier, S. Dental CT metal artefact reduction based on sequential substitution. *Dento-Maxillo-Facial Radiology*; 2011: **40**: 184-190

Troulis, M.J., Everett, P., Seldin, E.B., Kikinis, R., & Kaban, L.B. Development of a three-dimensional treatment planning system based on computed tomographic data. *International Journal of Oral and Maxillofacial Surgery*; 2002: **31**: 349-57

Uechi, J., Okayama, M., Shibata, T., Muguruma, T., Hayashi, K., Endo, K., & Mizoguchi, I. A novel method for the 3-dimensional simulation of orthognathic surgery by using a multimodal image-fusion technique. *American Journal of Orthodontics and Dentofacial Orthopedics*; 2006; **130**: 786-98

Valiathan, A., Dhar, S., & Verma, N. 3D CT imaging in Orthodontics: Adding a New Dimension to Diagnosis and Treatment Planning. *Trends Biomater.Artif.Organs*; 2007; **21**: 116-120

Vannier, M.W., Hildebolt, C.F., Conover, G., Knapp, R.H., Yokoyama-Crothers, N., & Wang, G. Three-dimensional dental imaging by spiral CT. A progress report. *Oral Surgery Oral Medicine Oral Pathology Oral Radiology and Endodontics*; 1997; **84**: 561-70

Veselko, M., Jenko, M., & Lipuscek, I. The use of the co-ordinate measuring machine for the study of three- dimensional biomechanics of the knee. *Computers in Biology and Medicine*; 1998; **28**: 343-357

Von, T.J. & Rivett, L.J. Applications of photogrammetry to orthodontics. *Australian Orthodontic Journal*; 1982; **7**: 162-167

Walker, F., Ayoub, A.F., Moos, K.F., & Barbenel, J. Face bow and articulator for planning orthognathic surgery: 2 articulator. *British Journal of Oral and Maxillofacial Surgery*; 2008a; **46:** 573-578

Walker, F., Ayoub, A.F., Moos, K.F., & Barbenel, J. Face bow and articulator for planning orthognathic surgery: 1 face bow. *British Journal of Oral and Maxillofacial Surgery*; 2008b; **46**: 567-572

White, S.C. & Pharoah, M.J. The evolution and application of dental maxillofacial imaging modalities. *Dental Clinics of North America;* 2008a; **52:** 689-705

Xia, J., Ip, H.H., Samman, N., Wong, H.T., Gateno, J., Wang, D., Yeung, R.W., Kot, C.S., & Tideman, H. Three-dimensional virtual-reality surgical planning and soft-tissue prediction for orthognathic surgery. *IEEE Transactions on Information Technology in Biomedicine*; 2001; **5**: 97-107

Yajima, A., Otonari-Yamamoto, M., Sano, T., Hayakawa, Y., Otonari, T., Tanabe, K., Wakoh, M., Mizuta, S., Yonezu, H., Nakagawa, K., & Yajima, Y. Cone-beam CT (CB Throne) applied to dentomaxillofacial region. *Bulletin of Tokyo Dental College*; 2006; **47**: 133-41

Young, J.M. & Altschuler, B.R. Laser holography in dentistry. *Journal of Prosthetic Dentistry*; 1977a; **38**: 216-25

Zhang S & Yau S T. High-resolution, real-time 3-D absolute coordinate measurement method based on a phase-shifting method. *Optics Express*; 2006; **14:** 7

Zhang, Y., Zhang, L., Zhu, X.R., Lee, A.K., Chambers, M., & Dong, L. Reducing metal artifacts in cone-beam CT images by preprocessing projection data. *International Journal of Radiation Oncology, Biology, Physics*; 2007; **67**: 924-932

Chapter Nine

Presentations and Awards

9 Presentations and Awards

9.1 Presentations

- **March 2009:** Orthodontics Technicians Association (OTA) annual conference, Milton Keynes: *Three dimensional imaging (3D) (Its virtually here)*.

- **May 2009:** Telford College, Edinburgh: *Three dimensional imaging (3D) (Its virtually here)*.

- **June 2010:** Hospital Laboratory Managers Association, Glasgow: *Three dimensional imaging (3D) (Its virtually here)*.

Abstract:

The term and use of 3D imaging is rapidly becoming more common place within the dental environment as clinical and technical members of the dental team strive to develop more accurate methods of prediction and planning of treatment.

Three Dimensional Imaging (3D), is any technique that has the ability to record or capture three dimensional data i.e. width, length and depth (x, y &z) of an object or create the illusion of depth in an image. There are a number of software computer programs that allow the user to visualise and manipulate the information captured in a virtual environment (*Virtual Reality (VR) refers to the technology on which a user is able to interact with a computer simulated environment*). 3D scanners can be categorized as either **contact** or **non-contact**:

Contact: these scanners examine the subject by touch (usually with use of a fine stylus) e.g. a coordinate measuring machine (CMM) This form of scanning can be very precise, but has significant limitations as the act of scanning has potential to damage the surface of the item being scanned and is a very slow method.

Non-Contact: these scanners omit a light, x-ray or ultrasound, e.g. laser scanning *(*Stereoscopic holography spiral computed tomography scanner (CT) or

more commonly used within dentistry a cone beam computed tomography scanner (CBCT).

CT scanning is widely regarded as the gold standard of creating 3D images of the hard tissue. The use of CT scans within dentistry is rapidly becoming common place, particularly in the planning of dental implants and the prediction of orthognathic outcomes. Although there may be significant levels of radiation and potential risk it is generally accepted that the benefits far outweigh the problems associated with CT. The introduction of cone-beam (CBCT) scanners, which create high-resolution images with a tenfold reduction in radiation have been specifically designed for maxillofacial imaging.

Gypsum based Orthodontic study models are still used routinely as an integral part of dental practise and research. For legal reasons these casts are a form of medical record and should retained for a minimum of 11 years post treatment or until the patient is 26 years old. These models can create a number of problems which 3D imaging may be able to overcome, storage/cost, archiving, weight, susceptibility to fracture, surface abrasion and recording of measurements.

The information that is obtained from 3D scanners is a collection of points in 3D space. Using specialised software these points can be connected using a variety of geometric entities to create a 3D model which can be displayed on a two-dimensional screen. Utilising reverse engineering the 3D information can be imputed in to a 3D printer. This is a machine that creates a physical object by layering and connecting very fine sections of material *e.g. plaster, corn starch or a variety of resins*.

3D imaging has the potential to revolutionise the way in which treatment planning of patients is undertaken. Although these systems may require more development and might not be cost effective in the archiving of dental casts, they go a long way to alleviating the problems associated gypsum models. 3D imaging might not be common place at the moment, but it's virtually here.

- **September 2010:** British Orthodontic Conference, Brighton: *An intra-oral registration technique for the replacement of the dentition in a cone beam CT (CBCT) scan.*

Abstract:

The increasing use of three dimensional (3D) imaging now enables clinicians to visualise the soft tissue, bone and dentition in a virtual environment. The use of cone beam CT (CBCT) is rapidly becoming a routine imaging modality due to the significant reduced radiation exposure to a patient, when compared to spiral CT. However, as with conventional CT it is not possible to reproduce an accurate representation of the occlusal surfaces of the teeth. When imaging patients using CBCT, any intra-oral metallic objects (e.g. restorations, jewellery, implants and orthodontic appliances) create streak artefacts.

These artefacts can obliterate the occlusal surfaces of the images of the teeth, rendering the virtual model useless in predicting intercuspal relationship and orthognathic wafer construction.
This presentation demonstrates a new and refined intra-oral technique in which the inaccurate dentition of the CBCT scan can be replaced with "clean" and accurate virtual dental models.

- **March 2011:** Orthodontics Technicians Association annual conference, Southampton: *How to remove an undesirable streak.*

- **June 2011:** hands on orthognathic course, Glasgow: *How to remove an undesirable streak.*

Abstract:

Cone beam CT (CBCT) is rapidly becoming a routine imaging modality specifically designed for the maxillofacial region and enables clinicians to visualize the soft tissue, bone and dentition in a virtual environment.
Imaging patients using CBCT who may have intra-oral metallic objects (e.g. restorations, jewellery, implants or orthodontic appliances) will create streak artefacts. These artefacts impair any virtual model by obliterating the occlusal surfaces of the teeth*).* This is a major obstacle for occlusal registration and the

fabrication of orthognathic wafers to guide the surgical correction of dentofacial deformities.

This presentation aims to demonstrate a new and refined intra-oral technique in which the inaccurate dentition of the CBCT scan can be replaced with "clean" and accurate virtual dental models. Impressions of the dentition were taken and cast using a high density, minimal expansion gypsum product. Acrylic baseplates were then constructed incorporating three hexagonal radiolucent registration markers. These appliances are then fitted to a dry skull and a CBCT scan performed. Alginate impressions were then taken of the dentition with the devices in situ and subsequent gypsum models were produced. The models are then CBCT scanned and a virtual model produced. Both the images of the dry skull and the model were imported into a CAD/CAM software program The hexagonal markers on both images were identified and aligned; this would align the dentition without relying on the teeth for superimposition and therefore allowed the occlusal surface of the dentition to be replaced with the occlusal image of the model.

To assess the accuracy of the method, distances between the meshes were measured at several anatomical dental points. These varied from 0.2mm to 0.4 mm. The accuracy of this technique is shown to be clinically acceptable, and could be a significant advancement in improving the accuracy of surgical prediction planning, with the ultimate goal of fabrication of a physical orthognathic wafer using reverse engineering.

9.2 Awards

- Awarded the Aldridge Medal, for best lecture at the 2009 OTA annual conference.